Nebraska Water Resources Center
Annual Technical Report
FY 2011

Introduction

Dr. Suat Irmak, professor in the Biological Systems Engineering Department at the University of Nebraska-Lincoln, took over as the interim director of the Water Center as of January 1, 2012. Lorrie Benson, J.D. serves as the assistant director. Steve Ress and Tricia Liedle serve as the communications specialist and program specialist, respectively. The Water Center staff also includes Rachael Herpel as the water outreach specialist. The Water Center also underwent a name change in February 2012 becoming the Nebraska Water Center, a part of the Daugherty Water for Food Institute at the University of Nebraska.

The Nebraska Water Center is currently housed in the School of Natural Resources, located in Hardin Hall (3310 Holdrege, Lincoln, NE 68583-0979). However, the Center is now part of the Robert B. Daugherty Water for Food Institute, which is located in Whittier Building in the Robert B. Daugherty Water for Food Institute, University of Nebraska, 234 Whittier Research Center, 2200 Vine Street, Lincoln, NE 68583-0857 U.S.A. The transition period to physically move the Nebraska Water Center to the Whittier Building is currently in progress.

The Water Center was the lead organizer for two major events fall 2011. First was a one-day science and policy symposium showcasing water-related research and programming in Nebraska, with a focus on climate, water and ecoysystems. The event, which was co-sponsored by the USGS Nebraska Water Science Center, featured speaker Matthew Larsen, associate director. The second event was a one-day water law conference, designed for practicing attorneys, but attended by many water policy makers and managers. It was co-sponsored by the University of Nebraska College of Law. The Water Center also assisted the UNL Office of Research with the third annual Water for Food conference an event drawing international speakers and attendees and sponsored by the University of Nebraska's Robert B. Daugherty Water for Food Institute.

The Water Center has continued to assist with development of the UNL water portal (water.unl.edu) and maintains the NIWR website (snr.unl.edu/niwr) through the Water Center. Along with these websites, we continue to focus on the Water Center’s home website (http://watercenter.unl.edu).

Research Program Introduction

For the 2011 fiscal year, four research seed grants received funding through the USGS 104(b) program. Areas chosen for funding were: (1) developing slow release persulfate to treat BTEX compounds at LUST sites; (2) a cost effective fixed film atrazine treatment utilizing nitrate as a nutrient; and (3) high-resolution imaging of the Platte river streambed using combined electromagnetic induction and hydraulic parameter estimation techniques; An additional three seed research grants were selected for possible funding during the 2012 fiscal year. Areas chosen for 2012 were: (1) analysis of potential groundwater trading programs for Nebraska; (2) developing a two-tier screen to evaluate the health of Nebraska's wetlands; and (3) direct monitoring of knickpoint progression.

The Water Sciences Laboratory continues as a core facility to assist water science faculty. Analyses and the number of faculty utilizing this cutting-edge analytical facility continued to grow. The overall usage of the laboratory has increased by over 20% in the past three years. Once again, analyses were conducted for several other universities, state and federal agencies, as well as for private companies and individuals, but the focus remains on UNL faculty.

Developing Slow Release Persulfate to Treat BTEX Compounds at LUST Sites

Basic Information

Title:	Developing Slow Release Persulfate to Treat BTEX Compounds at LUST Sites
Project Number:	2011NE216B
Start Date:	3/1/2011
End Date:	2/29/2012
Funding Source:	104B
Congressional District:	Nebraska 1st
Research Category:	Engineering
Focus Category:	Treatment, Toxic Substances, Groundwater
Descriptors:	
Principal Investigators:	Steve Douglas Comfort, Xu Li

Publication

1. No Publications

2011 Project Report: Developing slow-release persulfate candles to treat BTEX compounds at LUST sites

PIs: Steve Comfort[1] and Xu Li[2]

[1] *School of Natural Resources, University of Nebraska, Lincoln, NE 68583-0915, USA*
[2] *Department of Civil Engineering, University of Nebraska, Lincoln, NE 68583-0531, USA*

ABSTRACT

The development of slow-release chemical oxidants for sub-surface remediation is a relatively new technology. Our objective was to develop slow-release persulfate-paraffin candles to treat BTEX-contaminated groundwater. Laboratory-scale candles were prepared by heating and mixing $Na_2S_2O_8$ with paraffin in a 2.25 to 1 ratio (w/w), and then pouring the heated mixture into circular molds that were 2.38 cm long and either 0.71 or 1.27 cm in diameter. Activator candles were prepared with $FeSO_4$ or zerovalent iron (ZVI) and wax. By treating benzoic acid and BTEX compounds with slow-release persulfate and ZVI candles, we observed rapid transformation of all contaminants. By using ^{14}C-labeled benzoic acid and benzene, we also confirmed mineralization or conversion to CO_2 occurred upon exposure to the candles. As the candles aged and were repeatedly exposed to fresh solutions, contaminant transformation rates slowed and removal rates became more linear (zero-order); this change in transformation kinetics mimicked the observed dissolution rates of the candles. By stacking persulfate and ZVI candles on top of each other in a saturated sand tank (14×14×2.5 cm) and spatially sampling around the candles with time, the dissolution patterns of the candles and zone of influence were determined. Results showed that as the candles dissolved and persulfate and iron diffused out into the sand matrix, benzoic acid or benzene concentrations (C_o = 1 mM) decreased by > 90% within 7 d. These results support the use of slow-release persulfate and ZVI candles as a means of treating BTEX compounds in contaminated groundwater.

---

1. Introduction

One of the biggest threats to groundwater quality in the United States is leaking petroleum from underground storage tanks (UST). Currently there are approximately 597,000 federally-regulated active UST at ~215,000 sites in the U.S. (USEPA, 2011). When petroleum tanks leak, they contaminate soil and groundwater with a number of soluble and hazardous compounds, most notably, BTEX compounds.

Over the last 25 yr, considerable progress has been achieved in developing various treatments for remediating soils and groundwater contaminated with petroleum products. Despite these advances, new technologies are still being sought to deal with UST located in difficult formations, such as low permeable aquifers. In situ chemical oxidation (ISCO) is the relatively mature practice of injecting liquid oxidants into groundwater for the treatment of contaminants such as BTEX and chlorinated solvents. Specific oxidants commonly used with ISCO include sodium and potassium permanganate, hydrogen peroxide (Fenton's reagent), ozone, and persulfate. While permanganate is the most frequently used oxidant with ISCO applications (Krembs et al., 2011), it is not effective in removing benzene, the regulatory driver for remediating most UST sites.

Persulfate (peroxydisulfate) is the newest chemical oxidant used for ISCO, having only come into consideration over the last few years. Persulfate has a standard reduction potential of 2.01 V (Latimer, 1952, House, 1962), which is higher than those of hydrogen peroxide ($E° = 1.77$ V) and permanganate ($E° = 1.67$ V) but lower than hydroxyl radicals ($E° = 2.7$ V) or ozone ($E° = 2.07$ V) (Latimer, 1952). Persulfate is known to react directly with some organic compounds but can be kinetically slow in transforming some contaminants (ITRC, 2005; Osgerby, 2006; Petri et al., 2011). In addition to direct accepting electrons, persulfate can be purposely induced to form sulfate radicals ($SO_4^{\bullet-}$). The sulfate radical has a redox potential of 2.6 V (Eberson, 1987), which gives it more potential to degrade a larger variety of contaminants than the parent persulfate molecule ($E° = 2.01$ V). Common activators used to produce persulfate radical formation include heat, Fe(II), H_2O_2 and alkaline pH.

Several researchers have reported positive results in treating BTEX compounds with persulfate in contaminated soil and water (Huang et al., 2005; Crimi and Taylor, 2007; Killian et al., 2007; Liang et al., 2008; Achugasim et al., 2011; Lemaire et al., 2011). Some examples include Huang et al. (2005), who used heat-activated persulfate to degrade 59 volatile organic compounds, which included BTEX, as well as some other benzene derivatives. Lemaire et al. (2011) degraded a BTEX mixture consisting mainly of xylenes with unactivated and Fe(II)-activated persulfate while Liang et al. (2008) compared Fe(II) chelating agents and showed that citric acid was most suitable in the iron activated persulfate system for treating benzene.

A challenge to successfully implementing ISCO in aquifers is when the contaminants of interest are present in low permeable zones. Most ISCO treatments to date have involved injecting liquid oxidants. A common problem with any chemical injection however, is that some sites may have finer textured soils that do not readily accept liquid injections. When this occurs, the chemical oxidant can be observed coming back out of the injection borehole because it offers the path of least resistance.

Difficulty in addressing contamination in low permeable soils may be alleviated to some degree by taking a passive approach where a slow-release oxidant is inserted into the formation and allowed to dissolve and intercept the contaminant over many years.

While the development and testing of slow-release permanganate has been investigated for a number of years (Ross et al., 2005; Lee and Schwartz, 2007a; Swearingen and Swearingen, 2008), the use of slow-release persulfate for BTEX treatment has only recently been reported. Liang et al. (2011) created a slow-release persulfate cement cube (4×6×7 cm) that consisted of persulfate (sodium or potassium), cement, sand, and water. Liang et al. (2011) evaluated these persulfate cubes in column experiments to quantify their efficacy in removing benzene and MTBE. When activated with Fe(II), the persulfate cube (270 g) was able to oxidize 95 to 99% of the benzene (0.2 mg L^{-1}) and 86 to 92% MTBE (0.3 mg L^{-1}) during miscible displacement for several pore volumes. These results support using slow-release persulfate as a means of treating petroleum contaminated groundwater.

Although several researchers have suggested creating in situ oxidant barriers as a means of halting the migration of contaminants (e.g., Ross et al., 2005; Lee and Schwartz, 2007a; Lee et al., 2009; Liang et al., 2011), field-scale testing of slow-release oxidants is only beginning. Christenson (2011) reported one of the first field trials where a slow-release oxidant was inserted into a trichloroethene (TCE)-contaminated aquifer at an abandoned landfill. In their study, multiple 91 cm (3 ft) long permanganate candles (paraffin wax – permanganate) were manufactured and inserted into the aquifer by either direct push or encased in carriers and lowered into permanent wells to create an ISCO barrier. Initial results showed a 64 to 82% reduction in TCE within the first year (Christenson, 2011). To expand on the research reported by Christenson (2011), our objective was to develop similar slow-release persulfate-paraffin candles that could potentially be used to treat BTEX-contaminated groundwater. We accomplish this by conducting a series of laboratory experiments that combined and tested the efficacy of various persulfate and activator candles. A prototype of a combined persulfate-zerovalent iron (ZVI) candle for field-scale use is also presented.

2.0. Materials and methods

2.1. Candle preparation

Initial attempts to produce slow-release persulfate candles began by manufacturing a single candle containing a mixture of persulfate, activator and chelator. Specifically, we blended paraffin, persulfate, Fe(II) ($FeSO_4 \cdot 7H_2O$) as an activator, and citric acid as an iron chelator. Because these mixed composition candles (herein after referred to as “mixed candles”) did not provide consistent performance and were short-lived (explained below), individual persulfate and activator candles were made. Details of how the candles (persulfate, Fe(II), zerovalent iron) are explained in Kambhu (2011).

2.2 Chemical release rates from candles

To quantify persulfate release rates, laboratory experiments were conducted with both size candles (0.71 and 1.27 cm dia). The 0.71 cm candles were placed in 125-mL Erlenmeyer flask filled with 100 mL distilled water; the 1.27-cm dia candles were placed in 250-mL flasks containing 200 mL water. Sample temperature was maintained at room temperature. Once the candles were immersed in water, the solution was sub-sampled via pipette every 30 min for the first 4 h, and approximately every 2-3 d until the remainder of the experiment. Immediately prior to each sampling, the solutions were gently swirled to mix. All samples were analyzed colormetrically with iodide on a Hach DR 2800 Visual Spectrum Spectrophotometer at 450 nm. When needed, samples were diluted with H_2O so that measured concentrations fell with the linear adsorbance range (< 150 mg L^{-1}).

To characterize the release of persulfate from the slow-release sodium persulfate candles, we determined cumulative persulfate released with time. Mass of release persulfate was calculated from the concentration of persulfate in solution (mg L^{-1}) and volume of the solution (L).

The ability of the ZVI candles to release iron was also quantified. A ZVI candle was placed in a plastic bottle with a persulfate candle and H_2O. At selected times, aliquots were withdrawn and total iron was measured colormetrically with 1,10-phenanthroline at a wavelength of 510 nm (Olson, 1965) using a HACH Spectrophotometer DR2800 (HACH, Loveland, CO). We included persulfate candles in the iron release experiments because they greatly increased the dissolution rates of the iron candles and therefore, results were more representative of the two candle system (persulfate and activator).

2.3 Kinetic experiments

Kinetic degradation experiments were conducted with benzoic acid, benzene and BTEX mixture and the various candles developed. Control experiments verified that persulfate, benzoic acid and benzene were not reacting or adsorbing to the paraffin wax matrix. Control experiments showing the efficacy of thiosulfate to quench persulfate and stop the further transformation of benzoic acid and benzene were also performed.

2.3.1 Benzoic acid

Quantifying the ability of the persulfate candles to transform contaminants began with batch experiments using benzoic acid. Benzoic acid ($C_7H_6O_2$, ASC Reagent grade, Sigma-Aldrich, St. Louis, MO) was used as a surrogate for BTEX because it is less volatile and negated the need for a zero headspace experimental unit (used in later experiments). Benzoic acid experiments were conducted in 250-mL Erlenmeyer flasks under batch conditions. To each flask, 200 mL of benzoic acid solution (C_o = 0.1 mM) was added to the flask with a slow release persulfate candle and a ZVI candle (or a mixed candle) and agitated on an orbital shaker. In some experiments, solutions were spiked with 1 mL of ^{14}C-benzoic acid (ring-^{14}C, Moravek Biochemicals, Brea, CA, specific activity: 60 mCi $mmol^{-1}$) so that mineralization rates (conversion to $^{14}CO_2$) could

also be quantified. Temporal changes in concentrations were obtained by removing 1 mL samples at selected times and quenching the reaction by mixing with 0.17 g of sodium thiosulfate (ReagentPlus, 99%, Sigma-Aldrich, St. Louis, MO) in a 1.5-mL microcentrifuge tube and centrifuging for 15 min at 14,000 *g*. The supernatant was then transferred to a glass vial and analyzed with HPLC. Temporal changes in radioactivity were determined by mixing 1 mL samples with 0.5 mL of 2 N H_2SO_4, to release CO_2 and then mixed with 6 mL of scintillation cocktail.

2.3.2 Repeated exposure experiments

Chemical dissolution rates from slow-release oxidants can be characterized as an initial flush followed by a slower and sustained release (Kang et al., 2004; Lee and Schwartz 2007a; Christenson, 2011). To quantify the longevity of the slow-release candles to continually transform benzoic acid (or BTEX compounds), a series of experiments were performed where fresh solutions of contaminants were added to the same candle in repetitive batches. This was accomplished by mixing the contaminant solution with the slow release candles (mixed, persulfate + ZVI) and temporally removing samples to quantify degradation rates (either every 3 or 24 h, depending on candle diameter size). Once the contaminant was transformed, the treated solution was discarded and fresh solution added so that temporal changes in contaminant concentration could be measured again. This process of adding fresh solution (benzoic acid or BTEX compounds) to the same candle or candles was repeated multiple times.

2.3.5 ^{14}C-Benzene and BTEX

The ability of the persulfate and ZVI candles to degrade BTEX compounds were performed in 100-mL gas tight syringes equipped with septum valves (SGE, Austin, TX) in a manner similar to that described by Huang et al. (2002). In these experiments, small diameter persulfate and ZVI candles, and a magnetic stirring bar were placed inside the syringe barrel before filling with 100 mL of benzene or a BTEX mixture (0.1 - 1.0 mM). Once filled, any trapped air inside the syringe was pushed out and the syringe was placed on a magnetic stirrer (Barnstead, Thermolyne Cimarec 2 Stirrer, S46725, Dubuque, IA).

Benzene solutions were prepared by mixing Ultra pure H_2O (that was sonicated prior to use to remove dissolved gases) and benzene stock solution to the desired concentration. For some experiments, ^{14}C-benzene (Moravek Biochemicals, Brea, CA specific activity: 100 mCi mmol^{-1}) was spiked into the benzene solution so that mineralization could also be quantified.

At selected times, 0.5 mL aliquots were withdrawn from the 100-mL syringe using a 1-mL gas tight syringe that was already prefilled with 0.1 mL 2 M sodium thiosulfate with zero headspace. Sodium thiosulfate was used to quench the persulfate and stop the reaction. The solution was then transferred to a HPLC vial that was prefilled with 1.2 mL acetonitrile (HPLC grade, Gibbstown, NJ) to prevent volatilization. BTEX compounds were then analyzed with HPLC. Experiments were repeated with a mixture of BTEX compounds (C_o = 0.10 mM benzene; 0.08 mM toluene, 0.07 mM ethylbenzene, and 0.07 mM of all three xylenes: *o*-xylene, *p*-xylene, *m*-xylene) using freshly prepared

persulfate and ZVI candles and candles that were aged for 48 h.

2.4 Tank Experiments

A 14 x 14 x 2.5 cm 2D tank was used to determine the radius of influence of the persulfate and ZVI candles. The 2D tank was equipped with a glass front for viewing and a solid back that contain 30 septa-sealed sampling ports, spaced 2 cm apart, and arranged in a 5 by 6 array. In the center of the tank, we placed a slotted PVC pipe (2 cm dia) to simulate a well. In that well, we placed large diameter persulfate and ZVI candles. Specifically, a two to one persulfate to ZVI candle ratio was used by stacking three persulfate (2.38 cm length) and three ZVI (1.19 cm) candles on top each other, such that the persulfate candles were separated by a ZVI candle.

To visualize dissolution patterns and zone of influence, we packed the tank with silica sand (297-420 µm mesh size) and flooded the tank with methylene blue dye (~0.2 g L^{-1}), which we found turned colorless upon exposed to persulfate and ZVI candles. Control tests verified the dye was neutralized (i.e., turned colorless) when exposed to persulfate and ZVI candles but not persulfate or ZVI alone. In this experiment, photographs of the 2D tank were taken every day to visually record the dissolution and diffusion patterns of the chemicals released from the candle.

A second and third set of experiments packed the tank with silica sand and flooded the tank with either 1 mM benzoic acid or benzene in separate experiments. Samples were removed from the sampling grid after 2 and 7 d to determine the radius of influence. Contour plots of benzoic acid and benzene concentrations were plotted with SigmaPlot scientific analysis and graphing software.

2.5 Chemical analysis

Details of analytical procedures used to quantify benzoic acid, BTEX compounds and ^{14}C-activity are presented in Kambhu (2011).

3. Results and discussion

3.1 Longevity of mixed candle

Using the mixed candle (persulfate + Fe(II) + citric acid) to transform 0.1 mM benzoic acid showed that the initial reaction rates was very fast, with 100% removal observed within 6 h (Fig. 1). However, when that same mixed candle was placed in fresh benzoic acid in subsequent batches, results showed that the longevity of the mixed candle was limited. By the time the candle had been immersed in solution for 2 d (third cycle, T = 2 d), only ~40% of benzoic acid was transformed within the next 12 h (Fig. 1a). The longevity of the mixed candle to mineralize ^{14}C-labeled benzoic acid was even shorter, with a significant decline in performance observed after the first cycle (Fig. 1b). While Christenson (2011) showed that slow-release permanganate candles exhibit a rapid release of permanganate, followed by a slower release rate, the inability of our mixed persulfate candle to continually transform benzoic acid can not solely be explained by the physical diffusion constraints of the paraffin matrix. Other reasons for

this reduced efficacy include compatibility issues between the persulfate, Fe(II) and citric acid, either during initial blending or afterwards while in the candle matrix. It was noted that the mixed candles appeared to pick up moisture upon standing (days) and change colors from greenish-yellow to white. Another problem with the mixed candle occurred during blending where we found that the ferrous sulfate was very sensitive to temperature and that overheating by just one or two degrees caused the candles to turn from green to yellow, indicating ferrous iron oxidation. When we separated the mixed candle components into individual candles of persulfate, $FeSO_4$ and citric acid, we observed that the citric acid was much more readily released from the paraffin matrix than persulfate or $FeSO_4$. For these reasons, candle experiments shifted to using zerovalent iron as an activator without citric acid.

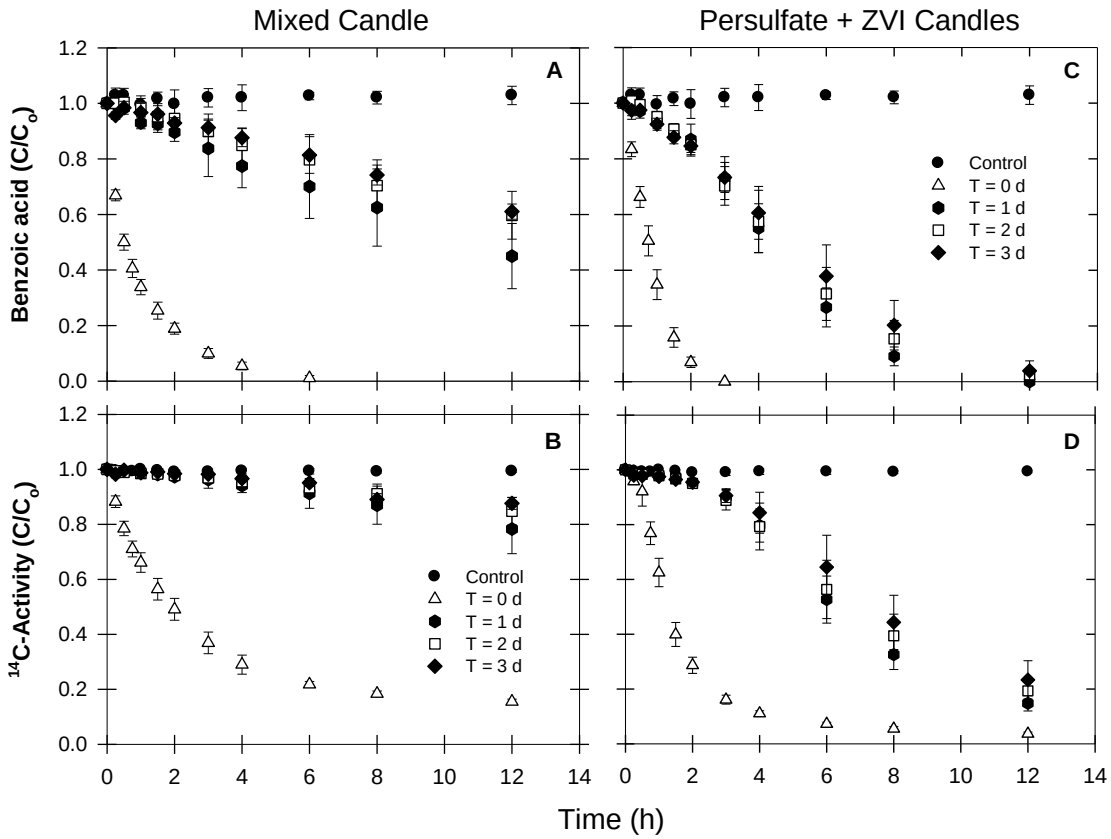

Figure 1 (A) Temporal changes in benzoic acid concentrations (C_o = 0.1 mM) and ^{14}C-activity (B) following treatment with mixed candle (persulfate, Fe(II), and citrate). (C) Temporal changes in benzoic acid concentrations (C_o = 0.1 mM) and ^{14}C-activity (D) following treatment with persulfate + ZVI candles. Bars on symbols represent sample standard deviations.

3.2 Treatment of benzoic acid with persulfate and ZVI candles

Treating benzoic acid with separate persulfate and ZVI candles showed that the initial reaction rate between the candles and benzoic acid were again fast with complete removal occurring within 3 h (Fig. 1c). Adding fresh benzoic acid to the candles every 24 h revealed that removal rates did not taper off as quickly as those observed with the mixed candle (Fig. 1a vs. 1c). For example, after 3 cycles of exposure (T = 2 d), the persulfate + ZVI candles were still able to transform ~100% of the benzoic acid within 12 h (Fig. 1c). The temporal changes in reaction kinetics upon repeated exposure can be explained by examining the release rates of persulfate and iron from the candles (See Sec. 3.3). Tracking changes in ^{14}C-concentrations confirmed mineralization was also occurring with the persulfate and ZVI candles (Fig. 1d) and this two candle system performed significantly better than the mixed candle (Fig. 1b).

3.3 Persulfate release rates

Release rates were measured from the large and small diameter persulfate candles with results confirming that candles dimensions influenced persulfate release. As observed with other slow-release oxidants (Kang et al., 2004; Lee and Schwartz 2007a; 2007b), large fluxes of persulfate were initially observed from the small and large diameter candles as the persulfate located on the surface of the candle dissolved into solution. This initial flux occurred within the first day for the small diameter candle and within the first 3 to 4 d for the large diameter candle. After this initial release (Fig. 2), the large diameter candles were much more consistent in releasing persulfate. After 4 d of being immersed in H_2O, the release rate was linear at 117 mg d^{-1}. By 25 d, the large diameter candle was spent and all of the persulfate (~100%) had been released. By contrast, the small candle had a slightly larger release rate (189 mg d^{-1}) but began to show signs of slowing down or releasing less persulfate by 3 d; by 6 d ~82% of the persulfate had been released. The observed change in dissolution patterns can be explained by the dissolution front retreating back into the paraffin matrix and the diffusion paths increasing. These changes in releases patterns were also manifested in the removal kinetics observed for benzoic acid (exponential decline vs. linear, Fig. 1c).

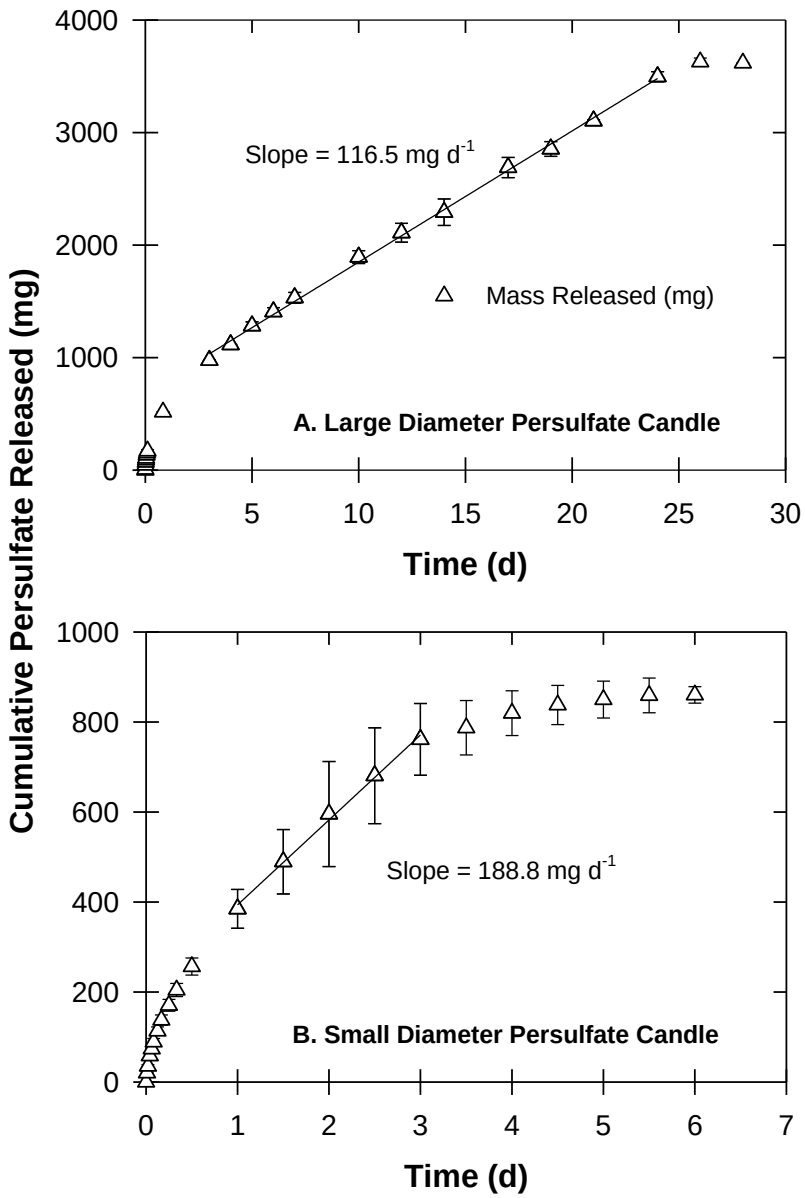

Figure 2 Chemical release characteristics from large and small diameter persulfate candles.

3.4 Comparison of iron sources as activators

Batch experiments confirmed that within the timeframe of the experiments, benzoic acid was not reactive to persulfate alone and activation to sulfate radicals was required to observed transformation. Liang and Lai (2008) and Liang and Guo (2010) showed that zerovalent iron was an effective activator for persulfate in treating TCE and naphthalene. Although the composition of analytical reagents is generally uniform between vendors, the chemical makeup of various cast irons can vary widely due to differences in manufacturing practices and feed stocks. By testing various iron sources as activators of persulfate, we found that degradation rates varied with particle size and source. A comparison of iron sources showed that the Aldrich iron powder resulted in the fastest removal of benzoic acid from solution followed by Peerless 50D USMD. One interesting observation was that all iron sources, except the Peerless 50D iron, showed visible signs of rusting or oxide formation on the iron surface during experimentation, while the 50D USMD iron did not. Based on these solution tests, ZVI candles were made with Aldrich iron powder and Peerless 50D and paired with persulfate candles for further testing.

A side by side comparison of the two ZVI candles immersed in a persulfate solution (spiked with benzoic acid) showed that the candle produced from Aldrich iron powder initially resulted in a more rapid loss of benzoic acid from solution than did the candle produced from Peerless 50D ZVI (Fig. 3a). However, after 7 d of aging, the removal of benzoic acid from solution was similar between iron sources (Fig. 3b). This similarity appears to be related to the iron release rates of the two ZVI candles. Because the Aldrich iron candle was made from a smaller grain size (i.e., powder) than the Peerless candle, initially iron released was much greater for the Aldrich candle during the first two days (Fig. 3c). After ~ 4 to 6 d, the release rates (i.e., slopes) were fairly similar between the two ZVI candles (Fig. 3c). Thus, when the candles were placed in fresh benzoic acid solution after 7 d, similar removal rates of benzoic acid were observed (Fig. 3b).

One practical question regarding using both persulfate and ZVI candles for treating BTEX compounds is what ratio of persulfate to iron candle should be used? To answer this, we paired a persulfate candle with different length ZVI candles. In this experiment, we sealed the ends of all candles so that chemical diffusion could only occur perpendicular to the axis. This was done because we envisioned stacking the persulfate and ZVI candles on top of each other to make a single candle for insertion into an aquifer rather than inserting two separate candles. Results showed that removal rates of benzoic acid (using fresh candles with sealed ends) were more constant or linear rather than the exponential decline observed in previous experiments. But as previously observed, the loss of benzoic acid mimicked the release rates of iron from the ZVI candles.

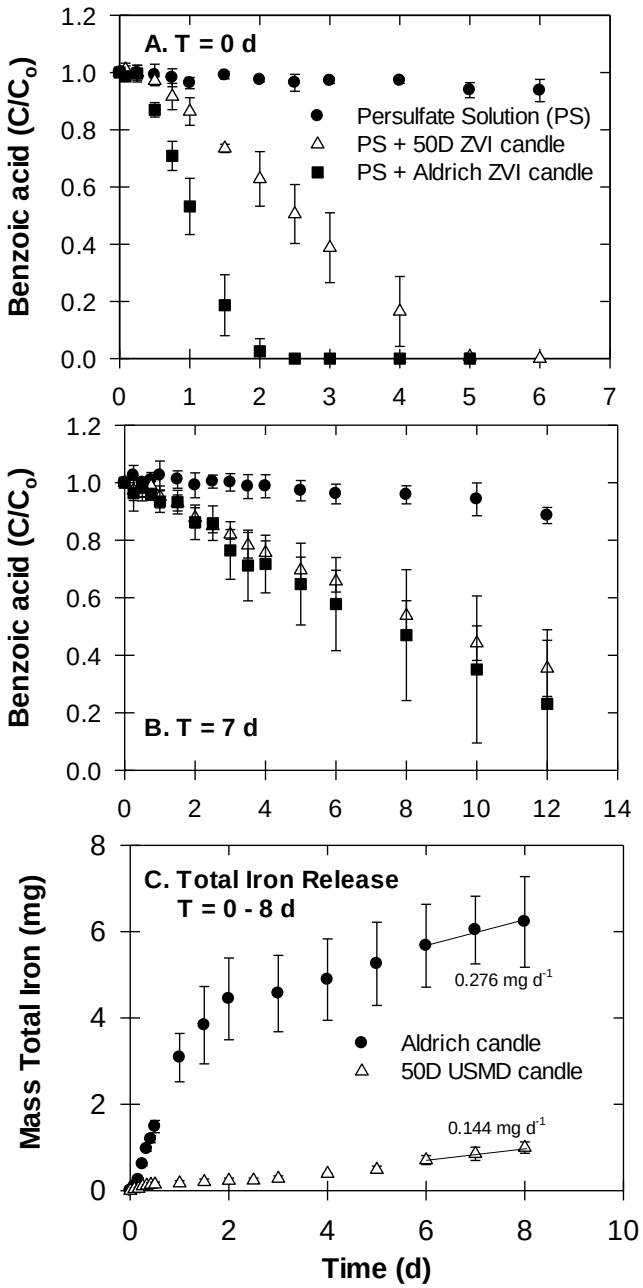

Figure 3 Changes in benzoic acid concentration (C_o = 0.10 mM) when treated with persulfate solution (10 mM) and two types of ZVI candles. (A) Results using fresh candles (T = 0 h); (B) Results using aged ZVI candles (T = 48 h); (C) Mass of iron released from ZVI candles. Note that Figures A, B, and C have different time scales

3.5 BTEX degradation by persulfate and ZVI candles

Treatment of three initial benzene concentrations (0.1, 0.5, 1.0 mM) with the small diameter persulfate and ZVI candles showed differences in removal kinetics. The loss of 0.1 mM benzene solution was exponential when treated with fresh candles and linear when treated with 48-h aged candles (Fig 4a, 4b). The greater the initial benzene concentration, the slower the reaction occurred. The effect of initial benzene concentrations on removal rates was more pronounced at T = 0 d (fresh candles) than at T = 48 h (aged candles). Again, benzene destruction rates were influenced by the dissolution rate of the candles. In Fig. 4c, we plotted persulfate released over 8 h for fresh persulfate candles versus candles that were exposed to the first benzene solution for 48 h. The persulfate release rates at T = 0 and 48 h mirrored the benzene removal kinetics observed (Fig. 4).

Treating a BTEX mixture with small diameter persulfate and ZVI candles verified that slow-release candles were able to effectively transform all BTEX compounds within 12 h (Fig. 5). We observed some differences in removal rates among the BTEX compounds with benzene being the slowest. Although the benzene concentration in the BTEX mixture was also 0.1 mM (as used in the previous experiment, Fig. 4), the collective concentration of the BTEX mixture was 0.46 mM and therefore the removal kinetics were similar to what we observed when we treated 0.5 mM benzene by itself (Fig. 4a, 4b).

Sra et al. (2008) studied persulfate treatment of BTEX, TMB, and naphthalene using different activation methods. They found BTEX responded well to nearly all activation methods, including alkaline, hydrogen peroxide, and chelated iron activation, as well as unactivated persulfate. However, TMB and naphthalene degradation were more extensive with hydrogen peroxide and alkaline activation (Petri et al., 2011). Crimi and Taylor (2007) also investigated the degradation of BTEX contaminants in porous media and noted that different activation methods yielded different chromatographs during sample analysis, potentially indicating that the organic intermediates and byproducts formed, as well as the reaction pathways may differ with activation methods. Using ^{14}C-labeled benzene, we were able to verify that CO_2 was major carbon-product produced from treatment with persulfate and ZVI candles.

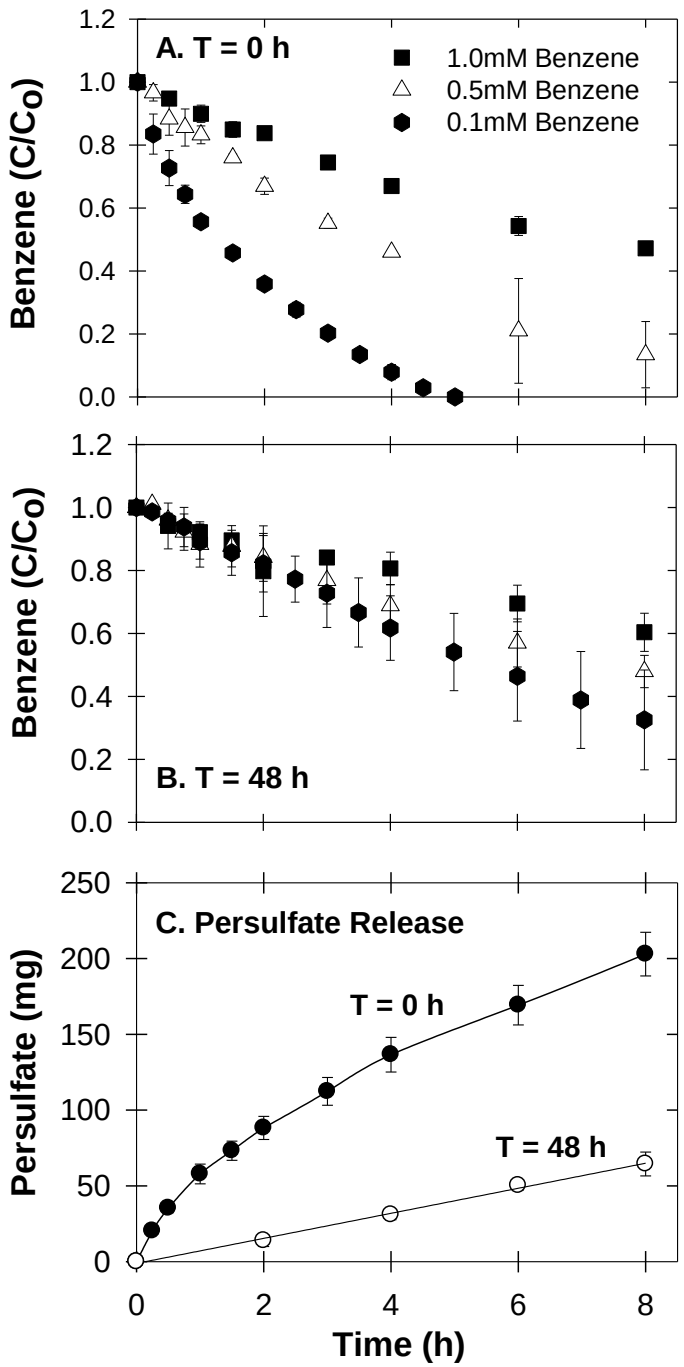

Figure 4 Changes in three initial benzene concentrations (C_o = 0.10 mM) following treatment with persulfate and ZVI candles using freshly prepared candles (A, T = 0 h) and candles that were aged for 48 h (B, T = 48 h). (C) Releases (0-8 h) from small persulfate candle at T = 0 and 48 h.

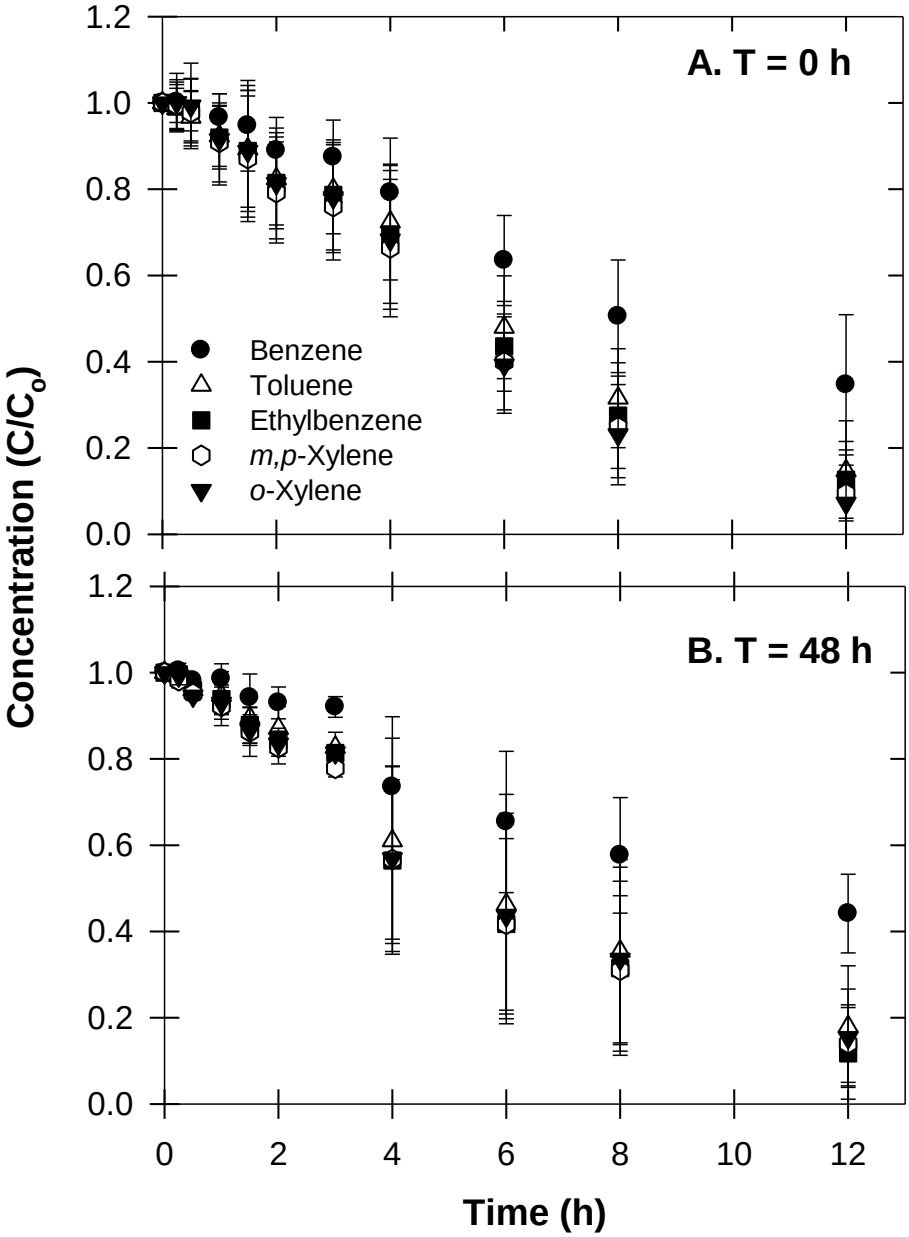

Figure 5 Treatment of mixed BTEX compounds (C_o = 0.10 mM benzene; 0.08 mM toluene, 0.07 mM Methylbenzene, 0.07 mM xylene) with persulfate and ZVI candles. Temporal changes using freshly prepared candles (A. T = 0 h) and candles that were aged for 48 h (B, T = 48 h).

3.6 Tank Experiments

To qualitatively visualize the radius of influence of the persulfate and ZVI candles, we flooded a 2-D tank with methylene blue and photographed temporal changes in color disappearance. Within 3 d, roughly half of the tank had the dye neutralized and by 7 d, ~ 85% of the tank had been treated. As observed by Christenson (2011) with their slow-release permanganate candles, the pattern of dye removal in our experiment indicates density driven flow likely occurred as the chemicals dissolved and diffused away from the central candle. This is based on the observance that the bottom of the tank was first affected and then the treatment zone vertically increased in a triangular pattern as the chemicals stacked up at the bottom of the tank (Fig. 6). Christenson (2011) was able to alter this diffusion pattern by adding pneumatic circulators to the bottom of their candles to induce upward flow paths below the candles and greatly accelerate the horizontal distribution of permanganate away from the slow-release permanganate candles. A similar approach could be used with the persulfate + ZVI candle system. Christenson (2011) initially developed slow-release permanganate candles to treat TCE in low permeable aquifers. He showed that in finer textured soils, density driven flow away from his permanganate candles was not observed. When we repeated his experiment with our persulfate + ZVI candles, we similarly observed an even spreading of oxidant away from the candles with no signs of density flow.

To quantify removal rates, we flooded the tanks with 1 mM benzoic acid and benzene in separate experiments. Using the spatial array of sampling ports, we sampled at 2 and 7 d and found that within 2 d, between 60 to 70% of the benzoic acid had been removed at the bottom the tank and by 7 d, ≥ 90% of the benzoic acid had been removed from most of the tank, except the top 2 cm (Fig. 7a). Results using benzene were similar where the majority of the sampling area had ≥ 98% of the benzene removed by 7 d (Fig. 7b).

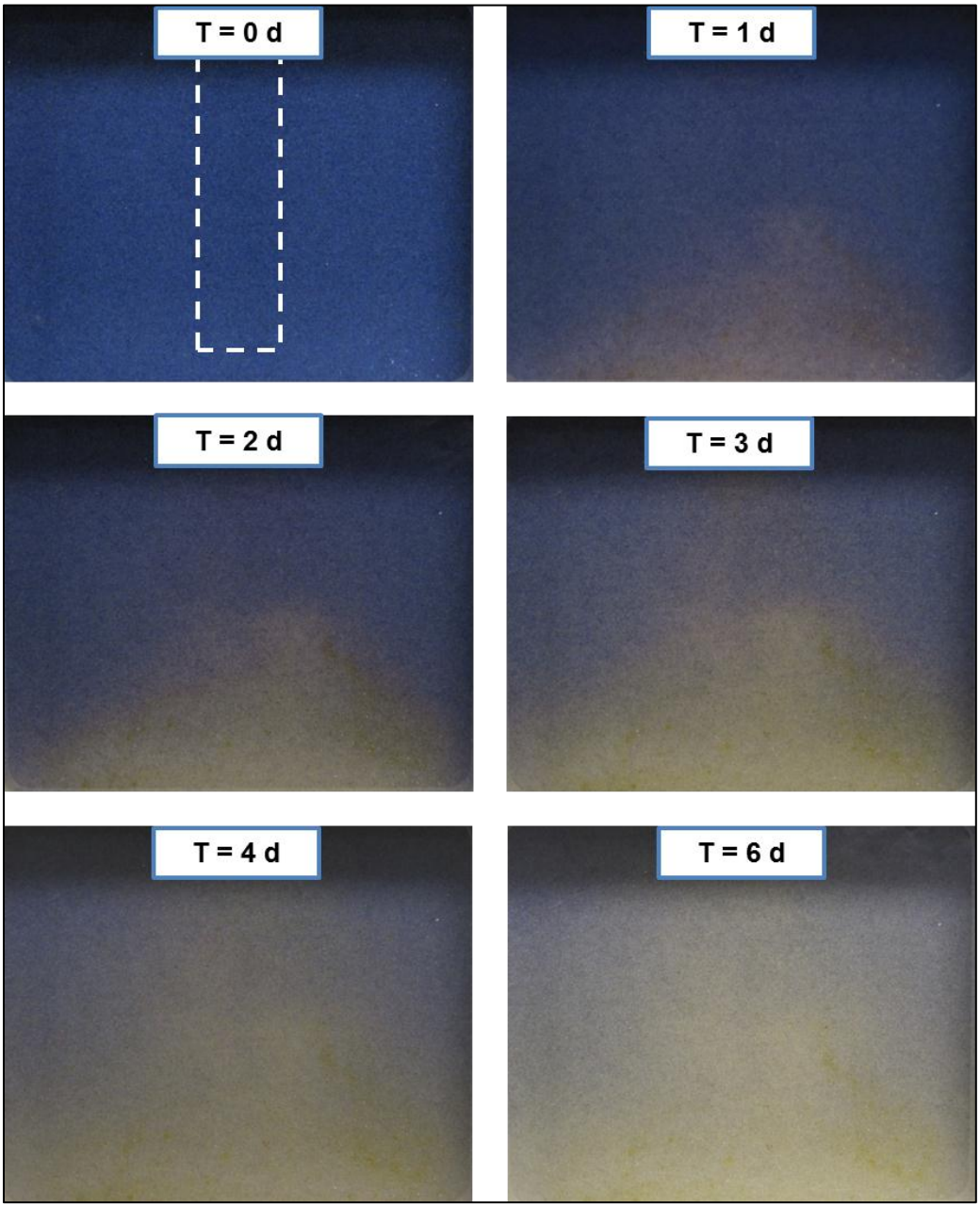

Figure 6 Temporal photographs of methylene blue neutralization caused by the dissolution and diffusion patterns of a central persulfate + ZVI candle.

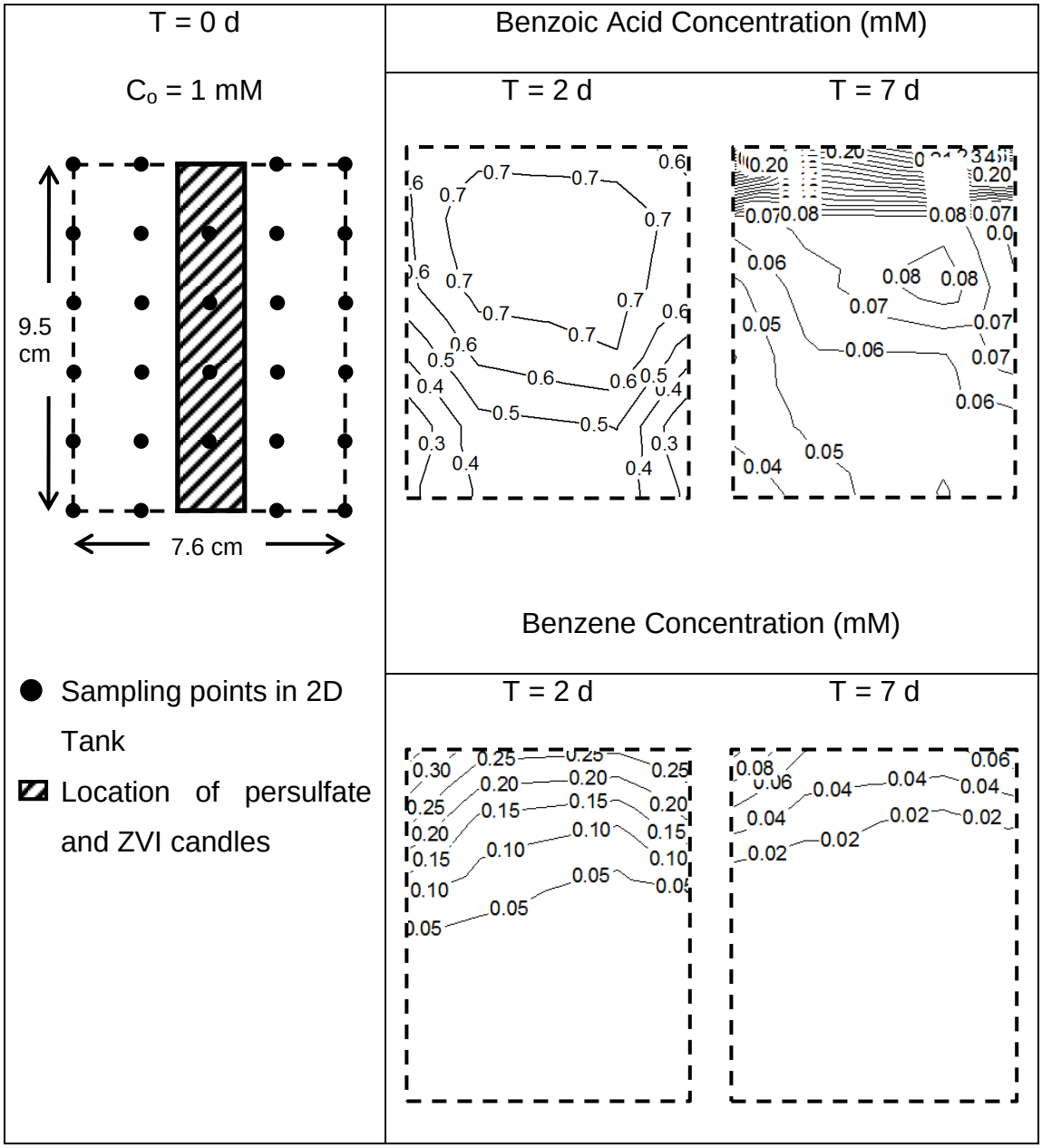

Figure 7 Changes in spatial benzoic acid concentrations (A) and benzene (B) in 2-D tank when treated with persulfate and ZVI candles at T= 2 d and T = 7 d.

4. Conclusions

Slow-release persulfate and zerovalent candles were developed and tested at the laboratory scale. Results show that the activated persulfate was able to transform all the BTEX compounds tested. Using ^{14}C-labled benzene, we confirmed that mineralization of benzene occurred in the presence of the persulfate + ZVI candle. These results support slow-release persulfate + ZVI candles as a technology for treating BTEX-contaminated groundwater. For future use, a prototype candle that could be used in the field was manufactured. Estimated material costs (US$) for this 5.1 cm dia by 91.4 cm length candle was $10.97.

References

Achugasim, D., Osuji, L.C., Ojinnaka, C.M., 2011. Use of activated persulfate in the removal of petroleum hydrocarbons from crude oil polluted soils. Research Journal of Chemical Sciences. 1, 57-67.

Christenson, M.D., 2011. Using Slow-release Permanganate to Remove TCE from a Low Permeable Aquifer at a Former Landfill. MS. Thesis. University of Nebraska-Lincoln: http://digitalcommons.unl.edu/natresdiss/29/

Crimi, M.L., Taylor, J., 2007. Experimental evaluation of catalyzed hydrogen peroxide and sodium persulfate for destruction of BTEX contaminants. Soil Sediment Contam. 16, 29-45.

Eberson, L., 1987. Electron Transfer Reactions in Organic Chemistry. Springer-Verlag, Berlin.

House, D.A., 1962. Kinetics and mechanism of oxidations by peroxydisulfate. Chem Rev. 62, 185-203.

Huang, K.C., Couttenye, R.A., Hoag, G.E., 2002. Kinetics of heat-assisted persulfate oxidation of methyl tert-butyl ether (MTBE). Chemosphere. 49, 413-420.

Huang, K.C., Zhao, Z., Hoag, G.E., Dahmani, A., Block, P.A., 2005. Degradation of volatile organic compounds with thermally activated persulfate oxidation. Chemosphere. 61, 551–560.

ITRC Interstate Technology & Regulatory Council 2005. Technical and Regulatory Guidance for In Situ Chemical Oxidation of Contaminated Soil and Groundwater, 2nd ed. Interstate Technology & Regulatory Council, Washington, DC.

Kambhu, A. 2011. Developing slow-release persulfate candles to treat BTEX-contaminated groundwater. University of Nebraska Master's thesis.

Kang, N., Hua, I., Rao, P.S., 2004. Production and characterization of encapsulated potassium permanganate for sustained release as an in situ oxidant. Ind. Eng. Chem. Res. 43, 5187-5193.

Killian, P.F., Bruell, C.J., Liang, C., Marley, M.C., 2007. Iron (II) activated persulfate oxidation of MGP contaminated soil. Soil Sediment Contam. 16, 523-537.

Krembs, F.J., Clayton, W.S., Marley, M.C., 2011. Evaluation of ISCO field applications and performance. In: Siegrist, R.L., Crimi, M., Simpkin, T.J. (Eds.) In Situ Chemical Oxidation for Groundwater Remediation. SERDP/ESTCP Environmental Remediation Technology Vol 3, Springer, New York. 319-353.

Latimer, W.M., 1952. Oxidation Potentials. 2nd ed. Prentice-Hall, Englewood Cliffs, NJ.

Lee, B.S., Kim, J.H., Lee, K.C., Kim, Y.B., Lee, E.S., Woo, N.C., Lee, M.K., 2009. Efficacy of controlled-release $KMnO_4$ (CRP) for controlling dissolved TCE plume in groundwater: A large flow-tank study. Chemosphere 74, 745-750.

Lee, E.S., Schwartz, F.W., 2007a. Characteristics and applications of controlled-release $KMnO_4$ for groundwater remediation. Chemosphere 66, 2058-2066.

Lee, E.S., Schwartz, F.W., 2007b. Characteristics and optimization of long-term controlled release system for groundwater remediation: A generalized modeling approach. Chemosphere. 69, 247-253.

Liang, C., Guo, Y.Y., 2010. Mass transfer and chemical oxidation of naphthalene particles with zerovalent iron activated persulfate. Environ. Sci. Technol. 44, 8203-8208.

Liang, C., Huang, C.F., Chen, Y.J., 2008. Potential for activated persulfate degradation of BTEX contamination. Water Res. 42, 4091-4100.

Liang, C., Lai, M.C., 2008. Trichloroethylene degradation by zero valent iron activated persulfate oxidation. Environ. Eng. Sci. 25, 1071-1077.

Liang, S.H., Kao, C.M., Kuo, Y.C., Chen, K.F., Yang, B.M., 2011. In situ oxidation of petroleum-hydrocarbon contaminated groundwater using passive ISCO system. Water Res. 45, 2496-2506.

Olson, R.V., 1965. Iron. In: Black, C.A. (ed.), Methods of Soil Analysis, Part II. Amer. Soc. Agronomy, Madison, Wisconsin, 9, 966-967.

Osgerby, I.T., 2006. ISCO technology overview: Do you really understand the chemistry? In: Calabrese, E.J., Kostecki, P.T., Dragun, J. (Eds.), Contaminated Soils, Sediments and Water, vol. 10 Successes and Challenges. Springer, New York, NY, USA, pp. 287-308.

Petri, B.G., Watts, R.J, Tsitonaki, A., Crimi, M., Thomson, N.R., Teel, A.L., 2011. Fundamentals of ISCO using persulfate. In: Siegrist, R.L., Crimi, M., Simpkin, T.J. (Eds.) In Situ Chemical Oxidation for Groundwater Remediation. SERDP/ESTCP Environmental Remediation Technology Vol 3, Springer, New York. 147-191.

Ross, C., Murdoch, L.C., Freedman, D.L., Siegrist, R.L., 2005. Characteristics of potassium permanganate encapsulated in polymer. J. Environ. Eng. 131, 1203-1211.

Sra, K., Thomson, N.R., Barker, J.F., 2008. In situ chemical oxidation of gasoline compounds using persulfate, Proceedings of the Petroleum Hydrocarbons and Organic Chemicals in Ground Water Conference, Houston, TX, Nov 3–5. pp. 76.

Swearingen, J., Swearingen, L., 2008. Patent No. US 7, 431,849 B1, Encapsulated Reactant and Process. United States of America.

USEPA, 2011. FY 2010 Annual Report On The Underground Storage Tank Program. Available at http://www.epa.gov/oust/pubs/fy10_annual_ust_report_3-11.pdf (verified Jan. 2012). U.S. Environmental Protection Agency.

A Cost Effective Fixed Film Atrazine Treatment Utilizing Nitrate as a Nutrient

Basic Information

Title:	A Cost Effective Fixed Film Atrazine Treatment Utilizing Nitrate as a Nutrient
Project Number:	2011NE218B
Start Date:	3/1/2011
End Date:	5/31/2012
Funding Source:	104B
Congressional District:	1
Research Category:	Water Quality
Focus Category:	Water Quality, Treatment, Nitrate Contamination
Descriptors:	
Principal Investigators:	Mohamed Dahab, Ahmed Hosni

Publications

There are no publications.

Principal investigator is currently out of the country and unable to provide an annual report at this time. Project will be completed May 31, 2012 and a final report will be given in June2013.

High-resolution imaging of the Platte River streambed using combined electromagnetic induction and hydraulic parameter estimation techniques

Basic Information

Title:	High-resolution imaging of the Platte River streambed using combined electromagnetic induction and hydraulic parameter estimation techniques
Project Number:	2011NE220B
Start Date:	3/1/2011
End Date:	9/30/2012
Funding Source:	104B
Congressional District:	1
Research Category:	Ground-water Flow and Transport
Focus Category:	Groundwater, Surface Water, Methods
Descriptors:	
Principal Investigators:	Jesse Thomas Korus, Xun-Hong Chen

Publications

There are no publications.

High-resolution imaging of the Platte River streambed using combined electromagnetic induction and hydraulic parameter estimation techniques

Jesse T. Korus and X. Hong Chen, School of Natural Resources, UNL

Statement of Problem

The exchange of water between aquifers and streams is a fundamental process linked to physical, chemical, and biologic conditions of riparian systems. This flow creates a shallow, narrow zone below the streambed with special significance for geochemical processes, water quality, aquatic habitat and biologic diversity, as well as water supply for human uses (Winter et. al, 1998). Many current water issues in Nebraska focus on processes in this zone. The vertical hydraulic conductivity (K_v) of streambed sediments is a key parameter controlling flows between aquifers and streams. Uncertainty and error associated with this parameter may result in poor management plans and stream/wetland restoration designs which could significantly impact environmental, agricultural, and socio-economic systems. Characterizing the spatial variability of streambed conductivity is therefore a basic research need in Nebraska.

Chen (2005, 2010) and Chen et al. (2008) clearly demonstrate cross-channel, downstream, and depth-dependent variation of K_v. This heterogeneity largely reflects lateral and vertical variations in the thickness of silt and clay layers and porosity variation with depth as opposed to salinity or temperature contrasts (Chen, 2010). Chen (2010) demonstrated an inverse correlation between electrical conductivity (EC) and K_v. This relationship suggests that EC contrasts obtained from geophysical methods can be exploited to infer gross 3-dimensionality of streambed K_v and perhaps to relate hydrologic and geophysical parameters.

This proposal focuses on using ground-based electromagnetic induction (EMI) because it measures subsurface electrical conductivity (EC) as a function of water content, porosity, salinity, temperature, soil texture, and mineralogy. These methods can be applied on the ground and through the air, allowing seamless 3-D integration of multi-scale datasets to create a high-resolution picture of the subsurface. EMI methods have furthermore proven useful for shallow subsurface characterization of stream channels (Crook et al., 2008; Sheets and Dumouchelle, 2009; Teeple et al., 2009).

Research Objectives

The goal of this project is to characterize the spatial variability of geophysical properties in relation to hydraulic properties in stream sediments. Our primary objectives are to 1) assemble existing and collect new geophysical and hydraulic data from multiple, co-located profiles at a stream site, and 2) assimilate data and generate multiple visualizations of apparent EC and streambed K_v. The work completed thus far has focused on assessing the effects of

traverse direction during data collection on the EM results as well as finding the optimal EM signal frequency for mapping streambed K_v.

Methods

We used the EMP-400 field portable, multi-frequency EMI tool manufactured by Geophysical Survey Systems, Inc. of Salem, NH. This tool offers portability, a built-in GPS, multi-frequency operation between 1 and 16 kHz, and up to 3 frequencies recordable at one time, thus giving three effective depths of penetration. The maximum depth of penetration is about 6 m. The primary user attended a training course on the use of this tool at the manufacturer's headquarters in Salem, NH. Data was collected on Clear Creek, a small tributary of the Platte River near Columbus, Nebraska. A grid survey was conducted over 100 x 60 ft. grid on a point bar for which K_v estimates have been derived. Data was collected at 15, 8, and 3kHz in both X-

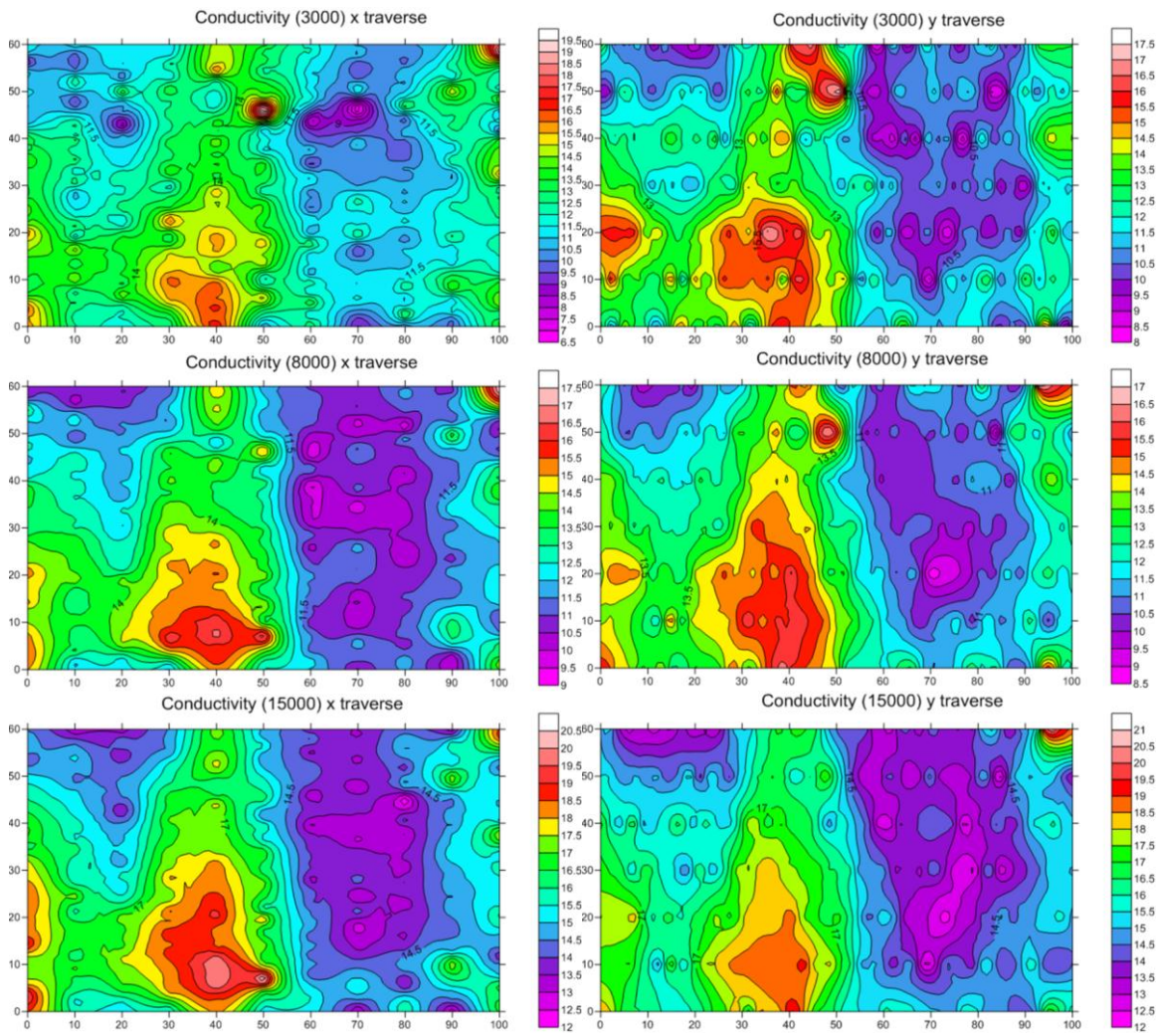

Figure 1. Comparison of EM-derived conductivity fields at 3, 8, and 15 kHz collected in x and y traverse directions.

and Y-oriented traverses. Line spacing was 10 ft. Data was downloaded, quality checked, and a spatial interpolation was performed using the Surfer® software program. A total of six grids were created and compared to check for anomalies and comparability (Fig. 1). A second survey was collected from a linear traverse along the length of the channel. The 15kHz, Y-traverse grid and the in-channel EM measurements were compared to maps of K_v for the same area (Fig. 2).

Initial findings

Conductivity fields collected at various frequencies and along different traverse directions are generally comparable (Fig. 1). Three main zones can be identified in all grids: a low conductivity zone right (east) of center, a high conductivity zone left (west of center), and a low conductivity zone in the upper left (northwest). The 3 kHz signal produced higher variability and larger range of values than the 8 and 15 kHz signals. The three conductivity zones were less well-defined in the 3 kHz grid than in the 8 or 15 kHz grids. Traverse direction has only a minor effect on the shape of the conductivity zones and can be considered negligible.

The north-south orientation of the conductivity zones corresponds to the direction of channel-bend and point-bar migration through time, as manifest in historical photographs dating to the 1940's (Fig. 2a). The relationship between K_v and conductivity, however, is not clearly inverse as was predicted. The K_v field, as determined by in-situ measurement just below the water table, suggests some zonation on the northern point bar that can be compared to the

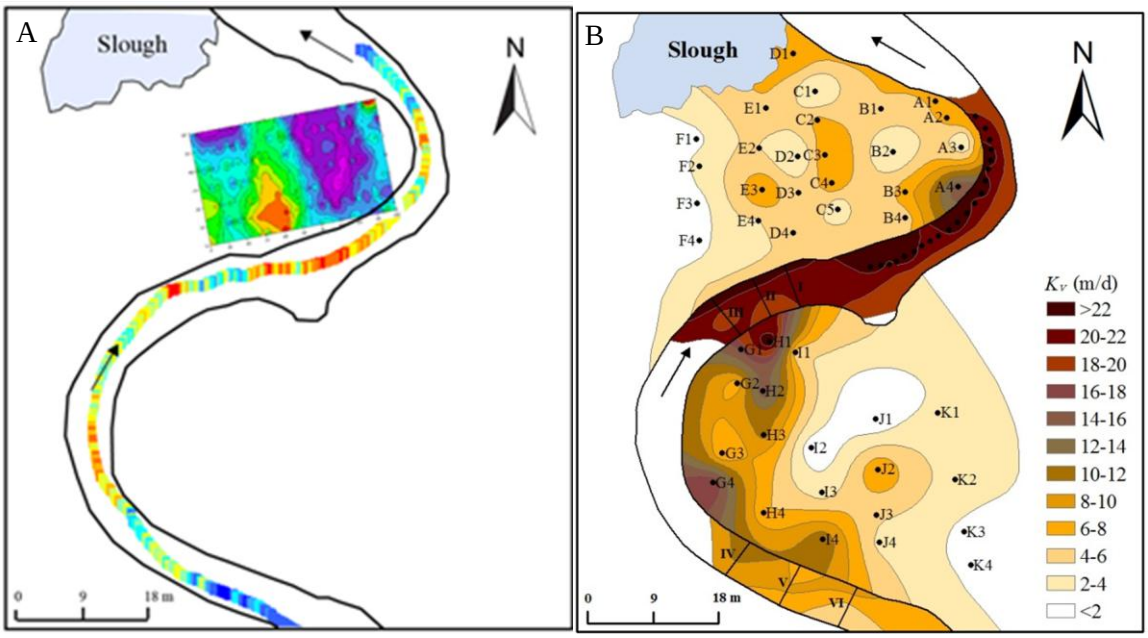

Figure 2. (A) EM grid and in-stream conductivity measurments. Warm colors are higher values and cool colors are lower values. (B) Vertical hydraulic conductivity field from in-situ measurement at the water table or in the streambed.

electrical conductivity field (Fig. 2b). In general, zones of high conductivity correspond to zones of higher K_v, but this relationship can only be established loosely. A zone of higher K_v exists near the center of the point bar at C2, C3, and C4, which corresponds to the area of high conductivity. This zone is surrounded by zones of slightly lower K_v at B1, B2, D2, and D3, which generally correspond to zones of lower conductivity. The zone of highest conductivity, however, corresponds to an area low K_v at C5, and the area of lowest conductivity corresponds to an area of high K_v at B3.

Comparison of the in-stream K_v and conductivity transect shows a good correspondence between the area of high conductivities and the area of high K_v near the northern meander bend. The southern meander bend is characterized by low conductivity and low $K_{v.}$

Overall, the general correspondence between K_v and conductivity is promising, but the lack of a well-defined inverse relationship as predicted suggests that additional field work is needed. Future efforts will aim to 1) collect data over a larger area, 2) resolve differences in sample density, and 3) resolve differences in the degree of vertical averaging. Additional data may need to be collected to investigate the effects of other physical parameters on conductivity, such as organic content, clay content, soil moisture, and water chemistry. Furthermore, data will need to be collected at several different sites to examine the effects of local geology. This study will continue through September, 2012.

References

Chen, X.H., 2005. Statistical and geostatistical features of streambed hydraulic conductivities in the Platte River, Nebraska. Environmental Geology 48: 693-701.

Chen, X.H., 2010. Depth-dependent hydrologic conductivity distribution patterns of a streambed. Hydrological Processes, DOI: 10.1002/hyp.7844 (online for early review).

Chen, X. H., M. Burbach, and C. Cheng, 2008. Electrical and hydraulic vertical variability in channel sediments and its effects on streamflow depletion due to groundwater extraction. Journal of Hydrology 352: 250-266.

Crook, N., A. Binley, R. Knight, D. A. Robinson, J. Zarnetske, and R. Haggerty (2008), Electrical resistivity imaging of the architecture of substream sediments, Water Resources Research 44, W00D13, doi:10.1029/2008WR006968

Sheets, R.A., and Dumouchelle, D.H., 2009, Geophysical investigation along the Great Miami River from New Miami to Charles M. Bolton well field, Cincinnati, Ohio: U.S. Geological Survey Open-File Report 2009–1025, 21 p.

Teeple, A.P., Vrabel, Joseph, Kress, W.H., and Cannia, J.C., 2009, Apparent resistivity and estimated interaction potential of surface water and groundwater along selected canals and streams in the Elkhorn-Loup Model study area, north-central Nebraska, 2006–07: U.S. Geological Survey Scientific Investigations Report 2009–5171, 66 p.

USGS Award no. G12AP20022 Evaluation of FEW NET Satellite Products for Drought Monitoring in Food Insecure Areas of Ethiopia

Basic Information

Title:	USGS Award no. G12AP20022 Evaluation of FEW NET Satellite Products for Drought Monitoring in Food Insecure Areas of Ethiopia
Project Number:	2012NE223S
Start Date:	11/21/2011
End Date:	2/20/2012
Funding Source:	Supplemental
Congressional District:	1
Research Category:	Climate and Hydrologic Processes
Focus Category:	Drought, Management and Planning, Agriculture
Descriptors:	
Principal Investigators:	Bruce Irvin Dvorak, Tsegaye Tadesse

Publications

There are no publications.

Evaluation of ETa Products for Drought Monitoring in Ethiopia

Tsegaye Tadesse
National Drought Mitigation Center (NDMC), School of Natural Resources, University of Nebraska-Lincoln,
e-mail ttadesse2@unl.edu

Gabriel Senay
USGS Earth Resources Observation and Science (EROS) Center, 47914 252nd Street, Sioux Falls, SD 57198
e-mail: senay@usgs.gov

Getachew Berhan Demisse
Addis Ababa University, P.O.Box 1176, Addis Ababa, Ethiopia,
e-mail: getachewb1@yahoo.com

ABSTRACT

Actual evapotranspiration (ETa) anomaly is currently one of the tools for African agricultural drought monitoring and food security status assessment. The objectives of this research were to: 1) develop an evaluation method specifically applicable for drought and food security models using crop yield and climate data, and 2) evaluate the ETa anomaly products using zonal (district level) crop yield and meteorological rainfall data. The yield data which was obtained from Central Statistical Agency of Ethiopia (CSA) was used for ETa model evaluation. The study showed that there is a trend of yield data increase almost for all crop yields assessed. The crop yield was detrended and the relationships between ETa (%) and detrended crop yield (Qt/ha) were assessed. For the climatic evaluation parameter, standardized precipitation index (SPI) was used. The spatio-temporal correlation analysis between ETa and cereals yield data showed that from the assessed 41 zones, the R^2 ranged from 0.01 to 0.8. The R^2 values for the spatio-temporal correlation analysis between ETa and climatic SPI data also ranged from 0.13 to 0.8. The overall evaluation result showed that there are positive relationships between average ETa (%) and yield data. It was observed that the increase or decrease of ETa percentage value can indicate the yield increase and deficit in the studied districts for Meher growing season. It was also found that ETa can be used for drought monitoring with future calibrations to much standard drought monitoring index SPI.

Key Words: Crop Yield; Drought Monitoring; ETa; Model Evaluation; SPI

Contents

ABSTRACT 1

1. INTRODUCTION 3

2. MATERIALS AND METHODS 4

2.1. Crop Yield Data 4

2.2. Using Crop Yield Data for Model Evaluation 4

2.3. Model Evaluation Study Sites Selection 6

2.4 ETa Model Description 7

2.5 Zonal Statistics Extraction for ETa 9

2.6 Spatial Regression Analysis of ETa and Yield Data 9

2.7. Standard Precipitation Index (SPI) for ETa Evaluation 10

3. RESULTS AND DISCUSSIONS 14

3.1 Preliminary ETa versus Cereal Yield Data Exploratory Analysis 14

3.2 Descriptive Statistics for ETa 15

3.3 Descriptive Statistics for Yield data 16

3.4 Spatial Regression Analysis of ETa and Yield Data 22

3.5. Evaluation of ETa using Climate Data 24

4. Conclusions 27

References 29

Appendix 1: List of Zones selected for ETa evaluation 30

Appendix 2: Average ETa zonal statistical analysis output for the year 2000 to 2010. 31

Appendix 3: Average Zonal Cereal Yield for the year 2000 to 2010. 32

Appendix 4: Average Zonal Teff Yield for the year 2000 to 2010. 34

Appendix 5: Average Zonal Barley Yield for the year 2000 to 2010. 36

Appendix 6: Average Zonal Wheat Yield for the year 2000 to 2010. 38

Appendix 7: Average Zonal Maize Yield for the year 2000 to 2010. 40

Appendix 8: Average Zonal Sorghum Yield for the year 2000 to 2010. 42

Evaluation of ETa Products for Drought Monitoring in Ethiopia

1. INTRODUCTION

Actual evapotranspiration (ETa) anomaly is currently one of the tool for African agricultural drought monitoring and food security status assessment (FEWSNET, 2011). This tool was developed based on the principles of surface energy balance model (Senay et al., 2011) of the environment.

In the environmental system, evapotranspiration (ET) is an important and primary component of the hydrologic budget because it expresses the exchange of mass and energy between the soil–water–vegetation system and the atmosphere. Prevailing weather conditions influence potential and reference ET through forcing variables such as radiation, temperature, wind, and relative humidity (Senay et al., 2011). ET comprised of two sub-processes: evaporation and transpiration. Evaporation occurs on the surfaces of open water bodies, vegetation, and bare ground. Transpiration involves the withdrawal and transport of water from the soil/aquifer system through plant roots, stems, and eventually an evaporation process from the interior of the plant leaves into the atmosphere (FEWSNET, 2011; Senay et al., 2011; Senay et al., 2007).

FEWSNET (2011) described that knowledge of the rate and amount of ET for a given location is an essential component in the design, development and monitoring of agricultural and environmental systems. The ETa anomaly for a given period expresses the surplus or deficit of ET compared to the same period historically. During the non-vegetative stage (for crop or rangeland areas), ETa anomalies are an expression of surplus or deficit in soil moisture. During the growing season, ETa anomalies express surplus or deficit of crop of water use, which is directly related to crop condition and biomass. Thus, positive ETa anomalies indicate greater-than-normal biomass, and negative ETa anomalies indicate less-than-normal biomass as compared to the median value, for the same period. Based on this assumption, ETa products are provided for 8-day cumulative and monthly ET anomalies for Africa for agricultural drought monitoring and food security status assessment (FEWSNET, 2011).

Drought monitoring is one of the most important aspects of drought risk management (Panu and Sharmat, 2002). For this purpose different methods and approaches had been developed in the past. Bastiaanssen et al.(2005) and Senay et al. (2011) indicated that ETa's dependence on land cover and soil moisture, and its direct relationship with carbon dioxide assimilation in plants, makes it an important variable to monitor and estimate crop yield and biomass for decision makers interested in food security.

Despite the general consensus in using ETa anomaly for drought monitoring and food security assessment, a comprehensive model evaluation was not done. Moreover, currently there are limited methodologies for evaluating drought and food security models. Taking these gaps in to account, this research has two major objectives: 1) develop an evaluation method specifically applicable for drought and food security models using crop yield and

climate data, and 2) to evaluate the ETa anomaly products using zonal (district level) crop yield and meteorological rainfall data.

In this article, section two presents details on crop yield data used for evaluation, data preprocessing, study site selection, ETa model description and zonal statistics extraction process. Section three presents the results and section four the conclusion of the research.

2. MATERIALS AND METHODS

There is no clearly defined model evaluation procedure which can be followed for our current research. Therefore, the method in this section develops a simplified and practical model evaluation approach for ETa and other drought and food security monitoring related models. For this model evaluation crop yield and rainfall data were used. This is due to the fact that crop yield is very important for deciding food assurance of a given region.

2.1. Crop Yield Data

The evaluation of the ETa product was done using the Meher season yield data obtained from Statistical Authority (CSA). The Meher season yield accounts for 90-95% of the annual crop production of Ethiopia (FEWSNET, 2003). The yield data anomaly observed in this season is crucial for characterizing the food security status of Ethiopia.

Crop yield data was obtained from CSA yearly report (from 2000 to 2010) (CSA, 2011) at zonal administrative level. The yield data was obtained using standard statistical data collection and analysis by CSA of Ethiopia.

According to CSA (2011), in order to select the sample a stratified two-stage cluster sample design was used. Enumeration areas were taken to be the primary sampling units and the secondary sampling units were agricultural households. An enumeration area in the rural parts of Ethiopia is a locality that is, in most of the cases less than, and only in some cases equal to a farmers' association in geographical area and usually consists of 150-200 households. A household may be either a one person household or a multi-person household who make provisions for his/their own living. Enumeration areas from each stratum were selected systematically using probability proportional to size sampling technique; size being number of agricultural households. The data collected using the standard CSA procedures were entered into the computers using the entry module of the CSPRO (Census and Survey Processing System) software, which is a software package developed by the United States Bureau of the Census. In the final report production of the tables, in addition to the CSPRO software, standard statistical estimation procedures were followed for each selected stratified samples.

2.2. Using Crop Yield Data for Model Evaluation

The yield data which was obtained from CSA was assessed for its suitability for ETa model evaluation. It was observed that there is a trend of yield data increase almost for all crop yields assessed (Figure 8). During the analysis

it was realized that the crop yield temporal increase due to farm management practice has to be deterended in order to use the data for model evaluation.

FAO (1999) described that the factors which affect the variability of agricultural yields can be roughly grouped in three categories according to their variations over time. The first factor is growing smoothly, such as more or less regular technology and management trends (i.e. mechanization, varieties, irrigation, and the farmers know-how), but growing more abruptly for several years in succession in the case of innovations. A typical innovation would be the new introduction of irrigation. The second factor is discontinuous, like extreme factors of various origins and policy decisions which affect management (e.g, farmers may decide to use less fertilizer if it is no longer subsidized) or infrastructure, such as the construction of a road which provides access to new markets. The third factor is pseudo-cyclic, such as weather. The theoretical illustrations of these factors that affect the variability of agricultural yields are presented on Figure 1. The current research for ETa model evaluation is focused on the effect of weather on crop yield data.

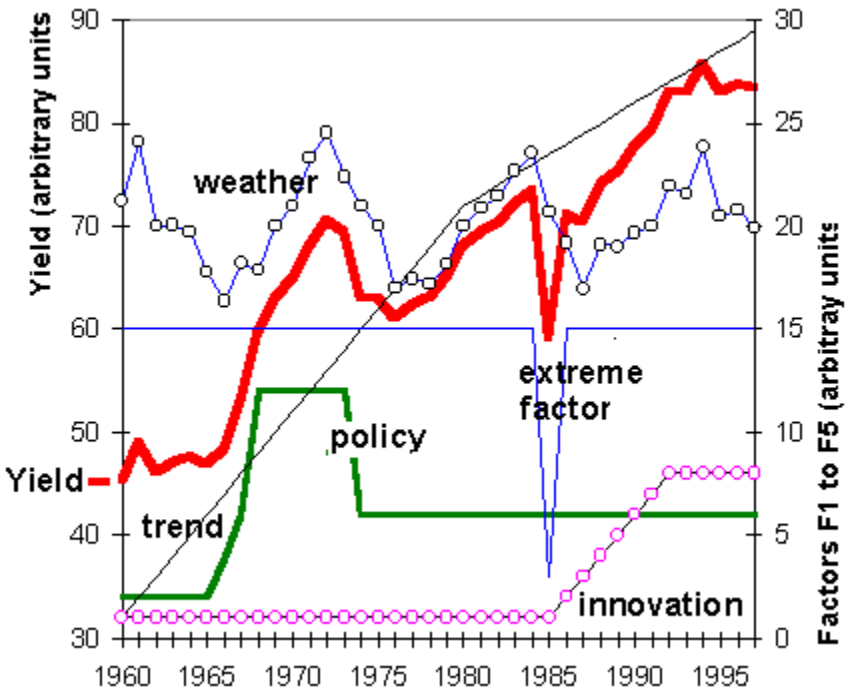

Figure 1: Factors affecting agricultural yields (represented by a heavy red line: technology and management trends, innovation, policy, extreme factors and weather) (adopted from FAO (1999)).

The crop yield data, which was obtained from CSA (2011) showed the pattern described by FAO (1999), and it was decided that before using the data, the trend has to be removed. The purpose of detrending the crop yield data here is to get a good estimate of yields that can be used for ETa model evaluation. FAO (1999) also recommended that "establishing a good series of yield data requires the application of some detrending statistics to get the so-called detrended yield. The hypothesis here is that "an upward (downward is not very likely) trend in yields caused by the factors mentioned above is eliminated from the statistics". After deternding, the data is the relative detrended yield,

which is the departure of yield values from the time-trend, assumed to take into account the technology and management component of yield (FAO, 1999).

The detrending of yield data was done in two steps. The first step was fitting of a smooth curve through the yield statistics. Such kind of fitting a function is described by Wu et al. (2007), where the detrending is the operation of removing the trend. The second step was calculating the actual detrended yield. Matlab Software (MathWorks, 2009) was used for this deterending analysis.

Detrending in this research is the operation of removing the crop yield increasing trend from the year 2000 to 2010 and after detrending, what remains is the variability of the residue of the crop yield data. It was believed that determining trend and implementing detrending operations are important steps in our data analysis. This is because the detrended crop yield data define a more meaningful variability of the yield variation caused by weather variability through the study periods. It was also assumed that ETa model captured the weather variability and it possible to correlate the two attributes using regression analysis.

2.3. Model Evaluation Study Sites Selection

After standard statistical data processing, CSA (2011) produced the yield data at Zonal (district) administrative level. The Zonal administrative level in Ethiopia is next to the regional administrative level. Currently there are 72 Zones in the country. From the 72 zones, 41 of them were selected for the current study (Figure 2). The zones were selected based on two criteria: 1) availability of yield data in the year 2000 to 2010 for Meher season, and 2) the Zones are in Meher crop growing district where annual cereal crops are grown. The lists of the selected Zones are attached at Appendix 1.

Over the selected 41 Zones, the cereals yield data was considered for ETa evaluation. According to CSA (2011), cereals are the major food crops both in terms of the area they are planted to and volume of production obtained in the selected Zones. Cereals are also produced in larger volume compared with other crops because they are the principal staple crops in these Zones.

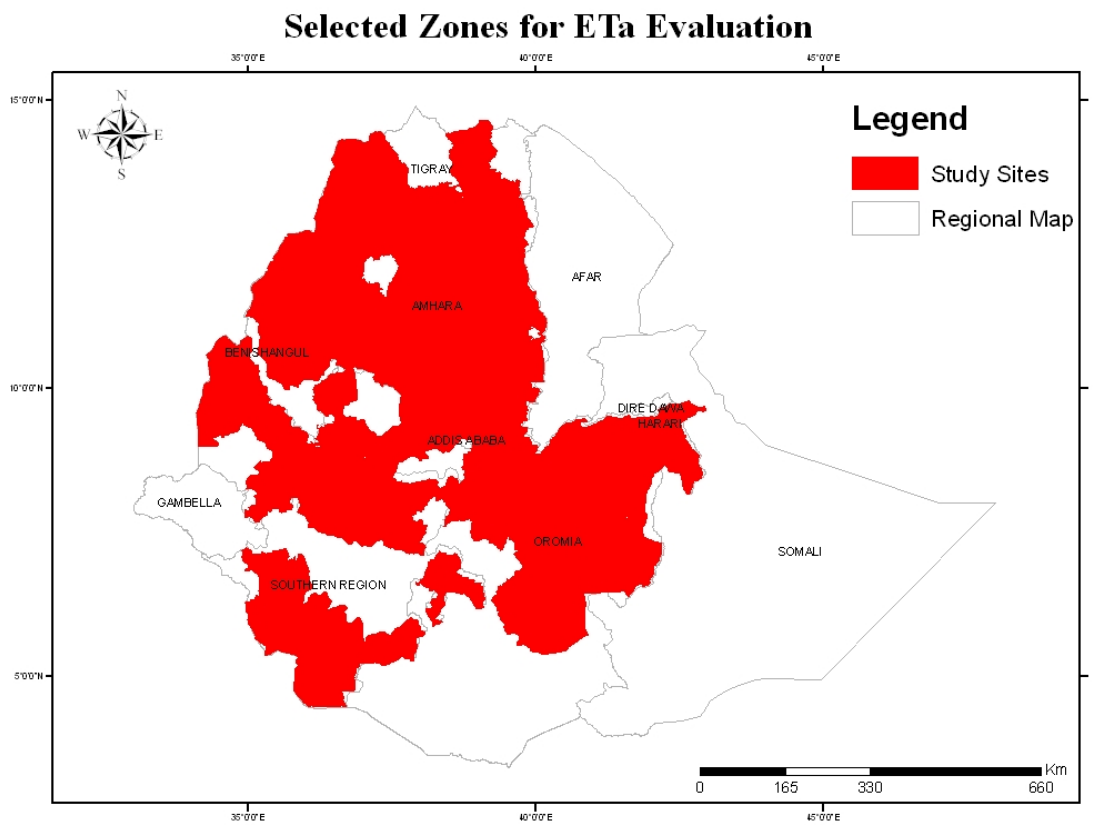

Figure 2: Spatial distribution of selected Zones (districts) on the regional map of Ethiopia (in red color).

2.4 ETa Model Description

In this subsection, the basic principle of ETa estimation from surface energy balance is presented. The overview of this basic principle is presented in order to understand the different data input of ETa and how these data combined using energy balance model, which helps us to compare later on the ETa anomaly with crop yield anomaly.

Senay et al. (2011) described that the approach of most energy balance models requires solving the energy balance as presented on equation 1. At the land surface, where the latent heat flux, comparable to ETa, is calculated as the residual of the difference between the net radiation to the surface and losses due to the sensible heat flux (energy used to heat the air) and ground heat flux (energy stored in the surface).

$$LE = Rn - G - H \qquad (1)$$

where LE = latent heat flux (energy consumed by evapotranspiration) (W/m^2); Rn = net radiation at the surface (W/m^2); G = ground heat flux (W/m^2); H = sensible heat flux (W/m^2).

The practical and simplified application of surface energy balance model was developed by Senay et al.(2007). The concept of the simplified surface energy balance (SSEB) was recently further explained by (Senay et al., 2011). They indicated that "SSEB is the joint use of reference ET and land surface temperature data. The surface energy balance is first solved for a reference crop condition (assuming full vegetation cover and unlimited water supply) using the standardized Penman–Monteith equation. ET fractions (ETf) account for differences in water availability in the landscape; and are used to adjust the reference ET (ETo) based on the LST of the pixel as presented on equation 2 for ETf (Senay et al., 2011). In the SSEB model formulation, ET fractions are calculated from the LST data sets based on the assumptions that hot pixels experience little or no ET, cold pixels represent maximum ET and with the simplified assumption, that ET can be scaled between these values in proportion to LST".

$$ETf = \frac{TH - Tx}{TH - TC} \qquad (2)$$

where TH is the average of the representative 3 hot pixels selected for hot bare areas.; TC is the average of representative 3 cold pixels selected from the irrigated fields; and Tx is the LST value for any given pixel in the image.

Senay et al. (2011) further described that the basic approach of calculating ETa involves only two steps: ETa is simply a product of the ET fraction (ETf) and ETo via Equations (3) and (4).

$$ETa = ETf \times ETm \qquad (3)$$

where ETa is actual ET, ETf is ET fraction, and ETm is maximum ET for the region. When grass reference ETo is calculated from weather data, ETm is estimated as:

$$ETm = \alpha \times ETo \qquad (4)$$

where the multiplier α is recommended to be 1.2 to estimate ET for tall, full cover crops such as alfalfa, corn and wheat.

FEWSNET (2011) described that the SSEB combines ET fractions generated from remotely sensed MODIS thermal imagery, acquired every 8 days, with reference ET using a thermal index approach. Using this dataset, ETa anomaly products (current vs. 2000 – 2010) are produced. The anomalies are the ratio of ETa and the corresponding median ETa, expressed as a percent value as presented on equation 5.

$$ETa(\%) = \frac{ETac}{ETam} \times 100 \qquad (5)$$

where $ETa(\%)$ is anomaly percentage value, $ETac$ is current ETa value and $ETam$ is median values of ETa from 2000 to 2010.

This ETa anomaly for a given period expresses the surplus or deficit ET compared to the same period historically. During the non-vegetative stage (for crop or rangeland areas), ETa anomalies are an expression of surplus or deficit in soil moisture. During the growing season, ETa anomalies express surplus or deficit crop water use, which is directly related to crop condition and biomass. Thus, positive ETa anomalies indicate greater-than-normal biomass (compared to the median value, for the same period), and negative ETa anomalies indicate less-than-normal biomass (compared to the median value, for the same period). The detailed methods used for deriving the ETa product is presented in Senay et al. (2007), Senay et al. (2011) and FEWSNET (2011).

2.5 Zonal Statistics Extraction for ETa

The ETa data was obtained from USGS for ten years (from 2000 to 2010). These raw data was extracted at zonal administrative level using zonal statistics tool of ArcGIS 10.0 (ESRI, 2011). This tool generated majority, maximum, mean, median, minimum, minority, range, standard deviation of the population, sum and variety of the ETa pixel values for each administrative districts. In this output the majority is the most frequently and minority is the least frequently occurring ETa values in each zone. The variety attribute is the number of unique ETa values observed in each zone.

For this model evaluation research we used the mean of the zonal statistics. The overall data extraction process is presented on Figure 3. The 10 years ETa data extracted using zonal statistical tool of ArcGIS 10 (ESRI, 2011) from 2000 to 2010 is also presented in Appendix 2.

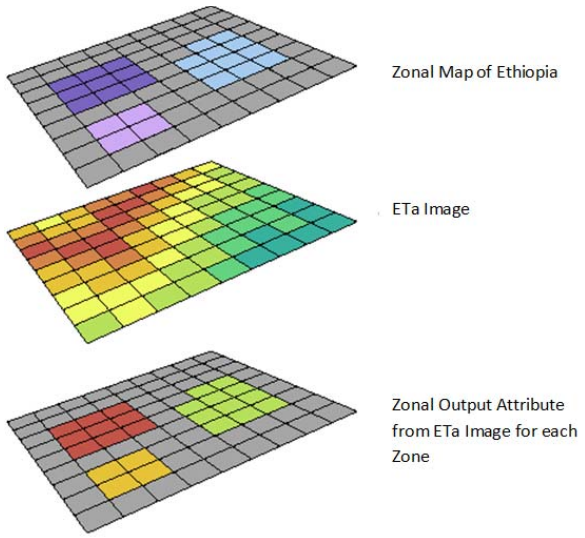

Figure 3: Data extraction for ETa zonal statistics (adapted from ESRI (2011)).

2.6 Spatial Regression Analysis of ETa and Yield Data

Both ETa and yield data have spatial dimensions. The spatial analysis of the relationship between ETa and yield data was done using ordinary least square (OLS) and geographically weighted regression (GWR).

OLS is the best known of all regression techniques, and it is also the proper starting point for all spatial regression analyses (Fotheringham et al., 1998). OLS provides a global model of the relationships between ETa and yield. The global relationship between ETa and yield was computed using equation 6 (Fotheringham et al., 1998). Fotheringham et al. (1998) described that OLS has the effect of producing average or global parameter estimates which are assumed to apply equally over the whole region under analysis. That is, the relationships being measured are assumed to be stationary over space.

$$y_{OLS} = a_0 + \sum_k a_k x_{ik} + \in_i \qquad (6)$$

where y_{OLS} is the global estimated average yield, a_0 is the intercept, x_{ik} is the average ETa value for given Zone, a_k is the coefficient for the average ETa, and $\in_i$ is the error.

Extending the OLS to spatial context, GWR was computed using equation 7 (Fotheringham et al., 1998).

$$y_{GWR} = a_0(u_i, v_i) + \sum_k a_k(u_i, v_i) x_{ik} + \in_i \qquad (7)$$

where y_{GWR} is the local estimated average yield, $a_0(u_i, v_i)$ is the intercept at coordinates of the ith point in space, $a_k(u_i, v_i)x_{ik}$ is the average ETa value for given Zone coordinates of the ith point in space, a_k is the coefficient for the average ETa, and $\in_i$ is the error.

GWR is one of several spatial regression techniques that provides a local model (Fotheringham et al., 1998) for estimating average yield. Fotheringham et al. (1998) and ESRI (ESRI, 2011) described that GWR helps to get a continuous surface of parameter values and measurements of this surface are taken at certain points to denote the spatial variability of the surface. It is also hoped that GWR provides powerful and reliable statistics for estimating linear relationships between ETa and yield.

2.7. Standard Precipitation Index (SPI) for ETa Evaluation

For the climatological evaluation of ETa product, SPI data was used. A total of 10 stations distributed in different part of the country were used for this evaluation analysis (Figure 4). We used the precipitation data from these 10 stations for deriving the SPI values. The stations were selected because we have got historical data for the last about 30 years.

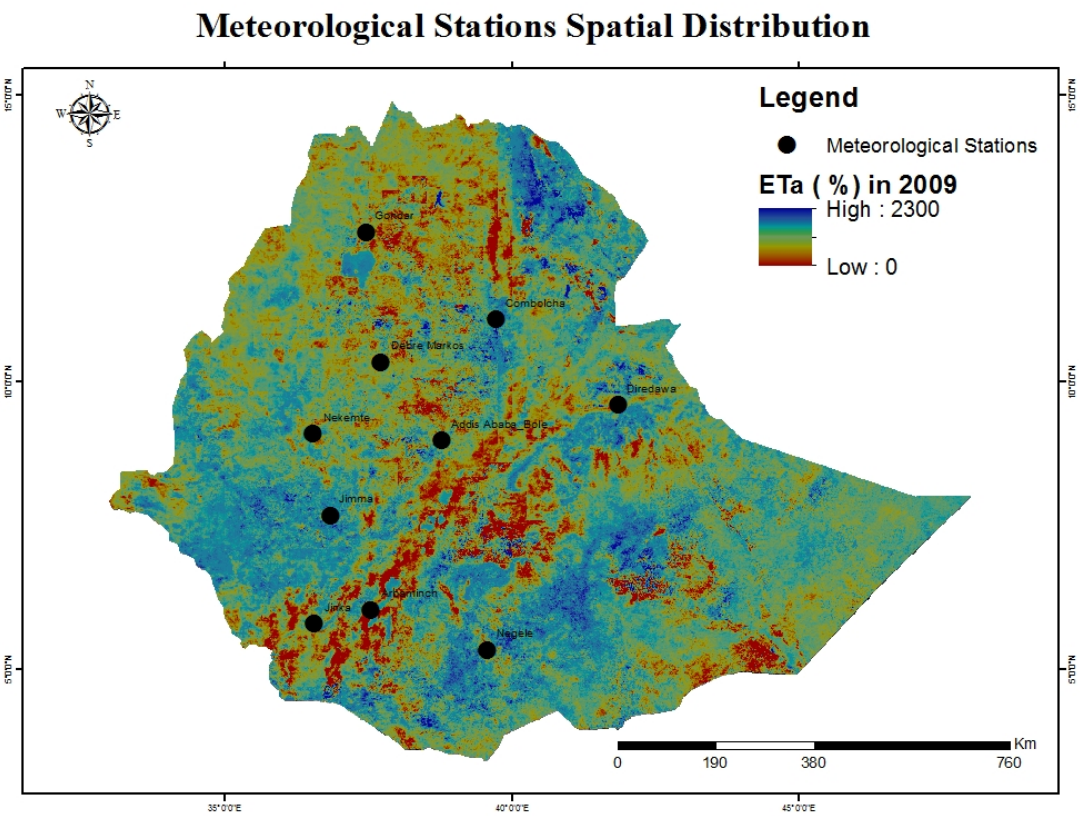

Figure 4: Spatial distribution of the selected meteorological stations.

In this study SPI represented the climatic data. McKee et al. (1993) and McKee et al. (1995) developed the SPI based on precipitation data. The SPI is calculated by fitting historical precipitation data to a Gamma probability distribution function for a specific time period and location, and transforming the Gamma distribution to a normal distribution with a mean of zero and standard deviation of one (Ji and Peters, 2003). Since the SPI is equal to the Z-value of the normal distribution, McKee et al. proposed a seven-category classification for the SPI: extremely wet (z > 2.0), very wet (1.5 to 1.99), moderately wet (1.0 to 1.49), near normal (-0.99 to 0.99), moderately dry (-1.49 to -1.0), severely dry (-1.99 to -1.5), and extremely dry (<-2.0).

Computation of the SPI involves fitting the Gamma probability density function to a given frequency distribution of precipitation totals for a station. The probability density function of the gamma distribution can be expressed in terms of the gamma function parameterized in terms of a shape parameter. The alpha and beta parameters of the Gamma probability density function are estimated for each station and for each month of the year. The Gamma distribution was defined by its frequency or probability density function using equation 8 (Chow et al., 1988; Ntale and Gan, 2003):

$$g(x) = \frac{1}{\beta^{\alpha}\Gamma(\alpha)} x^{\alpha-1} e^{\frac{-x}{\beta}} \quad \textbf{(8)}$$

where $g(x)$ is probability function, x is the precipitation amount, $\Gamma(\alpha)$ is the gamma function, α and β are and scale parameters, respectively.

Maximum likelihood solutions are used to optimally estimate α and β using equation 9 (Edwards and McKee, 1997).

$$\hat{\alpha} = \frac{1}{4A}\left(1 + \sqrt{\frac{4A}{3}}\right), \hat{\beta} = \frac{\hat{x}}{\hat{\alpha}} \textbf{ and } A = \ln\left(\hat{x}\right) - \frac{\sum \ln(x)}{n} \quad \textbf{(9)}$$

whre n is number of precipitation observations.

The resulting parameters are then used to find the cumulative probability of an observed precipitation event for the given month and time scale for the station in question. Since g(x) is undefined for x=0 and a precipitation distribution may contain zeros, the cumulative probability is obtained using equation 10 (Edwards and McKee, 1997):

$$H(x) = q + (1-q)G(x) \quad \textbf{(10)}$$

where q is the probability of a zero and $G(x)$ is the cumulative probability of the incomplete gamma function. If m is the number of zeros in a precipitation time series, then q can be estimated by m/n. By applying Equation 10, errors are eventually introduced to parameters a and b of Gamma distribution. These errors depend on the number of months with null precipitation (x=0) and they are evident only for the 1-month precipitation. For larger time scales (e.g. 3-month) the probability of null precipitation is usually zero (Ntale and Gan, 2003).

The cumulative probability, H(x), after its computation, is transformed to the standard normal random variable Z with mean equal to zero and variance of one, which is the value of the SPI. SPI value is more easily obtained computationally using an approximation that converts cumulative probability to the standard normal random variable Z using equation 11 and 12 (UNL, 2000).

$$Z = SPI = -\left(t - \frac{C_0 + C_1 t + C_2 t^2}{1 + d_1 t + d_2 t^2 +_{d_3} t^3} \right) \textbf{ for } 0 < H(x) <= 0.5 \qquad \textbf{(11)}$$

$$Z = SPI = \left(t - \frac{C_0 + C_1 t + C_2 t^2}{1 + d_1 t + d_2 t^2 +_{d_3} t^3} \right) \textbf{ for } 0.5 < H(x) <= 1 \qquad \textbf{(12)}$$

where $t = \sqrt{\ln \frac{1}{(H(x))^2}}$ for $0 < H(x) <= 0.5$ and $t = \sqrt{\ln \frac{1}{(1.0 - H(x))^2}}$ for $0.5 < H(x) <= 1$. Estimations are done for the variables C_0 =2.515517, C_1 = 0.802853 1 C_2 = 0.010328 d_1 = 1.432788 d_2 = 0.189269 and d_3 = 0.001308.

From SPI equation, it was observed that three month SPI of a given month would use the precipitation total of the previous two months and also the precipitation total of the that specific month of interest. For example, the SPI of September uses the precipitation total of July, August and September itself. Three month SPI is preferred and can give optimum estimation of short term drought condition and provides a seasonal estimation of precipitation (Ji and Peters, 2003). Therefore, we used three month SPI at the month of September for ETa evaluation. The three month SPI of the selected stations for the month of September from 2000 to 2009 is presented in Table 1.

Table 1: SPI values from 2000 to 2009 for the selected stations.

No	Station	LONG	LAT	2000	2001	2002	2003	2004	2005	2006	2007	2008	2009
1	Arbaminch	37.55277	6.0251	0.06	0.32	-0.15	0.12	0.09	-0.52	-0.32	2.5	1.27	-1.83
2	Addis Ababa_Bole	38.794	8.972	0.03	0.26	-0.31	0.02	0.15	-0.47	1.31	0.37	1.1	0.16
3	Combolcha	39.73723	11.07908	1.09	0.44	-0.13	-0.05	-0.51	0.3	0.76	-0.32	-0.5	0.75
4	Debre Markos	37.72639	10.33735	-0.36	0.51	0.41	0.12	0.08	-0.3	1.3	0.4	-0.78	-0.55
5	Diredawa	41.85723	9.594522	0.04	1.4	-0.34	-0.22	-0.56	-0.23	0.33	0.73	-0.29	-1.11
6	Gondar	37.46152	12.59992	1.03	0.23	-0.59	0.52	0.12	1.05	1.39	0.39	0.1	-0.95
7	Jimma	36.84389	7.673039	0.68	0.48	-0.43	-0.19	0.32	1.09	1.13	0.68	-0.16	0.55
8	Jinka	36.56446	5.783633	-0.05	0.25	-0.65	1.13	-0.26	-0.29	0.08	0.82	0.68	-1.02
9	Negele	39.57613	5.333612	-0.9	0.55	0.89	-0.32	-0.66	-1.02	-0.19	0.03	0.45	0.26
10	Nekemte	36.54856	9.091251	-0.07	0.04	-0.24	0.79	0.5	0.66	0.5	0.53	0.52	0.4

3. RESULTS AND DISCUSSIONS

The results and discussions are presented by exploring the relationship between ETa (%) and yield data. This includes the descriptive statistical analysis of ETa and yield data. After brief exploratory analysis the spatial relationships of the two parameters are analyzed. Finally, the climatic parameter SPI is used to evaluate ETa product with standard drought severity classes.

3.1 Preliminary ETa versus Cereal Yield Data Exploratory Analysis

The comparison of average ETa and average cereals yield from the year 2000 to 2010 is presented on 2-dimensional line graph on Figure 5. The X axis shows the zone numbers with order presented in Appendix 1. As it can be observed from the graph, there is a spatial relationship between average ETa and average yield for the selected zones. Except few zones, the increase and decrease of the two values were correlated.

Figure 6 presents, the overall temporal average for both ETa and cereal yield. There were two years missing (2002 and 2009) from CSA yield data and the ETa data were also excluded from the analysis. As it can be observed from the graph, there were increase and decrease through the study years for ETa values. The yield values shows an overall increase from 2000 to 2010.This shows the need of further study on the yield data before statistical comparison of the two datasets.

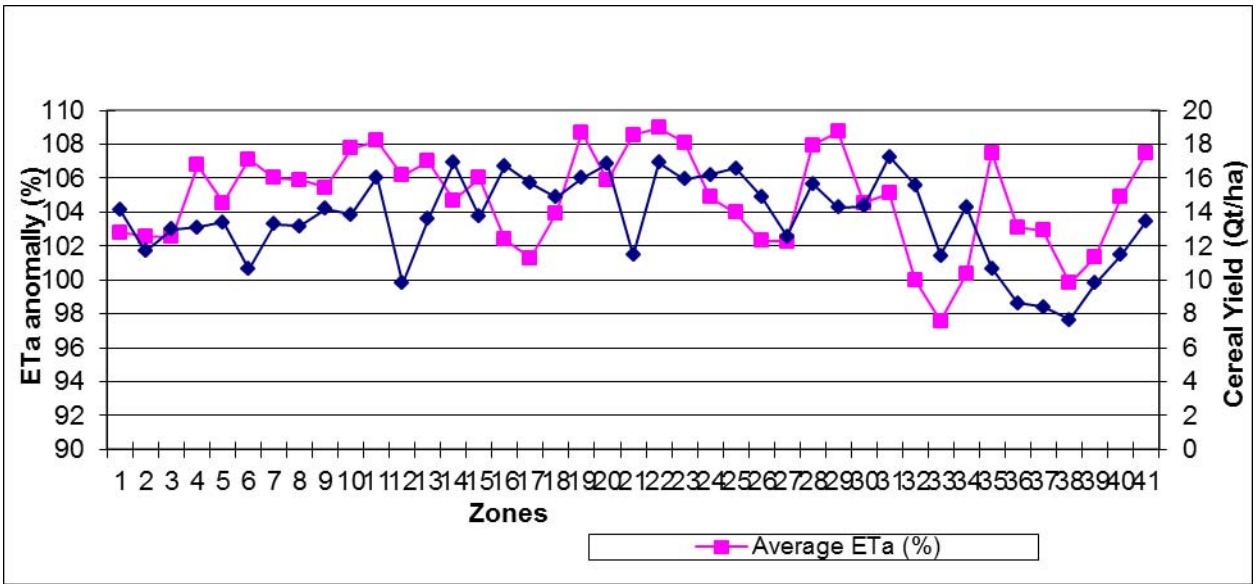

Figure 5: Spatial average ETa and yield comparison.

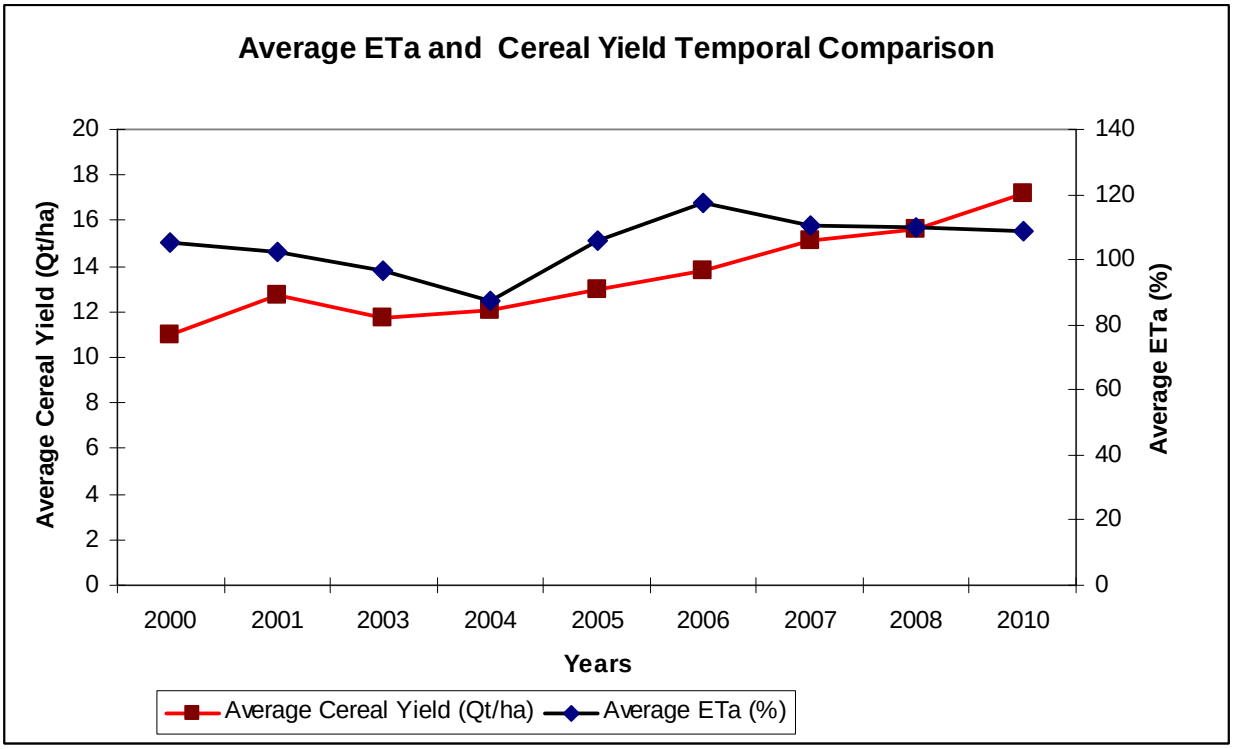

Figure 6: Temporal average ETa and yield data comparison for all zones.

3.2 Descriptive Statistics for ETa

The descriptive statistics for average ETa values in space and time dimensions is presented in Table 2. The minimum mean ETa was observed for the year 2002 followed by 2003. The maximum standard deviation was also observed for the year 2002. The year 2002 was drought year in Ethiopia (FAO, 2003) and the overall descriptive statistics (Table 2) of ETa also reflects this reality. The maximum mean ETa was for the year 2006 followed by 2008.

Table 2: Descriptive statistics for ETa values for all zones from 2000 – 2010.

No	Descriptive Statistics	Years										
		2000	2001	2002	2003	2004	2005	2006	2007	2008	2009	2010
1	Mean	105.38	102.42	79.54	96.27	87.60	106.06	117.27	110.15	109.62	80.32	108.89
2	Median	108.80	104.21	82.10	96.17	89.69	104.81	116.12	108.92	109.08	80.25	108.80
3	Standard Deviation	14.49	7.01	14.81	6.34	8.36	6.87	7.92	10.59	9.68	7.87	9.21
4	Range	65.16	34.29	56.27	26.32	34.62	25.00	28.56	48.73	38.27	36.27	36.73
5	Minimum	59.99	81.91	51.36	84.31	65.00	94.34	104.94	93.42	91.81	60.43	95.57
6	Maximum	125.15	116.20	107.63	110.63	99.62	119.34	133.50	142.15	130.09	96.70	132.29

FEWSNET (2011) used median values instead of the mean values. For getting a clear understanding of these values, the median and mean values of ETa in space and time dimensions were compared (Figure 7). Both the mean and median have almost same values and pattern (Figure 7). From this Figure, it can be observed that there were droughts in the years 2002, 2003, 2004 and 2009 compared to other years. In the year 2002, the percentage

anomalies of ETa and the corresponding median ETa were found to be below 80%. This means that there was a deficit in soil moisture for plant normal growth and yield deficit is expected at this year. The year 2003, 2004 and 2009 were also observed to be in below average ETa anomaly category.

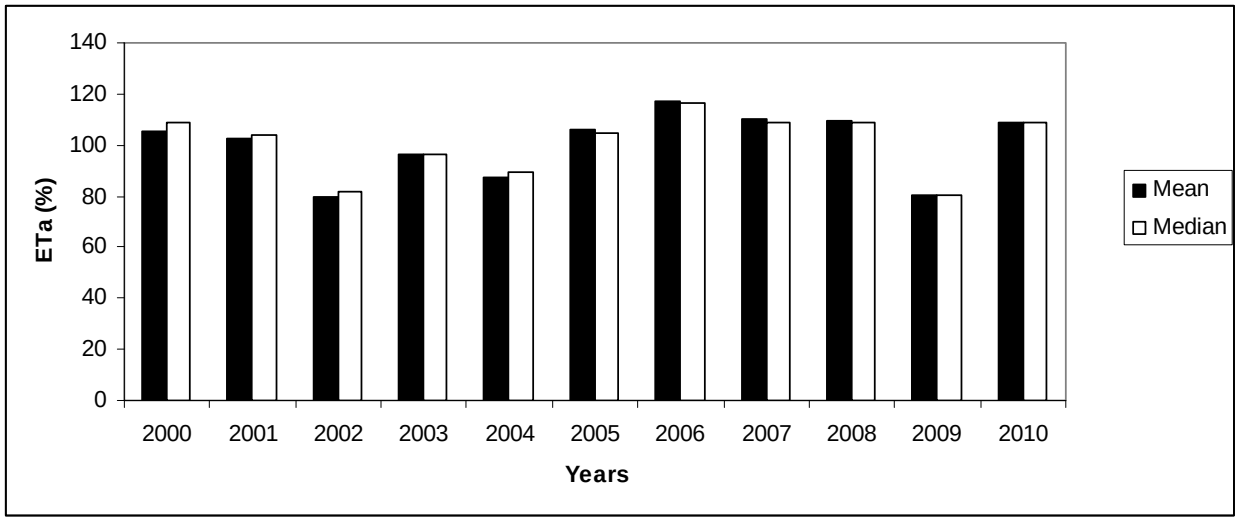

Figure 7: Comparison of ETa percentage mean and median

3.3 Descriptive Statistics for Yield data

The average yield data in space and time dimensions were explored. For this purpose, cereal yield, which is the overall average of Teff, barley, wheat, maize, sorghum, millet and oat, and also for each of the crops, the average values were explored. The descriptive statistics for cereal is presented in Table 3. The cereal yield data varies both temporally and spatially. The spatio-temporal average yield analysis output is also presented on Figure 8. Unfortunately, in all of these Figures the year 2002 and 2009 were missing, since these two years data were missing in CSA crop yield data reports.

Table 3: Descriptive statistics for cereal yield (Qt/ha) for all zones from 2000 – 2010.

No	Descriptive Statistics	Years								
		2000	2001	2003	2004	2005	2006	2007	2008	2010
1	Mean	10.92	12.73	11.70	12.14	13.00	13.77	15.10	15.64	17.22
2	Median	11.45	13.52	12.39	12.47	13.25	14.26	14.62	15.72	17.39
3	Standard Deviation	2.72	2.83	3.48	3.19	3.32	3.55	3.38	2.16	2.71
4	Range	12.62	12.75	15.87	12.74	15.32	15.17	16.39	8.35	11.36
5	Minimum	4.85	4.73	2.11	5.35	4.64	4.75	9.43	12.05	10.32
6	Maximum	17.47	17.48	17.98	18.09	19.96	19.93	25.82	20.40	21.68

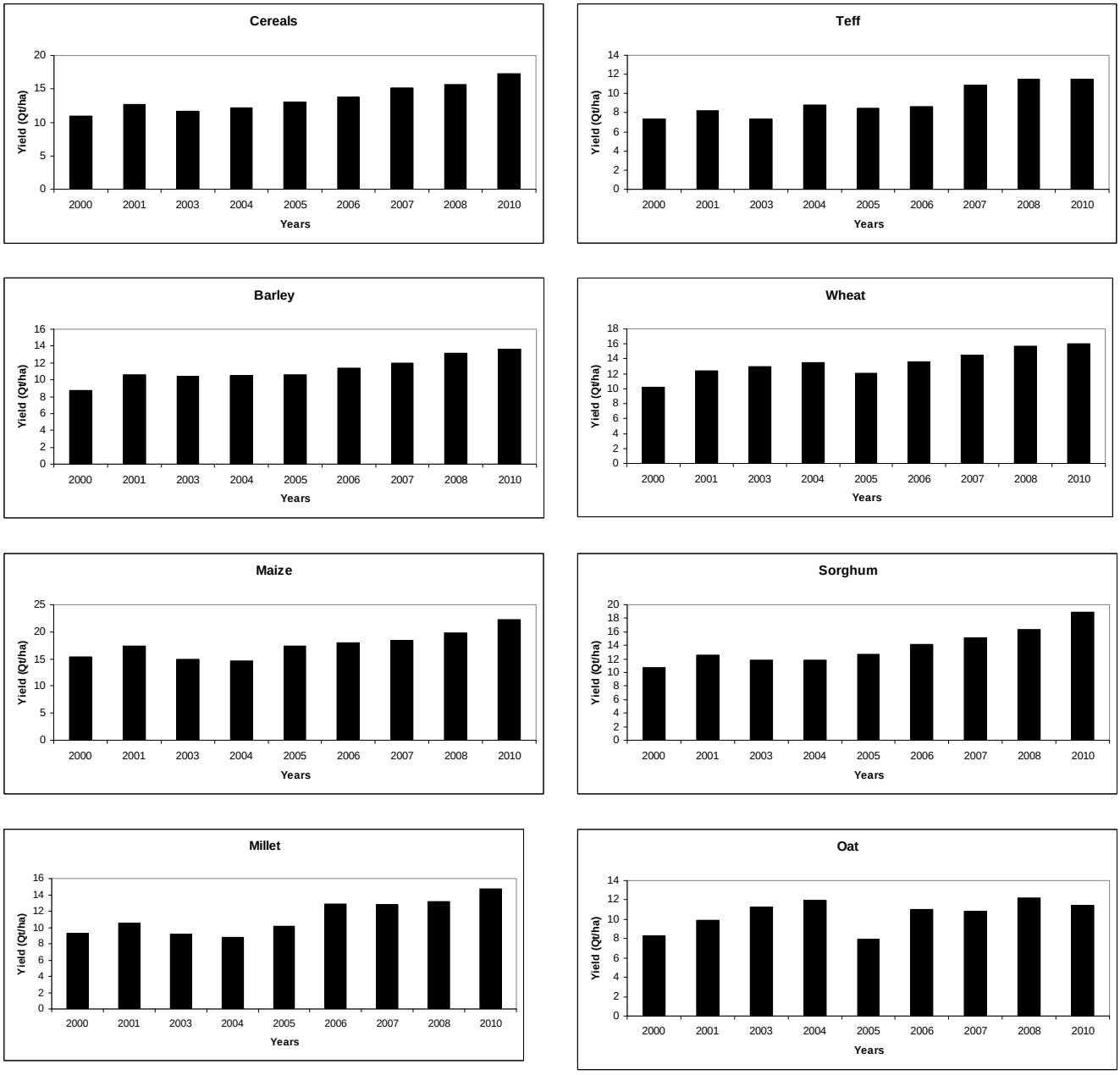

Figure 8: Crop yield pattern for the past 10 years in the studied zones.

All of the average crop yields showed almost the same pattern in that there is gradual increase in yield value except oat. The average yield value for oat showed an increase up to 2004 and decrease in 2005 and then a gradual increase pattern up to 2010.

The overall yield increase through years is assumed to be due to improved farm management, such as fertilizer, pesticide applications and improved farming systems through agricultural extensions. The challenge now is how to use these yield data, which is increasing gradually from year to year, with ETa data which is assumed to increase when there is surplus production (favorable weather condition) and decrease when there is deficit in crop yield (due

to unfavorable weather condition). In other words, in the ETa evaluation using the crop yield data, the expectation was that when there is a decrease in ETa percentage value, there is a decrease in yield value. This way it is possible to observe drought incidence on the ground. All of the crop data that we assessed have a gradual increase in yield from the year 2000 to 2010. This means there is a trend in all the crop yield data. If we simply test the correlation between ETa data and crop data without removing the inherent trend in crop yield data unexpected and/or misleading results can be produced. Therefore, we first removed the trend and then test the correlation between the two attributes. For this purpose, we detrended the crop yield data.

From the four crops assessed above, there is one interesting pattern observed in Teff average yield data (Figure 8). There was a yield decrease in 2003 compared to the year 2001 and 2004. This year was also found to have below average ETa anomaly category (Figure 7). Even before applying crop yield detrending, it is possible to observe the drought situation during 2003 on Teff average yield data.

Detrending is removing linear trends from regularly sampled time-domain input-output data (FAO, 1999). This data processing operation helps to estimate more accurate linear models because linear models cannot capture arbitrary differences between the input and output signal levels. After deterending, the linear models can estimate from detrended data the relationship between the ETa and crop yield data.

The detrended average crop yield for cereal, Teff, sorghum, maize, barley and wheat are presented on Figure 9. This is the average temporal yield for all zones for each of the crops. Since, the year 2002 and 2009 were missing, the average values of 2001 and 2003 for 2002, and 2008 and 2010 for 2009 were used for these two years. The spatial and temporal deterended values (for each zones from 2000 to 2010) for all these crops is presented in Appendix 2. It is not possible to show graphically the sptio-temporal detrended values for all zones and only the tables are presented in this Appendix.

The cereals yield data showed that the year 2003 to 2006 were below average value (zero) and for all other years above average values of cereal yield (Figure 9a). Teff yield showed the yearly variation clearly. There year 2003, 2005 and 2006 below average values (Figure 9b). Sorghum yield was observed to be below average from 2003 to 2008 (Figure 9c). Maize was observed to be below average for the year 2003, 2004 and 2007. Barley yield was observed to be below average for the years 2000, 2003, 2004 – 2007. Wheat yield was found to be below average for the year 2000, 2005 and 2007.

Cereals, Teff, Sorghum and Barley showed the decrease in yield in 2003 and this is in agreement with ETa below average ETa anomaly category. The year 2003 was also reported to be drought year by other authors, such as Meze-Hausken (2004) and FEWSNET (2003).

The year 2002 and 2009 were missing CSA data and average values were taken. The effect of this average value on the overall correlation of crop yield and ETa values were assessed using Waghimra Zone cereal data (which has relatively high correlation) (Figure 10). When these average values were included in the analysis data, the R^2 was found to be decreased. Therefore, these two years average data were not included in the subsequent analysis.

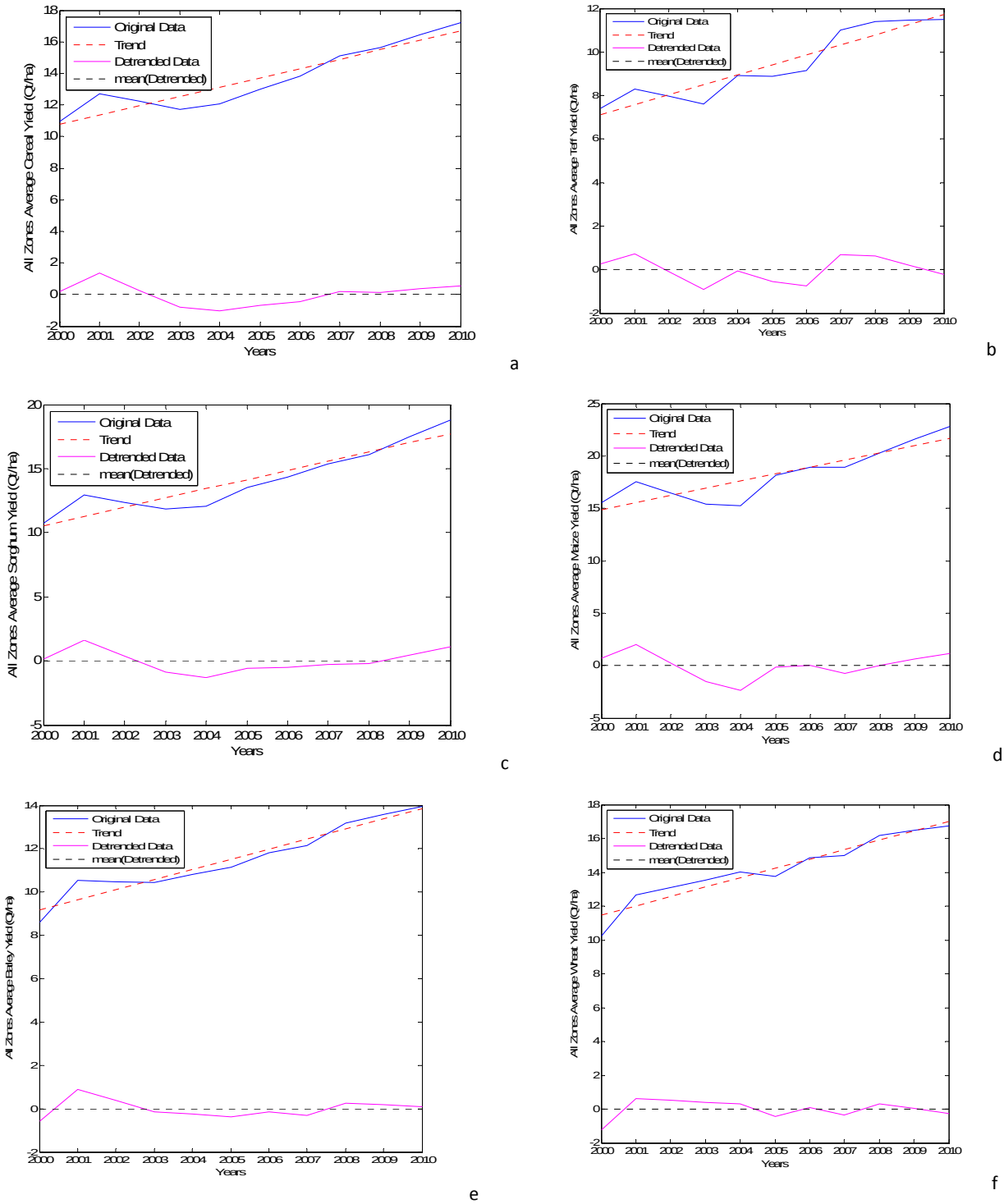

Figure 9: Detrended average spatiotemporal crop yield data, (a)cereals, (b)Teff, (c) sorghum, (d) maize, (e) barley, and (f) wheat.

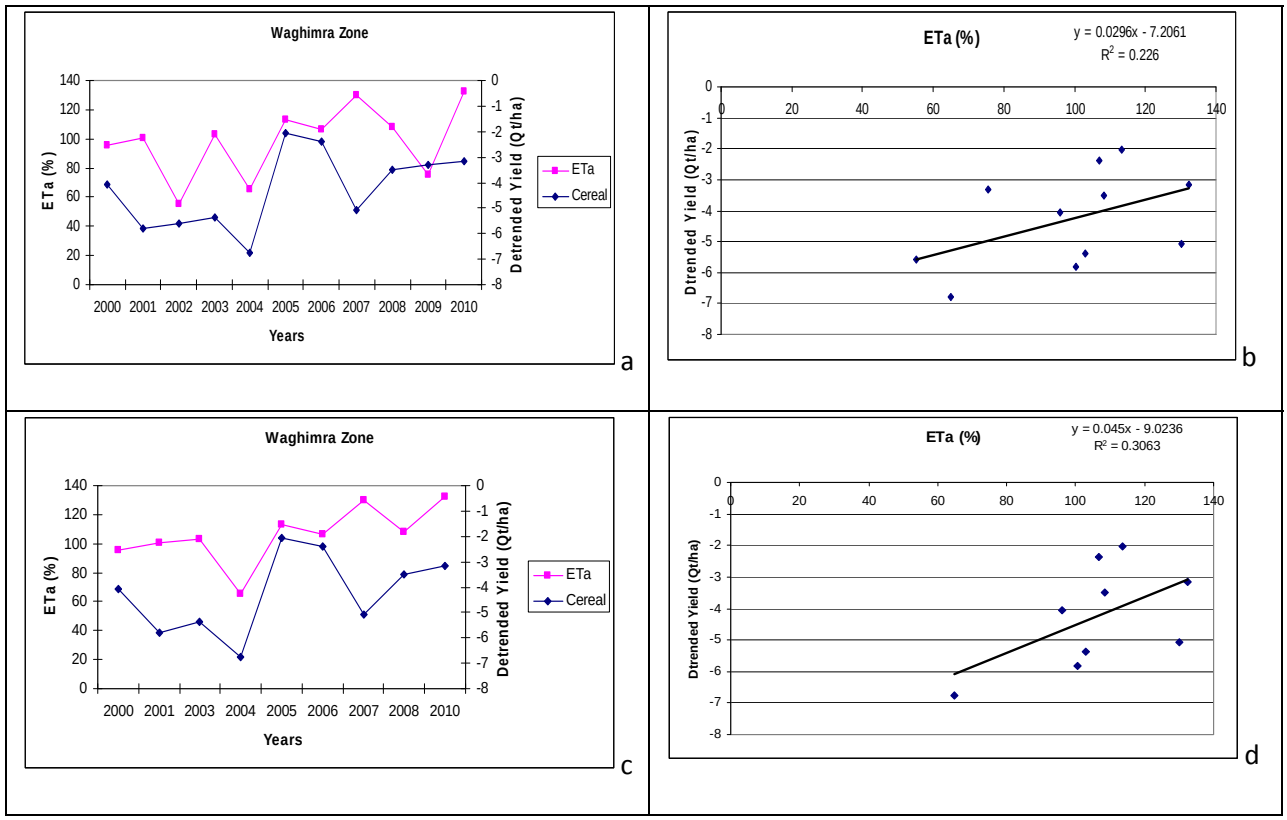

Figure 10: Correlation between crop yield and ETa (%) before removing 2002 and 2009 year data (a & b) and after removing 2002 and 2009 year data (c & d).

Yield anomaly was calculated from the deterended yield data for comparing with ETa anomaly. The same as ETa anomaly, the yield anomaly was calculated using median detrended cereals yield. The correlation and scatter plots for some of the selected Zones (those with relatively higher R^2 values) are presented on Figure 11 a – f.

From the assessed zones about 17% were found to have R^2 values of 0.5 - 0.8, about 20% 0.4 – 0.5, about 10% 0.3 – 0.4, about 5% 0.2 – 0.3, about 22% 0.1 – 0.2 and about 26% less than 0.1 (Table 4). The highest correlation coefficient was obtained for Gurage Zone of Southern Nation and Nationalities Peoples Region. The lowest correlation coefficient was North Shewa Zone of Amhara Region. From DEM data observation Gurage Zone has low elevation compared to North Shewa Zone. Senay et al. (2011) also indicated that ETa model may be influenced by heterogeneity in elevation. With this in mind, the influence of elevation on the correlation coefficient of the relationships between ETa and yield data was assessed. It was observed that DEM can explain only about 7% of the variability in the correlation coefficient (R^2) of the relationships between ETa and yield data.

In overall, the analysis results showed that there is a relationship between ETa anomaly and crop yield anomaly. The decrease or increase of ETa (%) data in space-time dimension can show the deficit or increase of yield data with optimum level of certainty. It was also realized that it is very difficult to decide the uncertainty levels of the relationships statistically. This is because inherently the two datasets are different and they were also produced for

different objectives. The detailed spatio-temporal analysis of the relationships between ETa and crop yield data is presented in the following subsections.

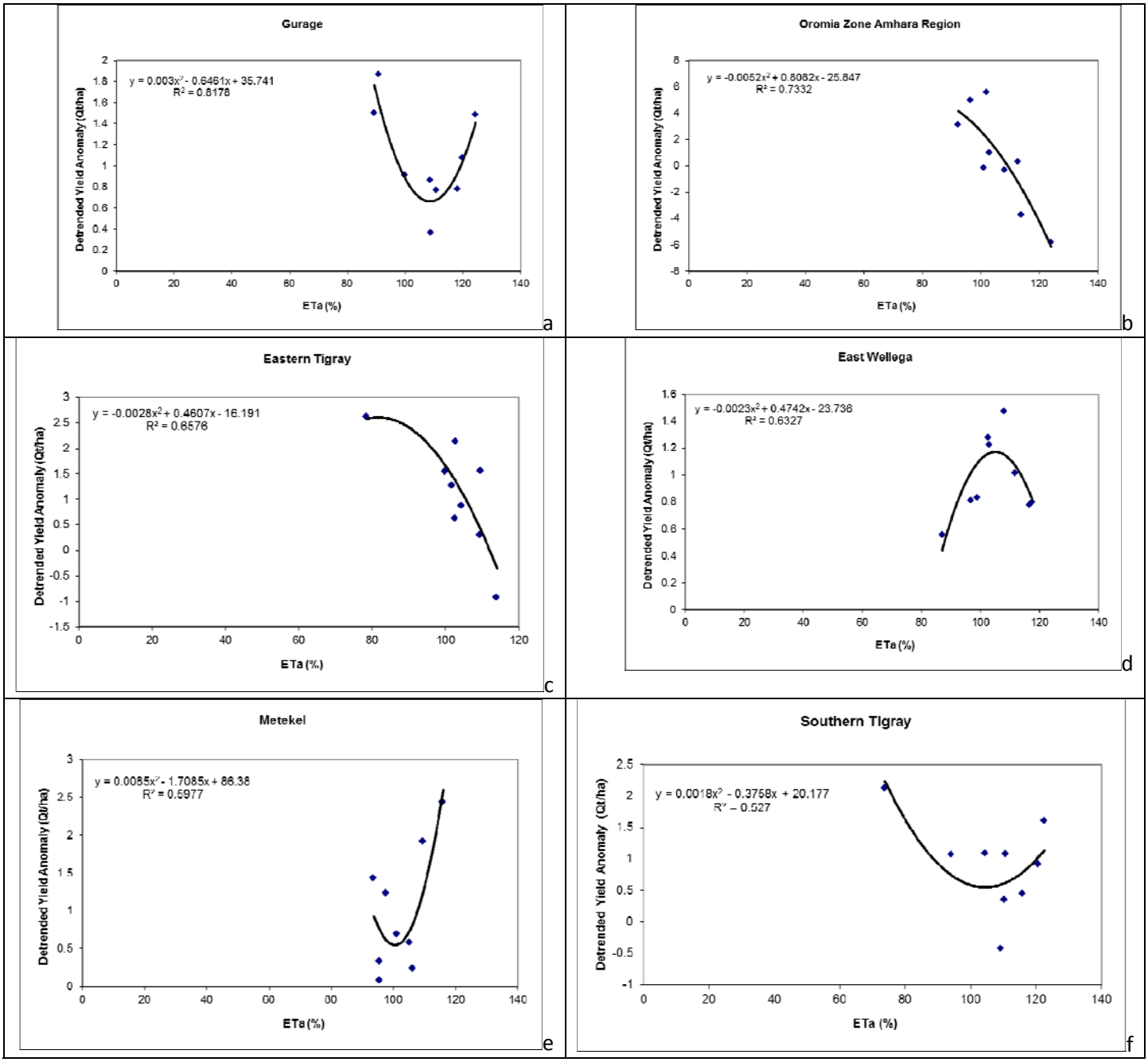

Figure 11: Scatter plots of the relationships between ETa (%) and cereal deterended yield.

Table 4: List of Zones in the correlation coefficient classes

Range of R2	Less than 0.1	0.1 - 0.2	0.2 - 0.3	0.3 - 0.4	0.4 - 0.5	0.5 - 0.8
Zone Names	East Harerge	Bench Maji	KAT	East Gojam	Amaro	Gurage
	Sidama	West Shewa	South Omo	East Shewa	North Shewa(R4)	Oromia
	Central	West Gojam		South Wollo	Arsi	Eastern
	Derashe	Dire Dawa		Hareri	Asosa	East Wellega
	Awi/Agew	Hadiya			Wag Himra	Metekel
	Western	Jimma			Ilubabor	Southern
	North Wollo	West Harerge			West Wellega	Gedio
	Bale	North Gonder			Burji	
	Yem	South Gonder				
	Konso					
	North Shewa(R3)					

3.4 Spatial Regression Analysis of ETa and Yield Data

A total of 41 Zones were used for the spatial analysis of the regression between ETa and yield data. The OLS temporal spatial analysis of the models for predicting yield using ETa data showed very low R^2 values (Table 5). For the intercepts of these models, the year 2003, 2006, 2007, 2008 and 2010 were found to be significant at $\alpha = 0.05$ level of significance. For the ETa coefficient, only the year 2000, 2004 and 2007 were found to be significant $\alpha = 0.05$ level of significance. This is also as expected, because OLS develop a global model and one equation applicable for the whole study areas.

GWR develops a local model extending the OLS to spatial context. For each year (from 2000 to 2010) the strength of the correlation between ETa and cereal yields were assessed. It was observed that there is variability in the coefficient of correlation between the different years. Maps for the years 2000 to 2004 from these analyses are presented on Figure 12. For this analysis, the R^2 ranges from 0.00 to 0.40 (Table 5). The highest R^2 was found for the year 2004 and the lowest for the year 2006. As expected the R^2 values in GWR were found to be higher compared to OLS. This happened due to the fact that GWR develops local model (Fotheringham et al., 1998) for predicting yield data compared to the global models of OLS. There is no spatio-temporal pattern for the high and low coefficient of determination values between ETa and yield data (Figure 12).

Overall, the correlation between ETa and yield was found to be weak both in the OLS and GWR and ETa may not be used for estimating the amount of yield. This is because these two datasets are different and they were also produced for different purposes. Even though their correlation is low the decrease or increase of ETa percentage value can indicate the deficit or increase of yield in Meher growing season of the studied Zones.

Table 5: Spatial analysis output for ETa and crop yield

No	Model Variable	Years								
		2000	2001	2003	2004	2005	2006	2007	2008	2010
1	Intercept	4.74	4.14	17.9	-4.2	10.3	26.9	29.5	8.7	14.9
2	Intercept standard error (SE)	2.93	5.74	5.22	4.06	6.2	9.6	4.19	3.6	5.06
3	Intercept t-statistics	1.62	0.72	3.43	-1.05	1.7	2.8	7.05	2.4	2.9
4	Intercept Probability	0.11	0.47	0.0015*	0.301	0.106	0.008*	0.000*	0.02*	0.005*
5	ETa Coefficient	0.059	0.08	-0.06	0.19	0.03	-0.11	-0.13	0.06	0.02
6	ETa Coefficient SE	0.026	0.05	0.05	0.05	0.06	0.08	0.04	0.03	0.045
7	ETa Coefficient t-statistics	2.24	1.53	-1.17	4.15	0.45	1.3	-3.5	1.9	0.46
8	ETa Coefficient Probability	0.03*	0.135	0.249	0.0002*	0.66	0.188	0.001*	0.06	0.648
9	OLS R^2	0.08	0.02	0.013	0.21	0.216	0.06	0.149	0.08	0.005
10	Average GWR R^2	0.13	0.10	0.2018	0.40	0.371	0.093	0.150	0.094	0.182

* Statistically significant.

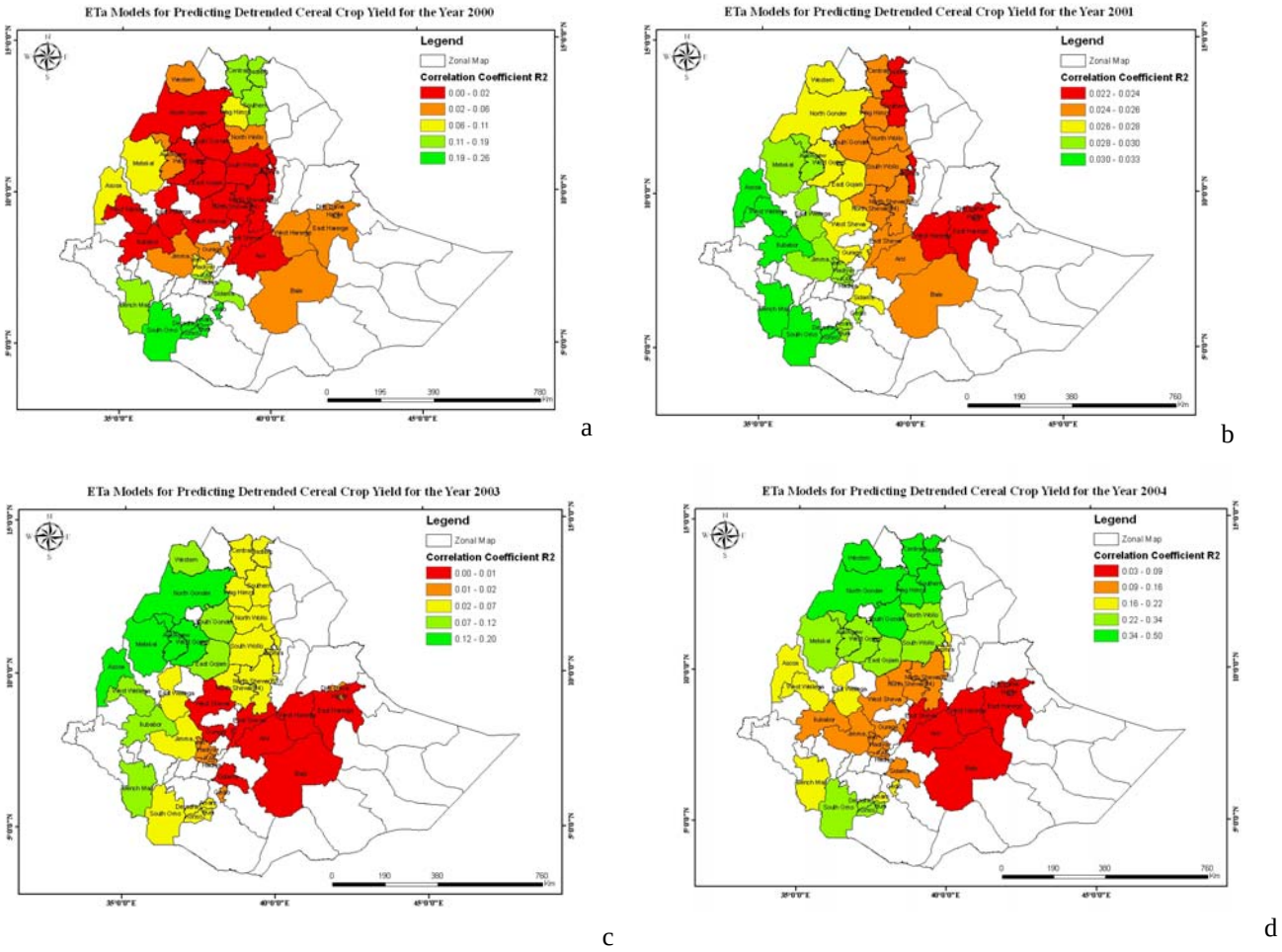

Figure 12: GWR spatial pattern of coefficient of determination (R^2) between ETa and yield data for the year (a) 2000, (b) 2001, (c) 2003, (d) 2004. The green colors are high and red colors are low coefficient of determination (R^2).

3.5. Evaluation of ETa using Climate Data

The historical SPI drought analysis of the selected stations is presented on Figure 13. The historical SPI analysis was done, since SPI should be explored at least for about 30 years to observe the trend and also to fit the Gamma probability. After deriving the SPI using the historical rainfall data, we correlated the SPI values from 2000 to 2009 with ETa percentage data. The year 2010 was not included in the analysis, since we did not get the data from Ethiopian Meteorological Agency.

As it can be observed from Figure 12, for all the stations analyzed the drought severity ranges from extremely dry (<-2.0) to extremely wet (> 2.0) in the year 2000 to 2009. The ETa point data was extracted for the selected 10 meteorological stations and the correlation of these values with SPI values were analyzed (Figure 13). From the analysis the coefficient of determination ranged from 0.13to 0.8. The highest correlation was observed for the year 2007 (Figure 14h and the lowest for the year 2008 (Figure 14i).

The evaluation of ETa percentage data using the climatological SPI data showed that there is a relationship between the two datasets. There is a variation in strength of these relationships between the years from 2000 to 2009. This needs further investigation in the ETa product. If ETa data is further refined and the correlation values between ETa and SPI are improved, it is possible to calibrate the ETa data, so that it can show the drought severity in space and time dimensions.

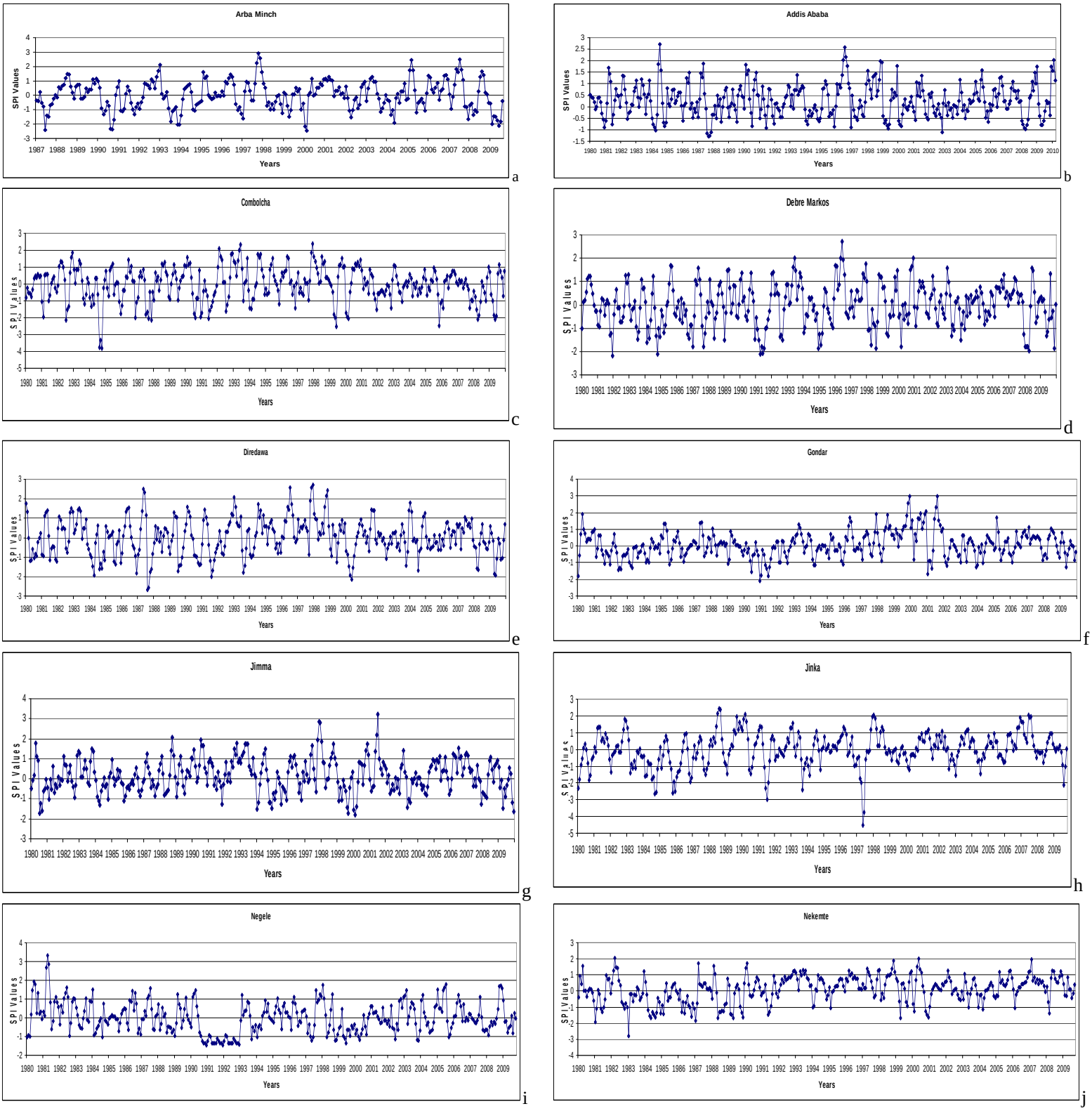

Figure 13: Historical drought trends in the selected station. The X-axis is the years and Y-axis is the SPI values.

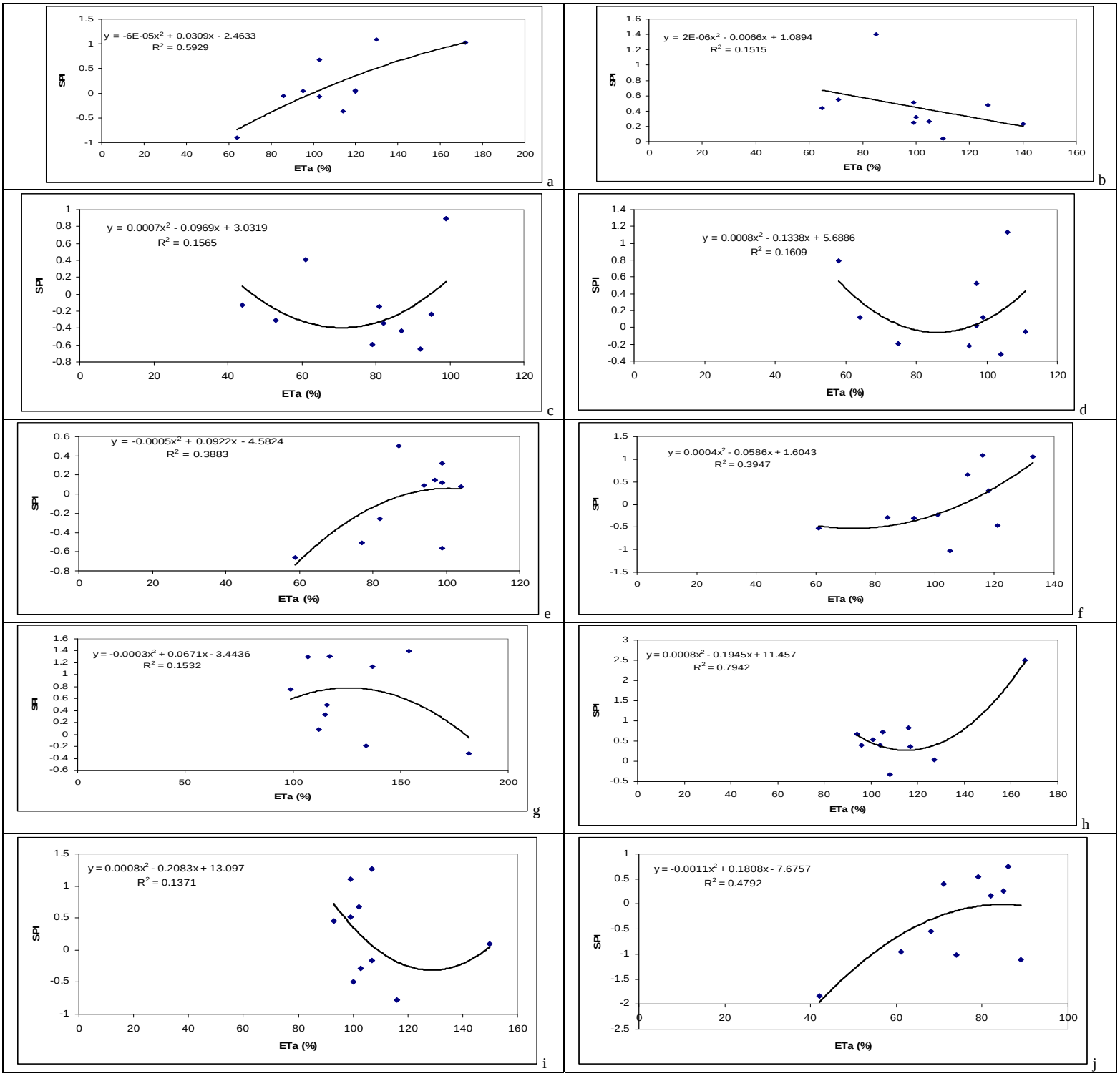

Figure 14: Scatter plots for the relationships between ETa and SPI values for the year (a) 2000, (b) 2001, (c) 2002, (d) 2003, (e) 2004, (f) 2005, (g) 2006, (h) 2007, (i) 2008, and (j) 2009

4. Conclusions

The objectives of this article were to: 1) develop an evaluation method specifically applicable for drought and food security models using crop yield and climate data, and 2) evaluate the ETa anomaly products using zonal (district level) crop yield data and clamatological rainfall data.

For the first objective, a simplified model evaluation method was developed. This method started by exploring the two attributes separately using statistical data exploratory techniques. It was found that crop yield data have trend through studied years from 2000 to 2010. Therefore, the trend had to be removed before the statistical relationships analysis. After removing the trend, both OLS and GWR regression analysis were conducted. The ETa percentage data was also evaluated using meteorological rainfall SPI data. The Correlation of ETa with SPI showed that there were differences between the different years analyzed from 2000 to 2009. If ETa data is further refined to fit the SPI data, it is possible to calibrate ETa for standard drought monitoring and food security assessment.

Concerning the second objective, it was found that there are positive relationships between ETa and crop yield data. In the ETa percent anomaly data the year 2002, 2003 and 2009 were reported to be drought years. Unfortunately, the year 2002 and 2009 were missing in the crop yield data. For the year 2003, the average cereal, Teff, maize and barley were found to be below average. This confirms that ETa can be used for drought and food security early assessment for Meher growing season.

Overall, there were weak correlations between ETa anomaly and cereal yield anomaly. The maximum coefficient of determination (R^2) was observed for the year 2004 and the minimum for the year 2005 (Table 5). The weak correlation between the two datasets can be attributed due to two major reasons: 1) the first reason is aggregation of both the yield and ETa data at Zonal administrative levels, and 2) the second reason is that inherently the two dataset are different.

The yield data was aggregated at Zonal district level, which is next to regional administrative levels in Ethiopia. This administrative level is very coarse resolution for yield data in that the report is not homogenous from an agricultural and agro-ecological point of view. Therefore, these coarse administrative level averages cancel local variability of yield and ETa data. One future research on evaluating the ETa model for food security and drought monitoring is to use high resolution administrative level crop yield data, such as Woreda administrative level (next high administrative resolution to Zone administrative level in Ethiopia).

It should be noted that even though we used yield data for evaluating ETa anomaly for showing the drought situation, inherently the two datasets are different and they may not be expected to show strong correlation. Interestingly, even though the two datasets were from different sources and were produced for different purposes, there were positive relationships. It was observed that the increase or decrease of ETa percentage value can indicate the yield increase and deficit in the studied districts for Meher growing season. This is also in agreement with Bastiaanssen et al.(2005) and Senay et al. (2011) recommendation that ETa's dependence on land cover and soil

moisture, and its direct relationship with carbon dioxide assimilation in plants, makes it an important variable to monitor and estimate crop yield and biomass for decision makers interested in food security. The correlation analysis of ETa data with standard climatic drought monitoring index SPI showed that there is a relationship between the two datasets. This further confirms that ETa can be used for drought monitoring with future calibrations to match with standard drought monitoring index SPI.

REFERENCES

Bastiaanssen, W.G.M., E.J.M. Noordman, H. Pelgrum, G. Davids, B.P. Thoreson, and R.G. Allen. 2005. SEBAL model with remotely sensed data to improve waterresources management under actual field conditions. Journal of Irrigation Drainage Engineering 131:85–93.

Chow, V.T., R.D. Maidment, and W.L. Mays. 1988. Applied Hydrology McGraw-Hill.

CSA. 2011. Annual Agricultural Sample Survey [Online]. Available by Central Statistical Agency of Ethiopia (CSA) http://www.csa.gov.et/index.php?option=com_content&view=article&id=59&Itemid=59 (verified 1 November).

Edwards, C.D., and T.B. McKee. 1997. Characteristics of 20th century drought in the United States at multiple time scales 634. Department of Atmospheric Sciences, Colorado State University.

ESRI. 2011. ArcGIS ArcMap Guide Environmental Systems Resource Institute (ESRI), Redlands, CA.

FAO. 1999. Production variability and losses [Online]. Available by Sustainable Development Department (SD), Food and Agriculture Organization of the United Nations (FAO) http://www.fao.org/sd/EIdirect/agroclim/losses.htm (verified 15 December, 2011).

FAO. 2003. Food and Agriculture Organization of the United Nations, Ethiopia: drought-hit farmers receive emergency aid [Online]. Available by FAO http://www.fao.org/english/newsroom/news/2003/18548-en.html (verified 10 December 2011).

FEWSNET. 2003. Estimating Meher crop production using rainfall in the 'long cycle' region of Ethiopia, June 21, revised October 6, http://www.fews.net/special/. Addis Ababa.

FEWSNET. 2011. Famine Early Warning Systems Network [Online]. Available by FEWSNET http://earlywarning.usgs.gov/fews/africa/web/imgbrowses2.php?extent=02ts (verified 03 December 2011).

Fotheringham, A.S., M.E. Charlton, and C. Brunsdon. 1998. Geographically weighted regression: a natural evolution of the expansion method for spatial data analysis. Environment and Planning 30:1905 - 1927.

Ji, L., and A.J. Peters. 2003. Assessing vegetation response to drought in the northern Great Plains using vegetation and drought indices. Remote Sensing of Environment 87:85 - 98.

MathWorks. 2009. MATLAB Neural Network Toolbox User's Guide Natick, MA: The MathWorks, Inc.

Mckee, T.B., N.J. Doesken, and J. Kleist. 1993. The relationship of drought frequency and duration to time scales. Paper presented at the 8th Conference on Applied Climatology, 17 - 22 January, Anaheim.

McKee, T.B., N.J. Doesken, and J. Kleist. 1995. Drought Monitoring with Multiple Time Scales. Preprints, 9th Conference on Applied Climatology, January 15–20, Dallas, Texas, 233–236.

Ntale, H., and T. Gan. 2003. Drought indices and their application to east Africa. International Journal of climatology 23:1335 - 1357.

Panu, U.S., and T.C. Sharmat. 2002. Challenges in drought research: some perspectives and future directions. Hydrotogical Sciences-Journal—des Sciences Hydrologiques 47(S):S19-S30.

Senay, G.B., M.E. Budde, and J.P. Verdin. 2011. Enhancing the Simplified Surface Energy Balance (SSEB) approach for estimating landscape ET: Validation with the METRIC model. Agricultural Water Management 98:606–618.

Senay, G.B., M. Budde, J.P. Verdin, and A. M. 2007. A Coupled Remote Sensing and Simplified Surface Energy Balance Approach to Estimate Actual Evapotranspiration from Irrigated Fields. Sensors 7:979-1000.

UNL. 2000. Weekly SPI Users Manual. National Drought Mitigation Center, University of Nebraska-Lincoln.

Wu, Z., N.E. Huang, S.R. Long, and C. Peng. 2007. On the trend, detrending, and variability of nonlinear and nonstationary time series. The National Academy of Sciences of the USA, PNAS 104:14889 – 14894.

Appendix 1: List of Zones selected for ETa evaluation

No	ZONENAME	Region
1	Western	Tigray
2	Central	Tigray
3	Eastern	Tigray
4	Southern	Tigray
5	North Gonder	Amhara
6	South Gonder	Amhara
7	North Wollo	Amhara
8	South Wollo	Amhara
9	North Shewa(R3)	Amhara
10	East Gojam	Amhara
11	West Gojam	Amhara
12	Wag Himra	Amhara
13	Awi/Agew	Amhara
14	Oromia Zone	Amhara
15	East Wellega	Oromia
16	West Wellega	Oromia
17	Ilubabor	Oromia
18	Jimma	Oromia
19	West Shewa	Oromia
20	East Shewa	Oromia
21	North Shewa(R4)	Oromia
22	Arsi	Oromia
23	West Harerge	Oromia
24	East Harerge	Oromia
25	Bale	Oromia
26	Metekel	Benshangul-Gumz
27	Asosa	Benshangul-Gumz
28	Gurage	SNNPR
29	Hadiya	SNNPR
30	KAT	SNNPR
31	Sidama	SNNPR
32	Gedio	SNNPR
33	South Omo	SNNPR
34	Bench Maji	SNNPR
35	Yem	SNNPR
36	Amaro	SNNPR
37	Burji	SNNPR
38	Konso	SNNPR
39	Derashe	SNNPR
40	Hareri	Hareri
41	Dire Dawa	Dire Dawa

Appendix 2: Average ETa zonal statistical analysis output for the year 2000 to 2010.

No	ZONENAME	Years										
		2000	2001	2002	2003	2004	2005	2006	2007	2008	2009	2010
1	Western	110.535	98.8069	91.6697	102.51	90.1287	102.696	111.537	103.876	103.327	79.1761	101.854
2	Central	101.694	96.9732	67.2815	101.352	83.8621	104.037	109.495	110.437	104.469	75.672	110.677
3	Eastern	101.72	104.47	67.95	102.53	78.50	102.75	109.64	113.99	99.90	77.25	109.34
4	Southern	115.768	109.143	72.4065	104.413	73.7766	110.541	110.252	120.576	93.9771	67.5013	122.459
5	North Gonder	110.023	108.154	79.5846	98.8038	89.1161	99.8818	116.248	110.654	108.519	77.3559	99.3007
6	South Gonder	113.678	105.4	62.8685	101.648	81.1821	102.535	117.83	108.944	130.089	76.5527	102.649
7	North Wollo	113.459	101.173	72.8742	107.918	74.4912	116.694	106.882	116.426	104.044	72.7514	112.951
8	South Wollo	115.729	102.095	61.0657	110.631	76.0593	118.183	109.185	109.379	99.0777	87.625	112.768
9	North Shewa(R3)	115.293	93.8335	57.7325	105.893	90.6075	114.64	107.426	111.323	104.325	84.5526	105.556
10	East Gojam	122.042	104.363	57.4578	91.5812	88.6767	105.591	112.622	110.269	123.223	80.167	111.416
11	West Gojam	113.845	113.502	71.8733	90.1165	93.2588	102.648	127.002	103.034	127.388	77.1396	103.114
12	Wag Himra	95.9654	100.368	55.3308	102.898	64.9995	113.424	106.855	130.216	108.389	75.542	132.291
13	Awi/Agew	119.998	116.204	85.4623	88.8893	93.7064	98.5462	124.544	106.615	116.122	80.91	98.4289
14	East Wellega	111.716	108.016	84.8522	87.0639	96.7494	102.992	117.584	98.8489	116.458	84.9619	102.616
15	Oromia	124.09	102.063	73.6162	102.972	92.2624	113.878	108.288	101.207	96.5065	91.0062	112.736
16	West Wellega	99.3166	100.406	94.0571	93.1265	95.5106	101.678	110.454	102.546	112.465	86.2761	106.028
17	Ilubabor	102.461	104.065	95.7604	88.8599	98.1968	98.9073	110.156	98.4706	108.678	91.2204	101.602
18	Jimma	110.383	107.719	91.5379	88.1405	97.1077	102.543	114.114	94.613	112.505	92.7667	108.261
19	West Shewa	123.07	108.812	63.9815	84.3073	92.0638	110.546	115.592	108.195	123.737	80.338	112.1
20	East Shewa	109.258	98.953	51.3607	101.745	79.7576	110.645	106.577	108.462	119.679	70.9515	117.79
21	North Shewa(R4)	125.149	107.45	62.0348	96.1429	90.0121	119.34	104.938	117.35	111.709	73.9851	104.714
22	Arsi	113.723	104.932	59.5888	98.5906	82.3244	111.918	128.304	109.973	111.141	70.4141	119.793
23	West Harerge	104.385	94.7369	65.2637	95.3246	89.7422	116.484	127.582	116.719	110.353	82.0576	117.452
24	East Harerge	105.287	93.7796	82.0706	97.4606	85.6401	110.051	122.378	110.842	107.806	84.8108	110.49
25	Bale	99.9417	92.7994	89.7566	99.6333	83.0967	109.469	129.903	104.865	105.032	88.0455	110.979
26	Metekel	101.178	105.297	89.6612	93.7265	95.6016	97.6935	115.993	106.147	109.484	84.3338	95.635
27	Asosa	99.8048	105.563	93.7033	92.8393	93.8746	96.5434	111.86	105.331	111.347	87.4407	103.105
28	Gurage	110.82	108.919	72.4612	89.3189	90.9173	108.798	120.054	99.9542	118.197	76.2297	124.465
29	Hadiya	117.947	110.442	84.2983	84.4413	94.2231	103.592	125.313	98.336	127.389	84.128	117.11
30	KAT	108.35	107.315	87.897	91.2463	95.4404	99.4333	120.475	98.0438	118.709	90.7191	101.924
31	Sidama	100.023	102.086	84.8448	95.5659	89.6421	101.475	129.183	103.399	114.005	76.5097	110.608
32	Gedio	97.4049	99.4234	98.2576	96.3812	98.4315	94.3449	112.799	101.977	103.61	90.2221	95.5655
33	South Omo	60.6977	89.6257	107.628	103.262	77.9464	98.2367	125.971	130.794	91.8145	72.8017	99.8487
34	Bench Maji	83.8378	105.627	91.7039	96.4502	92.6049	96.1979	119.45	111.814	99.9995	88.0341	97.1106
35	Yem	115.131	109.989	82.1389	87.0066	96.6825	109.317	120.857	93.4206	121.754	77.8704	113.241
36	Amaro	99.0891	104.001	91.1571	98.1908	88.4421	101.418	114.637	123.933	99.4682	71.8372	98.6425
37	Burji	84.2806	97.2202	94.1841	96.1215	87.9337	105.738	126.037	125.861	102.236	71.8814	100.675
38	Konso	59.9911	93.1674	103.668	96.19	71.6544	106.531	133.495	142.154	95.5062	60.4325	99.5143
39	Derashe	82.0599	104.546	100.53	94.4795	74.8182	95.7863	127.866	129.792	102.115	68.6906	100.818
40	Hareri	104.45	81.91	94.0053	92.8307	84.5608	109.495	123.96	108.886	120.696	96.7037	116.992
41	Dire Dawa	104.031	90.2842	77.9437	98.6839	85.9972	113.418	121.886	114.288	109.735	82.3724	129.153
42	Region 14	118.535	107.861	68.9872	93.8993	99.6209	116.077	109.925	104.134	99.1777	84.2784	121.581

Appendix 3: Average Zonal Cereal Yield for the year 2000 to 2010.

Table 3-1: Original Zonal Cereal Yield for the year 2000 to 2010

No	ZONENAME	Years										
		2000	2001	2002	2003	2004	2005	2006	2007	2008	2009	2010
1	Western	13.05	13.94		13.10	10.53	13.32	14.14	14.01	16.86		18.49
2	Central	11.29	9.77		9.12	8.22	11.89	10.93	11.99	13.50		18.62
3	Eastern	9.98	12.12		12.22	8.54	11.93	13.38	17.06	13.37		18.21
4	Southern	11.03	13.93		11.38	9.00	13.18	14.92	14.36	13.94		16.16
5	North Gonder	7.84	11.21		9.85	13.53	13.47	15.01	13.46	16.49		19.87
6	South Gonder	7.33	10.07		8.42	7.48	10.46	10.71	12.04	12.86		16.38
7	North Wollo	10.88	11.80		12.95	10.85	12.21	12.46	17.21	15.35		15.99
8	South Wollo	10.95	11.74		12.94	13.83	13.11	13.13	13.46	13.30		16.18
9	North Shewa(R3)	8.88	10.96		12.97	13.18	17.21	19.51	13.56	14.11		17.29
10	East Gojam	11.96	13.52		11.45	13.40	12.26	13.59	15.87	16.40		16.31
11	West Gojam	11.90	15.76		13.13	13.38	15.33	16.82	19.75	18.96		19.38
12	Wag Himra	7.30	7.23		7.01	5.35	11.92	12.32	10.36	12.08		14.78
13	Awi/Agew	9.89	14.00		11.93	12.32	12.79	14.06	16.24	14.86		16.41
14	East Wellega	14.37	17.48		13.95	14.59	17.49	16.95	17.91	17.98		21.68
15	Oromia	12.68	11.52		11.92	11.32	14.58	14.49	15.37	14.34		17.61
16	West Wellega	14.69	15.90		14.64	18.09	18.22	16.36	16.66	16.57		19.47
17	Ilubabor	13.75	14.52		13.20	13.66	14.80	16.61	16.52	17.88		20.41
18	Jimma	11.79	16.17		12.57	15.36	13.61	14.38	15.42	16.40		18.04
19	West Shewa	11.27	15.43		14.67	15.47	18.03	18.22	14.54	16.48		19.99
20	East Shewa	13.43	15.85		15.99	13.58	19.96	19.93	17.67	17.88		17.39
21	North Shewa(R4)	9.40	9.75		10.09	10.68	11.53	11.23	11.86	13.77		14.81
22	Arsi	12.15	16.98		17.98	18.03	15.92	15.37	15.42	18.93		21.53
23	West Harerge	17.47	14.79		14.76	12.35	13.75	15.01	21.12	15.72		18.32
24	East Harerge	13.14	14.40		15.74	12.37	12.06	16.29	25.82	15.78		20.05
25	Bale	13.58	14.21		15.75	15.38	15.13	16.95	18.79	20.40		18.98
26	Metekel	11.85	13.49		13.64	12.58	14.48	17.29	15.30	18.77		16.95
27	Asosa	11.67	11.05		9.17	10.70	11.77	12.36	14.62	15.12		16.75
28	Gurage	12.42	13.34		14.63	16.33	14.27	15.64	16.94	17.48		20.07
29	Hadiya	11.88	13.85		13.42	13.88	14.58	15.14	13.64	17.09		15.03
30	KAT	11.61	13.81		14.75	12.78	13.33	12.53	19.92	16.17		14.08
31	Sidama	13.38	15.52		16.70	16.25	16.81	16.70	19.92	19.85		20.22
32	Gedio	13.66	15.32		15.08	16.66	15.80	18.94	13.24	13.88		17.81
33	South Omo	8.27	10.95		8.04	11.18	8.60	9.72	11.02	15.26		19.93
34	Bench Maji	13.49	14.25		10.02	8.53	14.18	15.60	17.48	15.75		19.48
35	Yem	8.25	9.66		9.56	10.03	11.19	11.51	10.83	12.05		12.91
36	Amaro	4.85	9.86		5.75	10.76	6.11	6.10	10.18	12.22		12.05
37	Burji	6.18	8.01		5.47	14.11	4.77	4.75	9.43	12.78		10.32
38	Konso	4.90	4.73		2.11	7.55	4.64	4.85	11.53	15.00		13.54
39	Derashe	7.72	8.37		4.35	10.21	9.22	8.54	12.40	15.70		11.74
40	Hareri	8.96	12.68		8.75	6.26	9.58	12.56	12.84	16.33		15.41
41	Dire Dawa	10.12	13.87		11.02	6.62	10.14	12.32	13.44	13.60		17.18

Table 3-2: Detrended Zonal Cereal Yield for the year 2000 to 2010

No	ZONENAME	Years										
		2000	2001	2002	2003	2004	2005	2006	2007	2008	2009	2010
1	Western	1.209	0.529		-0.149	-1.665	-1.798	-1.611	-1.850	1.341		-0.313
2	Central	-0.507	-3.613		-4.044	-3.965	-3.125	-4.718	-3.823	-2.026		-0.098
3	Eastern	-1.772	-1.221		-0.877	-3.645	-2.974	-2.182	1.283	-2.163		-0.427
4	Southern	-0.678	0.618		-1.635	-3.175	-1.617	-0.540	-1.383	-1.600		-2.405
5	North Gonder	-3.824	-2.064		-3.084	1.360	-1.228	-0.356	-2.249	0.945		1.384
6	South Gonder	-4.290	-3.175		-4.441	-4.683	-4.129	-4.556	-3.625	-2.684		-2.023
7	North Wollo	-0.695	-1.408		0.164	-1.311	-2.276	-2.711	1.583	-0.203		-2.330
8	South Wollo	-0.581	-1.433		0.228	1.683	-1.272	-1.954	-2.133	-2.262		-2.064
9	North Shewa(R3)	-2.607	-2.176		0.335	1.038	2.936	4.525	-1.995	-1.454		-0.874
10	East Gojam	0.517	0.418		-1.103	1.266	-1.913	-1.303	0.350	0.828		-1.780
11	West Gojam	0.501	2.685		0.650	1.250	1.267	2.029	4.276	3.376		1.372
12	Wag Himra	-4.054	-5.804		-5.388	-6.774	-2.042	-2.379	-5.078	-3.507		-3.151
13	Awi/Agew	-1.420	1.003		-0.398	0.196	-1.065	-0.537	0.833	-0.735		-1.442
14	East Wellega	3.104	4.511		1.705	2.478	3.738	2.445	2.544	2.378		3.911
15	Oromia	1.458	-1.412		-0.251	-0.788	0.935	0.075	0.039	-1.259		-0.079
16	West Wellega	3.513	2.998		2.543	5.989	4.679	2.045	1.368	0.964		1.856
17	Ilubabor	2.617	1.651		1.182	1.566	1.366	2.393	1.271	2.264		2.882
18	Jimma	0.701	3.345		0.625	3.271	0.280	0.259	0.205	0.774		0.584
19	West Shewa	0.225	2.632		2.799	3.388	4.805	4.189	-0.638	0.850		2.618
20	East Shewa	2.429	3.088		4.197	1.505	6.837	5.994	2.531	2.245		0.099
21	North Shewa(R4)	-1.556	-2.979		-1.621	-1.396	-1.482	-2.610	-3.246	-1.870		-2.406
22	Arsi	1.238	4.291		6.347	5.961	3.010	1.629	0.356	3.280		4.394
23	West Harerge	6.602	2.133		3.203	0.291	0.942	1.360	6.094	0.069		1.261
24	East Harerge	2.316	1.771		4.257	0.317	-0.637	2.737	10.835	0.122		3.073
25	Bale	2.801	1.617		4.343	3.336	2.531	3.498	3.836	4.737		2.077
26	Metekel	1.115	0.937		2.310	0.537	1.994	3.929	0.381	3.096		0.133
27	Asosa	0.979	-1.468		-2.078	-1.337	-0.620	-0.905	-0.258	-0.554		0.010
28	Gurage	1.773	0.848		3.453	4.299	1.989	2.474	2.104	1.797		3.413
29	Hadiya	1.277	1.402		2.324	1.860	2.402	2.072	-1.157	1.402		-1.551
30	KAT	1.052	1.393		3.725	0.765	1.262	-0.445	5.155	0.478		-2.423
31	Sidama	2.866	3.140		5.756	4.239	4.846	3.816	5.192	4.146		3.793
32	Gedio	3.190	2.968		4.215	4.653	3.944	6.150	-1.447	-1.829		1.467
33	South Omo	-2.156	-1.365		-2.747	-0.817	-3.155	-2.965	-3.630	-0.451		3.667
34	Bench Maji	3.109	1.974		-0.698	-3.457	2.527	3.006	2.869	0.029		3.296
35	Yem	-2.087	-2.585		-1.077	-1.959	-0.352	-0.990	-3.747	-3.675		-3.193
36	Amaro	-5.443	-2.352		-4.815	-1.218	-5.326	-6.304	-4.359	-3.515		-3.975
37	Burji	-4.069	-4.170		-5.012	2.137	-6.569	-7.556	-5.070	-2.958		-5.631
38	Konso	-5.305	-7.414		-8.295	-4.416	-6.592	-7.359	-2.933	-0.745		-2.327
39	Derashe	-2.440	-3.738		-5.981	-1.755	-1.904	-3.577	-2.024	-0.045		-4.050
40	Hareri	-1.156	0.604		-1.505	-5.695	-1.441	0.539	-1.550	0.574		-0.296
41	Dire Dawa	0.048	1.824		0.839	-5.330	-0.774	0.397	-0.909	-2.161		1.548

Appendix 4: Average Zonal Teff Yield for the year 2000 to 2010.

Table 4-1: Original Teff Yield for the year 2000 to 2010

No	ZONENAME	Years										
		2000	2001	2002	2003	2004	2005	2006	2007	2008	2009	2010
1	Western	10.4	8.08		7.33	7.34	9.21	9.07	12.78	16.72		10.46
2	Central	8.07	7.01		7.13	6.78	8.7	8.74	10.03	11.67		13.72
3	Southern	9.71	9.88		8.25	4.73	9.04	11.53	11.26	10.89		12.5
4	North Gonder	6.17	8		7.1	9.96	8.57	8.72	10.85	12.22		13.41
5	South Gonder	6.77	7.98		7.33	6.81	8.8	8.12	9.21	10.54		12.58
6	North Wollo	8.7	8.54		10.26	9.23	8.51	9.78	13.1	13.91		11.78
7	South Wollo	10.16	8.88		9.84	11.59	10.18	11.17	11.19	11.4		12.51
8	North Shewa(R3)	7.08	8.01		9.84	10.46	13.96	15.98	12.11	12.27		10.98
9	East Gojam	10.48	11.6		10.78	11.66	10.01	10.9	13.61	12.5		14
10	West Gojam	6.96	8.7		8.11	8.22	8.44	8.34	15.31	14.66		12.42
11	Wag Himra	6.64	5.72		5.38	3.79	9.75	10.25	9.34	11.23		10.87
12	Awi/Agew	6.9	7.96		7.1	8.68	7.34	7.82	9.93	11.14		11.67
13	East Wellega	8.01	9.47		7.4	10.62	9.62	8	12.17	13.09		11.8
14	Oromia	7.46	8.79		8.62	9.61	11.96	13.14	11.46	10.03		13.25
15	West Wellega	4.69	6.86		7.67	8.31	8.92	5.07	9.99	10.26		9.67
16	Ilubabor	7.38	8.84		8.63	11.18	9.44	9.55	14.67	12.06		10.84
17	Jimma	6.35	9.36		8.33	9.47	7.83	7.99	10.51	10.53		12.24
18	West Shewa	9.91	11.21		10.13	12.35	13.44	13.5	11.28	11.95		13.74
19	East Shewa	8.62	8.68		7.99	10.89	13.72	14.82	12.81	11.6		13.95
20	North Shewa(R4)	8.63	8.15		8.57	10.11	9.35	9.43	9.74	11.56		13.88
21	Arsi	7.74	9.25		8.74	8.96	7.83	7.47	10.45	10.33		12.71
22	West Harerge	8.46	11.58		14.65	9.04	9.8	9.21	12.58	9.62		9.3
23	Bale	10.62	6.7		5.24	6.33	6.41	9.32	9.73	10.87		11.49
24	Metekel	7.84	8.89		9.24	11.66	9.49	10.86	11.87	10.32		10.95
25	Asosa	3.58	3.65		2.51	2.86	3.22	3.9	7.07	9.76		4.53
26	Gurage	6.26	7		7.57	9.76	7.74	9.07	10.67	9.78		11.46
27	Hadiya	7.33	9.33		7.49	9.7	8.27	7.94	9.68	10.66		11.28
28	South Omo	8.24	8.2		5.41	5.08	7.61	7.35	13.61	10.86		6.24
29	Bench Maji	3.7	6.19		6.4	6.66	8.08	7.9	12.07	9.59		14.7
30	Yem	7.26	8.42		7.4	7.04	8.34	8.91	8.03	10.66		9.91
31	Amaro	4.12	9.29		2.83	12.33	5.88	5.91	10.1	12.1		10.51
32	Burji	4.8	6		3.88	14.64	5.16	4.02	6.1	10.77		7.65
33	Derashe	5.41	7.91		3.91	8.14	8.51	7.84	10.28	10.89		12.3

Table 4-2: Detrended Teff Yield for the year 2000 to 2010

No	ZONENAME	Years										
		2000	2001	2002	2003	2004	2005	2006	2007	2008	2009	2010
1	Western	1.521	-0.685		-1.871	-1.043	-1.070	-1.767	0.636	3.971		-2.401
2	Central	-0.717	-1.726		-1.971	-1.635	-1.492	-1.991	-2.044	-0.995		0.944
3	Southern	1.015	1.173		-0.752	-3.718	-1.065	0.905	-0.743	-1.691		-0.190
4	North Gonder	-2.433	-0.679		-1.802	1.479	-1.448	-1.799	-1.083	-0.277		0.805
5	South Gonder	-1.741	-0.670		-1.473	-1.704	-1.131	-2.293	-2.652	-1.873		0.061
6	North Wollo	0.281	-0.082		1.557	0.683	-1.333	-0.527	1.308	1.581		-0.654
7	South Wollo	1.833	0.287		1.237	3.010	0.424	0.969	-0.532	-0.846		0.162
8	North Shewa(R3)	-1.155	-0.554		1.336	1.847	4.291	5.885	0.459	0.108		-1.283
9	East Gojam	2.337	3.064		2.376	3.014	0.429	0.911	2.029	0.422		1.823
10	West Gojam	-1.091	0.193		-0.195	-0.459	-1.054	-1.542	3.799	2.666		0.328
11	Wag Himra	-1.319	-2.759		-2.825	-4.921	0.343	0.474	-2.100	-0.680		-1.137
12	Awi/Agew	-0.967	-0.490		-1.006	-0.064	-1.979	-1.850	-1.440	-0.686		-0.251
13	East Wellega	0.235	1.049		-0.606	1.843	0.388	-1.564	0.871	1.347		-0.036
14	Oromia	-0.223	0.397		0.713	0.800	2.815	3.682	0.231	-1.629		1.500
15	West Wellega	-2.901	-1.504		-0.137	-0.533	-0.137	-4.282	-1.169	-1.315		-1.995
16	Ilubabor	-0.120	0.504		0.923	2.304	0.470	0.304	3.582	0.569		-0.739
17	Jimma	-1.058	1.053		0.722	0.561	-1.053	-1.150	-0.508	-0.877		0.746
18	West Shewa	2.594	2.932		2.622	3.408	4.645	4.466	0.333	0.627		2.332
19	East Shewa	1.396	0.430		0.581	1.915	5.012	5.892	1.933	0.360		2.627
20	North Shewa(R4)	1.498	-0.071		1.261	1.103	0.729	0.608	-1.067	0.404		2.642
21	Arsi	0.700	1.057		1.530	-0.080	-0.703	-1.246	-0.286	-0.742		1.558
22	West Harerge	1.512	3.416		7.540	-0.033	1.354	0.600	1.914	-1.368		-1.767
23	Bale	3.764	-1.435		-1.771	-2.776	-1.949	0.816	-0.866	-0.034		0.509
24	Metekel	1.076	0.783		2.329	2.521	1.218	2.462	1.345	-0.500		0.054
25	Asosa	-3.092	-4.428		-4.301	-6.312	-4.964	-4.391	-3.385	-0.977		-6.280
26	Gurage	-0.320	-1.050		0.858	0.555	-0.357	0.885	0.286	-0.873		0.735
27	Hadiya	0.842	1.309		0.878	0.462	0.260	-0.139	-0.634	0.091		0.640
28	South Omo	1.844	0.208		-1.103	-4.191	-0.312	-0.623	3.366	0.375		-4.314
29	Bench Maji	-2.604	-1.774		-0.013	-2.643	0.245	0.033	1.897	-0.811		4.231
30	Yem	1.048	0.485		1.086	-2.296	0.592	1.149	-2.073	0.343		-0.473
31	Amaro	-2.000	1.383		-3.384	2.961	-1.780	-1.745	0.067	1.866		0.212
32	Burji	-1.228	-1.878		-2.234	5.238	-2.413	-3.529	-3.862	0.620		-2.562
33	Derashe	-0.526	0.061		-2.105	-1.295	1.024	0.397	0.388	0.824		2.173

Appendix 5: Average Zonal Barley Yield for the year 2000 to 2010.

Table 5-1: Original Barley Yield for the year 2000 to 2010

No	ZONENAME	Years										
		2000	2001	2002	2003	2004	2005	2006	2007	2008		2010
1	Central	10.32	8.79		9.27	9.93	10.14	9.43	11.37	13.52		17.25
2	Eastern	10.8	12.41		12.7	8.68	12.06	13.63	12.67	14.58		18.39
3	Southern	10.23	11.27		10.4	7.08	10.93	11.84	15.4	16.23		18.14
4	North Gonder	5.46	10.67		10.36	10.56	12.54	13.73	12.54	14.47		17.33
5	South Gonder	6.45	9.55		8.61	6.84	9.82	10.11	8.95	11.43		13.23
6	South Wollo	8.95	13.36		13.53	15.34	12.55	12	12.44	12.46		13.07
7	North Shewa(R3)	7.74	10.72		11.8	12.69	17.22	17.54	14.08	17.05		14.42
8	East Gojam	8.57	11.54		9.53	11.78	10.18	12.38	11.83	13.69		11.66
9	West Gojam	5.81	11.44		7.51	9.7	12.67	14.7	10.13	11.33		11.25
10	Wag Himra	6.92	7.51		9.06	8.21	11.45	12.51	8.98	9.73		13.7
11	Awi/Agew	7.75	11.32		11.04	10.53	7.95	10.43	11.71	13		7.69
12	East Wellega	11.11	11.38		11.06	8.57	11.27	8.34	10.65	12.69		14.01
13	Oromia	8.87	10.88		9.95	7.12	11.28	11.05	11.12	15.02		10.43
14	West Wellega	6.82	8.01		8.16	10.86	9.02	12.1	10.76	9.45		8.09
15	Ilubabor	7.43	7.33		6.77	7.07	8	9.27	10.86	12.62		11.06
16	Jimma	8.69	11.77		9.1	8.94	7.77	9.15	13.15	11.06		12.74
17	West Shewa	8.66	12.89		12.74	11.97	16.02	16.05	12.85	16.84		15.79
18	East Shewa	9.71	14.57		14.85	12.69	16.32	17.48	15.19	12.78		12.47
19	North Shewa(R4)	8.81	9.3		9.56	8.21	10.91	10.28	13.38	14.1		12.48
20	Arsi	10.62	15.91		16.41	18.81	14.54	14.68	16.45	17.93		23.75
21	Bale	12.66	13.92		16.91	16.44	15.17	18.13	18	18.83		16.66
22	Gurage	14.63	13		17.36	19.58	16.72	17.55	15.57	17.98		26.32
23	Hadiya	9.97	10.12		10.29	8.2	11.55	11.71	13.4	15.63		14.45
24	KAT	9.37	9.67		10.71	13.29	12.16	12.64	11.49	12		14.44
25	Bench Maji	7.41	8.85		6.56	7.19	9.15	8.76	14.26	11.2		15.42
26	Yem	6.62	8.58		8.22	9.62	8	8.25	9.54	9.1		9.5
27	Amaro	7.68	9.46		9.28	8.06	5.54	6.33	9.99	10.45		13.62
28	Burji	3.52	5.34		4.18	15.31	3.32	3.76	4.38	8.19		7.7
29	Derashe	7.93	6.41		6.55	9.98	8.62	9.2	11.13	9.07		9.8

Table 5-2: Detrended Barley Yield for the year 2000 to 2010

No	ZONENAME	2000	2001	2002	2003	2004	2005	2006	2007	2008	2009	2010
1	Central	1.639	-2.716		-1.738	0.482	-2.329	-3.853	-1.005	-0.810		2.366
2	Eastern	2.124	0.972		1.733	-0.864	-0.314	0.451	0.311	0.332		3.572
3	Southern	1.560	-0.100		-0.526	-2.561	-1.348	-1.235	3.057	2.064		3.388
4	North Gonder	-3.205	-0.632		-0.524	0.822	0.357	0.759	0.214	0.385		2.644
5	South Gonder	-2.209	-1.683		-2.233	-2.995	-2.267	-2.757	-3.360	-2.573		-1.390
6	South Wollo	0.297	2.195		2.728	5.409	0.558	-0.763	0.146	-1.462		-1.484
7	North Shewa(R3)	-0.908	-0.377		1.040	2.662	5.323	4.881	1.803	3.210		-0.068
8	East Gojam	-0.072	0.511		-1.189	1.655	-1.621	-0.176	-0.431	-0.068		-2.763
9	West Gojam	-2.827	0.480		-3.168	-0.521	0.964	2.248	-2.115	-2.347		-3.107
10	Wag Himra	-1.711	-3.382		-1.577	-2.108	-0.160	0.162	-3.249	-3.865		-0.591
11	Awi/Agew	-0.876	0.496		0.445	0.115	-3.565	-1.814	-0.502	-0.514		-6.535
12	East Wellega	2.490	0.625		0.506	-1.942	-0.150	-3.800	-1.546	-0.742		-0.149
13	Oromia	0.255	0.193		-0.563	-3.488	-0.044	-0.986	-1.060	1.670		-3.663
14	West Wellega	-1.789	-2.609		-2.311	0.155	-2.209	0.168	-1.404	-3.819		-5.937
15	Ilubabor	-1.174	-3.221		-3.660	-3.732	-3.133	-2.559	-1.287	-0.567		-2.901
16	Jimma	0.092	1.288		-1.289	-1.958	-3.268	-2.575	1.019	-2.046		-1.155
17	West Shewa	0.067	2.476		2.393	0.975	5.077	4.429	0.735	3.816		1.961
18	East Shewa	1.123	4.224		4.544	1.598	5.473	5.963	3.092	-0.162		-1.293
19	North Shewa(R4)	0.228	-0.978		-0.705	-2.979	0.158	-1.133	1.298	1.239		-1.217
20	Arsi	2.044	5.701		6.187	7.525	3.883	3.371	4.384	5.151		10.119
21	Bale	4.089	3.779		6.728	5.058	4.609	6.924	5.950	6.132		3.095
22	Gurage	6.065	2.927		7.219	8.101	6.254	6.448	3.537	5.364		12.821
23	Hadiya	1.410	0.115		0.190	-3.375	1.180	0.712	1.383	3.096		1.017
24	KAT	0.816	-0.266		0.652	1.618	1.885	1.746	-0.511	-0.453		1.073
25	Bench Maji	-1.139	-1.018		-3.457	-4.579	-1.030	-2.030	2.276	-1.171		2.119
26	Yem	-1.923	-1.220		-1.756	-2.246	-2.084	-2.436	-2.428	-3.190		-3.735
27	Amaro	-0.858	-0.271		-0.654	-3.902	-4.449	-4.252	-1.962	-1.758		0.451
28	Burji	-5.012	-4.323		-5.713	3.251	-6.573	-6.719	-7.556	-3.936		-5.403
29	Derashe	-0.596	-3.185		-3.302	-2.176	-1.178	-1.175	-0.789	-2.975		-3.237

Appendix 6: Average Zonal Wheat Yield for the year 2000 to 2010.

Table 6-1: Original Wheat Yield for the year 2000 to 2010

No	ZONENAME	Years										
		2000	2001	2002	2003	2004	2005	2006	2007	2008	2009	2010
1	Central	11.61	9.85		11.23	11.82	12.01	12.17	13.85	16.44		20.06
2	Eastern	9.14	12.08		13.25	9.43	12.01	14.33	14.4	10.52		19.61
3	Southern	10.49	12.45		11.29	9.26	13.61	15.82	14.32	14.55		18.54
4	North Gonder	7.18	9.67		11.1	12.92	13.22	15.53	13.05	14.9		19.49
5	South Gonder	7.13	10.3		8.59	7.54	9.83	10.41	11.68	12.5		17.14
6	North Wollo	10.07	11.62		15.28	11.89	12.31	12.31	12.74	15.02		13.41
7	South Wollo	12.41	12.2		12.17	15.36	12.36	13.63	14.35	15.94		14.14
8	East Gojam	11.9	15.7		13.04	16.44	13.68	13.65	19.77	19.04		16.95
9	West Gojam	9.36	15.68		15.83	21.38	17.29	16.09	20.03	17.12		17.1
10	Wag Himra	8.84	7.72		8.14	8.55	11.5	14.07	10.85	10.25		12.11
11	Awi/Agew	6.89	11.98		11.48	9.23	9.65	11.63	16.95	13.18		13.67
12	Jimma	9.65	12.71		11.18	15.12	10.88	12.13	16.34	14.51		14.21
13	West Shewa	10.54	15.64		15.37	18.84	19.26	21.65	15.03	17.81		18.26
14	East Shewa	14.63	15.77		17.21	15.84	19.81	23.37	16.6	19.32		17.77
15	North Shewa(R4)	10.79	10.52		10.73	11.6	13.11	14.17	12.46	15.19		13.25
16	Arsi	13.19	17.65		20	20.63	17.48	16.79	16.44	21.14		21.94
17	Bale	14.87	16.76		17.72	17.26	16.14	18.12	21.83	23.85		23.19
18	Gurage	9.93	13		18.77	20.84	17.47	19.11	17.58	21.52		21.26
19	Hadiya	12.87	17.21		18.12	16.26	18.44	18.74	19.06	22.07		18.74
20	KAT	11.84	15.65		19.83	16.39	17.9	17.63	14	17.52		17.38
21	Yem	7.81	9.63		11.15	11.32	11.83	12.58	13.67	13.51		13.81
22	Burji	3.88	4.48		6.22	10.27	3.35	3.27	4.55	10.36		6.83

Table 6-2: Detrended Wheat Yield for the year 2000 to 2010

No	ZONENAME	Years										
		2000	2001	2002	2003	2004	2005	2006	2007	2008	2009	2010
1	Central	1.639	-1.983		-0.244	0.356	-0.663	-1.947	-1.043	2.360		2.160
2	Eastern	-0.856	0.169		1.580	-2.276	-0.768	0.141	-0.501	-3.762		1.818
3	Southern	0.470	0.462		-0.576	-2.688	0.727	1.559	-0.589	0.067		0.856
4	North Gonder	-2.865	-2.396		-0.962	0.729	0.231	1.197	-1.868	0.216		1.914
5	South Gonder	-2.939	-1.844		-3.668	-4.893	-3.264	-3.995	-3.246	-2.385		-0.328
6	North Wollo	-0.024	-0.601		2.826	-0.786	-0.890	-2.167	-2.194	-0.067		-3.950
7	South Wollo	2.292	-0.099		-0.480	2.442	-0.945	-0.919	-0.592	0.652		-3.112
8	East Gojam	1.758	3.323		0.194	3.280	0.270	-0.971	4.819	3.551		-0.194
9	West Gojam	-0.807	3.226		2.788	7.977	3.774	1.397	5.071	1.429		0.064
10	Wag Himra	-1.351	-4.812		-5.098	-5.095	-2.121	-0.695	-4.117	-5.642		-4.818
11	Awi/Agew	-3.326	-0.630		-1.954	-4.657	-4.076	-3.207	1.975	-2.913		-3.150
12	Jimma	-0.590	0.023		-2.450	0.990	-2.952	-2.779	1.356	-1.784		-2.502
13	West Shewa	0.275	2.875		1.544	4.468	5.323	6.669	0.038	1.314		1.656
14	East Shewa	4.341	2.927		3.188	1.225	5.767	8.317	1.600	2.623		1.274
15	North Shewa(R4)	0.476	-2.400		-3.488	-3.257	-1.038	-0.955	-2.548	-1.708		-3.138
16	Arsi	2.852	4.652		5.586	5.531	3.227	1.593	1.423	4.041		5.660
17	Bale	4.507	3.684		3.110	1.918	1.781	2.851	6.805	6.549		7.017
18	Gurage	-0.457	-0.153		3.964	5.256	3.006	3.769	2.547	4.018		5.195
19	Hadiya	2.458	3.979		3.118	0.434	3.871	3.327	4.018	4.367		2.783
20	KAT	1.404	2.341		4.632	0.321	3.225	2.145	-1.050	-0.384		1.531
21	Yem	-2.651	-3.756		-4.244	-4.991	-2.950	-2.977	-1.388	-4.596		-1.931
22	Burji	-6.605	-8.984		-9.370	-6.284	-11.535	-12.359	-10.516	-7.947		-8.803

Appendix 7: Average Zonal Maize Yield for the year 2000 to 2010.

Table 7-1: Original Maize Yield for the year 2000 to 2010

No	ZONENAME	Years										
		2000	2001	2002	2003	2004	2005	2006	2007	2008	2009	2010
1	Western	19.45	19.78		17.49	14.08	18.76	20.88	15.33	20.25		25.93
4	Southern	16.86	15.49		10.3	7.1	17.29	17.93	14.66	15.68		21.64
5	North Gonder	10.58	16.72		13.17	19.31	20.01	22.24	17.78	22.55		23.66
6	South Gonder	11.18	16.16		11.8	10.66	15.13	15.99	16.07	16.93		22.11
8	South Wollo	12.7	16.13		13.93	9.79	16.1	16.3	20.03	15.09		22.38
9	North Shewa(R3)	12.07	10.05		12.07	12.29	18.69	20.62	16.24	18.55		21.23
10	East Gojam	17.95	20.37		14.63	18.05	17.93	22.91	21.87	28.04		25.91
11	West Gojam	20.2	26.02		22.11	19.35	24.18	26.55	27.64	26.04		27.63
12	Wag Himra	11	6.61		8.8	4.34	11.27	12.55	12.69	13.01		14.65
13	Awi/Agew	17.62	28.4		21.43	20.51	25.11	24.89	25.56	20.8		28.66
14	East Wellega	23.5	28.36		20.42	23	26.55	25.81	24.9	23.57		28.26
15	Oromia	17.8	10.97		16.66	11.61	16.86	14.92	16.97	17.02		17.95
16	West Wellega	21.78	22.33		19.51	21.11	25	22.79	21.7	23.25		26.68
17	Ilubabor	18.84	19.83		17.26	15.76	20.75	21.2	19.06	22.71		26.83
18	Jimma	19.9	24.22		18.73	22.86	23.47	23.44	20.89	24.82		26.09
19	West Shewa	22.25	28.23		20.89	19.42	27.59	23.58	21.46	24.01		29.92
20	East Shewa	18.25	22.3		23.67	15.95	27.94	28.53	27.26	27.14		23.9
21	North Shewa(R4)	10.09	14.99		10.61	11.86	10.56	11.11	15.81	17.62		23.1
22	Arsi	16.18	22.42		21.99	20.03	23.14	19.83	18.58	22.59		24.69
23	West Harerge	19.58	16.79		16.33	12.22	16.87	17.56	19.48	17.49		18.93
24	East Harerge	13.91	19.69		19.77	13.27	18.89	21.26	24.57	21.83		22.17
25	Bale	14.04	19.68		15.74	15.65	19.02	19.87	19.5	26.98		18.19
26	Metekel	18.69	24.45		24.3	21.94	21.99	24.76	21.31	29.38		27.29
27	Asosa	15.98	16.01		12.55	15.91	16.06	15.43	18.41	19.91		25.95
28	Gurage	18.34	18		22.16	21.7	22.26	25.21	22.71	20.45		28.76
29	Hadiya	16.31	15.5		15.5	17.41	18.13	20.67	15.69	18.88		18.31
31	Sidama	14.51	17.91		19.85	19.47	21.14	20.97	22.05	21.4		27.53
33	South Omo	9.4	14.66		11.29	18.85	9.84	11.92	11.41	16.49		22.44
34	Bench Maji	20.27	16.2		10.3	8.53	19.29	24.19	16.52	18.33		27
35	Yem	13.46	13.14		12.22	13.92	19.45	18.44	14.29	14.2		18.7
37	Burji	15.72	16.89		8.99	17.81	5.74	6.89	15.67	17.57		14.63
38	Konso	8.12	7.52		3.9	9.75	6.56	7.36	14.53	17.35		18.03
39	Derashe	7.1	7.15		4.65	10.93	8.97	9.2	14.38	18.25		14.73
40	Hareri	11.46	8.75		13.02	8.83	13.01	16.19	16.59	20.24		20.04
41	Dire Dawa	9	12.82		12.77	10.92	12.17	11.18	19.71	12.34		15.77

Table 7-2: Detrended Maize Yield for the year 2000 to 2010

No	ZONENAME	Years										
		2000	2001	2002	2003	2004	2005	2006	2007	2008	2009	2010
1	Western	1.659	-0.985	-0.501	-0.017	-1.457	-3.136	-1.743	-4.858	-1.322	-0.407	0.509
4	Southern	-0.799	-5.086	-6.084	-7.083	-8.421	-4.387	-4.476	-5.452	-5.818	-4.724	-3.630
5	North Gonder	-6.947	-3.667	-3.878	-4.089	3.805	-1.447	0.050	-2.256	1.127	-0.166	-1.458
6	South Gonder	-6.215	-4.039	-4.687	-5.334	-4.829	-6.107	-5.984	-3.890	-4.419	-3.638	-2.857
8	South Wollo	-4.563	-3.880	-3.480	-3.080	-5.683	-4.918	-5.458	0.146	-6.185	-4.310	-2.436
9	North Shewa(R3)	-5.061	-9.772	-7.294	-4.816	-3.166	-2.108	-0.922	-3.568	-2.650	-3.042	-3.434
10	East Gojam	0.951	0.737	-0.697	-2.132	2.610	-2.649	1.584	2.138	6.914	4.156	1.397
11	West Gojam	3.334	6.576	6.024	5.473	3.926	3.821	5.441	7.984	4.989	4.129	3.268
12	Wag Himra	-5.734	-12.646	-10.179	-7.713	-11.068	-8.870	-8.343	-6.890	-7.967	-8.764	-9.560
13	Awi/Agew	1.018	9.333	7.187	5.041	5.118	5.190	4.213	6.056	-0.103	2.249	4.601
14	East Wellega	7.030	9.481	6.819	4.156	7.624	6.850	5.349	5.472	2.742	3.547	4.352
15	Oromia	1.462	-7.720	-3.600	0.520	-3.750	-2.621	-5.325	-2.381	-3.734	-4.770	-5.806
16	West Wellega	5.574	3.829	3.661	3.494	5.767	5.739	2.761	2.425	2.571	2.823	3.075
17	Ilubabor	2.766	1.517	1.443	1.368	0.433	1.708	1.388	-0.139	2.105	2.741	3.376
18	Jimma	3.958	6.096	4.529	2.963	7.549	4.648	3.844	1.767	4.289	3.539	2.788
19	West Shewa	6.440	10.295	7.771	5.247	4.125	8.987	4.200	2.413	3.554	5.161	6.769
20	East Shewa	2.572	4.553	6.352	8.151	0.671	9.557	9.366	8.289	6.758	3.829	0.900
21	North Shewa(R4)	-5.455	-2.568	-3.676	-4.785	-3.403	-7.603	-7.838	-3.085	-2.687	-1.218	0.252
22	Arsi	0.767	5.050	5.885	6.720	4.784	5.196	1.098	-0.239	2.357	2.175	1.993
23	West Harerge	4.299	-0.391	0.396	1.184	-3.010	-0.854	-0.955	0.737	-2.669	-3.142	-3.616
24	East Harerge	-1.239	2.698	3.723	4.748	-1.944	1.385	2.961	5.903	1.746	0.761	-0.224
25	Bale	-0.977	2.876	1.859	0.843	0.452	1.735	1.787	0.910	6.970	1.459	-4.053
26	Metekel	3.805	7.835	8.681	9.527	6.758	4.924	6.893	2.796	9.445	7.321	5.198
27	Asosa	1.227	-0.417	-1.258	-2.099	0.744	-0.786	-2.221	-0.028	0.049	2.029	4.010
28	Gurage	3.719	1.762	4.699	7.635	6.551	5.634	7.776	4.348	0.663	3.817	6.971
29	Hadiya	1.821	-0.549	0.275	1.100	2.277	1.723	3.452	-2.596	-0.832	-2.080	-3.328
31	Sidama	0.153	2.049	3.812	5.574	4.353	4.953	3.968	3.840	1.762	3.903	6.044
33	South Omo	-4.824	-1.012	-1.937	-2.862	3.749	-6.128	-4.866	-6.724	-3.074	-0.984	1.105
34	Bench Maji	6.178	0.716	-1.506	-3.728	-6.555	3.542	7.620	-1.538	-1.159	2.329	5.816
35	Yem	-0.500	-2.155	-1.919	-1.683	-1.149	3.921	2.086	-3.692	-5.215	-3.774	-2.332
37	Burji	1.892	1.784	-1.503	-4.789	2.758	-9.569	-9.247	-2.236	-1.770	-4.011	-6.251
38	Konso	-5.576	-7.398	-8.576	-9.755	-5.286	-8.529	-8.561	-3.300	-1.916	-2.308	-2.700
39	Derashe	-6.464	-7.579	-8.230	-8.880	-4.090	-5.900	-6.505	-3.373	-0.942	-3.395	-5.848
40	Hareri	-1.972	-5.791	-3.088	-0.386	-6.174	-1.640	0.701	-1.087	1.123	0.368	-0.387
41	Dire Dawa	-4.300	-1.532	-1.022	-0.512	-4.068	-2.261	-4.093	2.109	-6.703	-5.604	-4.506

Appendix 8: Average Zonal Sorghum Yield for the year 2000 to 2010.

Table 8-1: Original Sorghum Yield for the year 2000 to 2010

No	ZONENAME	Years										
		2000	2001	2002	2003	2004	2005	2006	2007	2008	2009	2010
1	Western	15.01	16.19	16.18	16.17	12.8	15.25	15.9	15.25	18.52	20.345	22.17
2	Central	9.29	12.38	11.385	10.39	7.76	14.9	12.84	13.76	15.22	19.35	23.48
3	Southern	12.42	23.43	21.62	19.81	18.47	18.69	20.79	18.28	16.05	15.665	15.28
4	North Gonder	9.1	12.7	11.605	10.51	15.57	15.54	17.18	15.01	18.62	20.47	22.32
5	North Wollo	13.07	14.21	15.09	15.97	14.09	14.68	14.38	21.01	16.47	19.865	23.26
6	South Wollo	11.9	13.59	15.315	17.04	14.75	16.69	15.53	16.45	13.22	18.175	23.13
7	North Shewa(R3)	9.79	13.16	14.385	15.61	13.61	17.76	19.17	15.59	15.91	19.515	23.12
8	Wag Himra	7.39	8.8	7.81	6.82	2.28	14.41	13.46	12.6	14.41	16.22	18.03
9	East Wellega	14.5	20.24	18.315	16.39	14.65	19.59	20.36	16.49	18.53	21.44	24.35
10	Oromia	12.63	12.72	12.415	12.11	11.94	14.85	14.83	16.85	15.1	17.035	18.97
11	West Wellega	13.52	15.51	14.615	13.72	19.78	16.7	16.43	17.24	16.98	18.775	20.57
12	Ilubabor	12.37	13.34	13.3	13.26	14.71	16.32	18.77	16.23	20.1	23.175	26.25
13	Jimma	11.88	14.05	12.84	11.63	17.48	13.34	14.23	15.12	15.86	16.405	16.95
14	West Shewa	6	17.41	17.835	18.26	16.99	18.62	19.98	14.76	16.54	20.58	24.62
15	East Shewa	9.97	12.44	14.24	16.04	10.86	17.38	21.48	20.44	14.99	19.105	23.22
16	North Shewa(R4)	10.82	12.12	12.905	13.69	14.67	14.92	14.48	14.01	18.01	19.65	21.29
17	West Harerge	16.95	14.75	14.45	14.15	13.13	13.18	14.59	23.95	15.06	17.325	19.59
18	East Harerge	12.92	12.17	13.475	14.78	11.74	11.96	14.92	28.49	13.6	16.985	20.37
19	Metekel	12.3	13.83	14.07	14.31	9.48	14.51	16.58	15.29	17.68	16.725	15.77
20	Asosa	12.04	10.21	9.38	8.55	9.17	11.06	12.21	14.77	14.39	14.915	15.44
21	Hadiya	10.69	9.52	9.395	9.27	11.56	13.25	14.73	11.69	15.67	14.875	14.08
22	South Omo	7.68	8.93	7.315	5.7	6.57	7.84	8.9	8.17	16.02	17.28	18.54
23	Bench Maji	12.87	14.79	13.565	12.34	11.55	12.93	12.92	18.88	18.38	18.705	19.03
24	Yem	9.37	10.15	9.385	8.62	11.62	9.03	10.28	10.76	14.13	13.625	13.12
25	Burji	5.47	6.06	4.71	3.36	11.45	3.88	3.4	4.9	14.72	13.665	12.61
26	Konso	4.28	3.45	2.59	1.73	5.76	3.83	3.77	10.15	13.36	10.84	8.32
27	Derashe	8.17	8.94	6.54	4.14	10.6	9.57	8.4	10.84	17.6	12.77	7.94
28	Hareri	8.14	16.55	12.26	7.97	5.61	8.98	11.67	12.09	15.25	15.105	14.96

Table 8-2: Detrended Sorghum Yield for the year 2000 to 2010

No	ZONENAME	Years										
		2000	2001	2002	2003	2004	2005	2006	2007	2008	2009	2010
1	Western	2.318	-0.101		-0.615	-2.063	-3.358	-3.152	-2.835	1.779		-2.110
2	Central	-3.257	-3.661		-6.031	-6.898	-3.334	-5.865	-4.121	-1.473		-0.395
3	Southern	0.018	7.639		3.753	4.017	0.830	2.433	0.604	-0.594		-8.190
4	North Gonder	-3.157	-2.841		-5.183	1.322	-1.946	-0.830	-2.462	2.024		-0.745
5	North Wollo	0.958	-1.081		0.641	0.047	-2.432	-3.283	3.743	-0.077		0.600
6	South Wollo	-0.067	-1.451		2.075	0.912	-0.048	-1.785	-0.613	-3.278		0.875
7	North Shewa(R3)	-2.032	-1.631		1.010	-0.023	1.396	2.202	-1.268	-0.540		1.270
8	Wag Himra	-4.286	-5.741		-7.416	-11.148	-1.580	-3.161	-4.054	-1.991		-3.415
9	East Wellega	2.969	5.949		2.518	1.427	3.974	4.086	0.041	2.177		3.310
10	Oromia	1.244	-1.321		-1.398	-1.078	-0.392	-1.096	0.606	-1.204		-1.666
11	West Wellega	2.279	1.719		0.576	6.968	1.832	0.851	1.200	0.725		0.339
12	Ilubabor	1.274	-0.201		0.480	2.103	1.826	3.538	0.395	3.893		6.424
13	Jimma	0.929	0.759		-0.786	5.078	-0.780	-0.654	-0.511	-0.298		-2.471
14	West Shewa	-4.806	4.369		6.209	4.793	4.874	5.443	-0.666	0.430		5.604
15	East Shewa	-0.691	-0.351		4.353	-1.132	4.008	7.290	5.218	-1.071		4.609
16	North Shewa(R4)	0.304	-0.421		2.367	2.883	1.922	0.637	-1.007	1.998		3.084
17	West Harerge	6.579	2.459		3.191	1.548	0.556	1.095	9.137	-0.904		1.789
18	East Harerge	2.694	0.129		4.185	0.363	-0.290	1.772	13.882	-2.315		2.974
19	Metekel	2.219	2.039		4.079	-1.692	2.634	3.779	0.887	1.813		-1.222
20	Asosa	2.104	-1.331		-1.316	-1.797	-0.442	-0.244	0.571	-1.428		-1.147
21	Hadiya	0.899	-1.771		-0.232	0.798	2.122	2.624	-2.304	-0.100		-2.102
22	South Omo	-1.966	-2.111		-3.438	-3.986	-2.914	-2.859	-5.620	0.299		2.763
23	Bench Maji	3.369	3.999		3.566	1.199	2.550	1.508	5.295	2.708		3.658
24	Yem	0.014	-0.391		0.210	1.474	-0.976	-0.784	-2.621	-1.494		-1.847
25	Burji	-3.740	-4.231		-4.686	1.509	-5.752	-7.317	-8.276	-0.855		-1.952
26	Konso	-4.785	-6.591		-5.952	-3.976	-5.428	-6.600	-2.822	-2.167		-5.837
27	Derashe	-0.750	-0.851		-3.177	1.069	0.686	-1.623	-1.927	2.122		-5.812
28	Hareri	-0.635	7.009		1.017	-3.716	0.470	1.995	-0.472	-0.179		1.612

Appendix 9: Comparisons of correlation coefficients between standardized and median cereals yield (Qt/ha) anomalies

No	Zone	R2 from StandardizedCereals	R2 from Median Anomally
1	Western	0.0913	0.0178
2	Central	0.0723	0.0618
3	Eastern	0.6576	0.6576
4	Southern	0.527	0.527
5	North Gonder	0.2442	0.134
6	South Gonder	0.1136	0.1136
7	North Wollo	0.0223	0.0144
8	South Wollo	0.6495	0.3332
9	North Shewa(R3)	0.0055	0.0036
10	East Gojam	0.3644	0.3644
11	West Gojam	0.165	0.165
12	Wag Himra	0.4169	0.4169
13	Awi/Agew	0.0326	0.0326
14	East Wellega	0.6327	0.6327
15	Oromia	0.7332	0.7332
16	West Wellega	0.4062	0.4062
17	Ilubabor	0.411	0.411
18	Jimma	0.1458	0.1458
19	West Shewa	0.1799	0.1799
20	East Shewa	0.3406	0.3406
21	North Shewa(R4)	0.4514	0.4514
22	Arsi	0.4353	0.4353
23	West Harerge	0.1377	0.1377
24	East Harerge	0.0787	0.0787
25	Bale	0.009	0.009
26	Metekel	0.5977	0.5977
27	Asosa	0.4277	0.4277
28	Gurage	0.8178	0.8178
29	Hadiya	0.1484	0.1484
30	KAT	0.2651	0.2651
31	Sidama	0.0661	0.0661
32	Gedio	0.5117	0.5117
33	South Omo	0.2546	0.2546
34	Bench Maji	0.1903	0.1903
35	Yem	0.0086	0.0086
36	Amaro	0.4685	0.4685
37	Burji	0.4028	0.4028
38	Konso	0.0051	0.0051
39	Derashe	0.0526	0.0526
40	Hareri	0.3248	0.3248
41	Dire Dawa	0.1609	0.1609

Information Transfer Program Introduction

The University of Nebraska-Lincoln (UNL) Water Center is actively pursued its tradition of vigorous and diverse information transfer programming in 2011. USGS funding continues to help underwrite a wide variety of public and professional information, public relations and education efforts, including: (1) four quarterly issues of the Water Current newsletter, which are mailed to more than 2,700 subscribers and appears as an online pdf; (2) updated and reprinted Water Center fact sheets and online UNL water faculty directories database; (3) 24 press releases reporting on water-related research and outreach programming or promoting Water Center and UNL water-related educational activities; (4) supporting four internet web sites; (5) publicity and supporting materials for an annual water law conference, public lecture series, colloquium, brown bag lectures, water and natural resources tour to western Nebraska; and (6) coordinating UNL Extension's largest public display and student recruitment event of the year at the Husker Harvest Days farm show.

Late in the year, the UNL Water Center affiliated with the Robert B. Daugherty Water for Food Institute, a global imitative involving all University of Nebraska water-related faculty and staff with a mission of greater global agricultural water management efficiency ("More crop per drop") and is beginning to collaborate with that entity on national and international publicity and information campaigns. This relationship is expected to become stronger in the coming year.

Information Transfer Plan/Water Education

Basic Information

Title:	Information Transfer Plan/Water Education
Project Number:	2008NE173B
Start Date:	3/1/2010
End Date:	2/29/2012
Funding Source:	104B
Congressional District:	1
Research Category:	Not Applicable
Focus Category:	Education, None, None
Descriptors:	None
Principal Investigators:	Bruce Irvin Dvorak, Steven W. Ress

Publications

1. Newsletter: The Water Current newsletter has a free, subscriber-based distribution of approximately 3,100 copies per issue, more than 95% of which are requested subscriptions. It is published quarterly in a full-color magazine format, and is available online. Water-related research, engagement, education and outreach faculty and water-related professional staff are featured in each issue. Guest columns and articles are encouraged. A director's column is published in each issue. News Releases: The Water Center produces about 30 press releases annually focused on research results or progress, extension programming, educational opportunities, public tours, seminars, lectures, symposiums and conferences, awarding of major research grants and other matters of public impact involving the Water Center and other natural resource-focused UNL entities. These releases support a wide variety of UNL water-related research and outreach that cross departmental and academic disciplines. They focus on public impacts of UNL-sponsored research and programming. The UNL Water Center writes these for many UNL environmental science-related departments and faculty members who do not have a staff communicator available to them. The Water Center coordinates public media requests for information and interviews with sources on any water-related topic of interest to them and devotes significant attention to cultivating long-term relationships with members of the working media. The Water Center has a long reputation as a willing and reliable "source" among local, state and regional media for water and natural resources news. Media calls are frequent and water-related faculty and staff are accustomed to fielding questions from the media, doing radio and television interviews, etc. The Water Center makes wide use of electronic and broadcast journalism sources, as well as more traditional print (newspaper) sources.
2. Brochures and pamphlets: All full color. Produced as needed. These include, but are not limited to, mission and programming of the UNL Water Center, UNL Water Sciences Laboratory, Tern and Plover Conservation Partnership, annual Water and Natural Resources Tour and for other units or programs affiliated with or sponsored by the Water Center. All have online versions, as well.
3. Water Center fact sheets: All full-color, generally one sheet. Used to inform and promote both general themes, such as the Water Center itself, or to announce specific programs, seminars, courses, etc. There are various editions, designed for specific internal and external audiences.
4. Nebraska Water Map: A 24 x 36" full-color map of Nebraska surface and groundwater resources. Includes inset maps, diagrams and photos that describe the basics of water quantity, quality and use in Nebraska. The map is used for educational purposes across the state, and is available online. More than 65,000 have been distributed statewide. A range of publications produced outside the UNL

Water Center, particularly fact sheets, research project results and other print materials from USGS, Nebraska Department of Environmental Quality, U.S. Environmental Protection Agency, U.S. Army Corps of Engineers, local Natural Resources Districts and University of Nebraska-Lincoln Extension, are available through Water Center and School of Natural Resources web sites or in print form. UNL Water Center assists with content, design, editing and production for many of these publications.

5. Electronic Resources: Print materials produced by the UNL Water Center, and other information, are available online. The Water Center co-sponsors, designs and maintains the following related Internet web sites: UNL Water: http://water.unl.edu UNL Water Center: http://watercenter.unl.edu/ Water Sciences Laboratory: http://waterscience.unl.edu UNL School of Natural Resources: http://snr.unl.edu/water/index.asp

Conferences, Seminars, Tours, Workshops, and Other Outreach:

Water and Natural Resources Seminars: A longstanding annual series of 12 to 14 free weekly public lectures from conducted from January to April. The series dates to the early 1970's and includes a broad range of water and natural resource-related topics, such as irrigation and other agriculture topics, fish and wildlife, drinking water and wastewater, watershed management, modeling, energy, climate change, law, economics, and political science. In 2011 the series included a mini sub-series of four stormwater management lectures co-sponsored by UNL Extension's Stormwater Management Team. Individual lectures attract an audience of 60 to 100, including approximately 15 graduate and undergraduate students who attend the lectures as a one-credit-hour course. Other audience members include faculty, government and organizational employees, policy makers and interested members of the public. News releases, mailings, brochures, posters and web-based information are produced supporting this series. Most lectures are posted online for viewing by those than cannot attend.

Summer Water and Natural Resources Tour: The tour is another long-standing Water Center activity, dating to UNL "Irrigation tours" first conducted in the 1970's. The 2011 tour explored water and agricultural issues in Western Nebraska's Sandhills region and was sold-out, as they typically are. Attendees include state legislators, congressional staff, faculty, and water scientists and managers from a wide variety of public and private entities. The event is co-sponsored and co-planned with the Kearney Area Chamber of Commerce, Nebraska Public Power District, Central Nebraska Public Power and Irrigation District and others. News releases, mailings and a brochure are produced supporting this event.

Water Law Conference: A one-day event focused on Nebraska water law issues such as water rights transfers, drainage issues, Clean Water Act enforcement, etc. It is targeted to practicing attorneys but open to all. Typically half those attending are water managers and policy-makers. The program is developed by a committee that includes Nebraska's top water lawyers, and is co-sponsored by the University of Nebraska College of Law.

Great Plains Climate, Water and Ecosystems Symposium: A one-day event following the water law conference focusing on Great Plains climate, water and ecosystems and showcasing impacts at the intersection of climate change or variability, water and all other disciplines, including infrastructure, design, hydropower, agriculture, ecosystem services, drinking water and many others. Geographic focus was centered on the Great Plains, including research or programming transferrable to the Great Plains.

Faculty/Staff/Student Networking and Mentoring Events: The Nebraska Water Center is particularly focused on assisting faculty who are interested in interdisciplinary research. In addition to helping link individual faculty members to groups, the Water Center sponsored three events to help connect faculty. First was a networking/social event, attended by 18 faculty. Second were two brownbag mentoring/networking events for assistant professors. The topics were digital data management and storage, and advice on post-grant administration. Attendance was 8 and 5, respectively. Finally, a mini-workshop on creating and presenting effective posters was offered to graduate students in water-related disciplines. Attendance was 21 students from 5 departments.

Mentoring: The Water Center prioritizes mentoring newer assistant professors to help them establish successful careers. Newer faculty from the many academic units associated with the Water Center attended several brown bag sessions during the year where they could get acquainted and get advice from senior faculty and external partners on topics such as working with stakeholders, multidisciplinary research, and managing large data sets over their careers.

Other Outreach: Water Center staff routinely provides talks for groups and respond to requests for information. For example, during 2010 the Water Center coordinated faculty testimony and white papers for the Nebraska Legislature related to impacts of a new oil pipeline through the ecologically fragile Nebraska Sandhills and over the High Plains aquifer, the largest aquifer in North America.

Educational Displays: The Water Center makes frequent public displays in association with conferences, symposiums, trade shows, educational open houses and water and environmental education festivals. Water Center staff make presentations and sit on steering committees for such annual educational and informational festivals as "Earth Wellness Festival," "Sunday with a Scientist, " "Gateway Farm Expo" and others. Water Center staff superintends UNL research exhibits at "Husker Harvest Days," one of the largest commercial agricultural expos in the country. More than 50,000 tour UNL exhibits during the three-day show.

Grant/Award: Clean Water Act Section 319 grant from the U.S. Environmental Protection Agency via the Nebraska Department of Environmental Quality (NDEQ) to develop, write and publish a print and online publication documenting the more than 10 years of work of the cooperative Community Lakes Restoration Program, conducted jointly by the NDEQ, University of Nebraska-Lincoln Extension and the Nebraska Game and Parks Commission. An 18-month grant in the amount of approximately $53,000 awarded to UNL Water Center communicator Steve Ress and interim director Bruce Dvorak.

Primary Information Dissemination Clientele:
U.S. Department of Agriculture
U.S. Environmental Protection Agency
U.S. Geological Survey
U.S. Bureau of Reclamation
U.S. Army Corps of Engineers
U.S. Bureau of Land Management
Nebraska Department of Natural Resources
Nebraska Department of Agriculture
Nebraska Health and Human Services System
Nebraska Department of Environmental Quality
Nebraska Environmental Trust Fund
Nebraska Association of Resources Districts (and 23 individual NRDs)
Nebraska Congressional delegation
Nebraska State Senators
Public and private power and irrigation districts
The Audubon Society
The Nature Conservancy
Nebraska Alliance for Environmental Education
Nebraska Earth Science Education Network
Other state Water Resources Research Institutes
University and college researchers and educators
NU students Public and parochial science teachers

Farmers
Irrigators
Irrigation districts and ditch companies
Private citizens

Cooperating Entities:
In addition to primary support from the USGS, the following agencies and entities have helped fund communications activities by the UNL Water Center during the past year.
U.S. Environmental Protection Agency
U.S. Department of Agriculture Nebraska Department of Environmental Quality Nebraska Research Initiative
Nebraska Game and Parks Commission
Nebraska Environmental Trust
Nebraska Department of Environmental Quality
National Water Research Institute
Nebraska Public Power District
Central Nebraska Public Power and Irrigation District
Farm Credit Services of America
Kearney Area Chamber of Commerce
Nebraska Association of Resources Districts
UNL Institute of Agriculture and Natural Resources
UNL Agricultural Research Division
UNL College of Agricultural Sciences and Natural Resources
UNL School of Natural Resources
University of Nebraska Robert B. Daugherty Water for Food Institute
NU College of Law
USGS Nebraska Water Science Center
Nebraska Center for Energy Sciences Research

USGS Summer Intern Program

None.

Student Support					
Category	**Section 104 Base Grant**	**Section 104 NCGP Award**	**NIWR-USGS Internship**	**Supplemental Awards**	**Total**
Undergraduate	0	0	0	0	0
Masters	1	0	0	0	1
Ph.D.	0	0	0	0	0
Post-Doc.	0	0	0	0	0
Total	1	0	0	0	1

Notable Awards and Achievements

Publications from Prior Years